

SANDIA REPORT

SAND2009-5804 Revision 1

Unclassified Unlimited Release

Printed September 2009

Revised November 2009

Polyethylene-Reflected Plutonium Metal Sphere: Subcritical Neutron and Gamma Measurements

John Mattingly

Prepared by
Sandia National Laboratories
Albuquerque, New Mexico 87185 and Livermore, California 94550

Sandia is a multiprogram laboratory operated by Sandia Corporation,
a Lockheed Martin Company, for the United States Department of Energy's
National Nuclear Security Administration under Contract DE-AC04-94AL85000.



Sandia National Laboratories

Issued by Sandia National Laboratories, operated for the United States Department of Energy by Sandia Corporation.

NOTICE: This report was prepared as an account of work sponsored by an agency of the United States Government. Neither the United States Government, nor any agency thereof, nor any of their employees, nor any of their contractors, subcontractors, or their employees, make any warranty, express or implied, or assume any legal liability or responsibility for the accuracy, completeness, or usefulness of any information, apparatus, product, or process disclosed, or represent that its use would not infringe privately owned rights. Reference herein to any specific commercial product, process, or service by trade name, trademark, manufacturer, or otherwise, does not necessarily constitute or imply its endorsement, recommendation, or favoring by the United States Government, any agency thereof, or any of their contractors or subcontractors. The views and opinions expressed herein do not necessarily state or reflect those of the United States Government, any agency thereof, or any of their contractors.



Polyethylene-Reflected Plutonium Metal Sphere: Subcritical Neutron and Gamma Measurements

John Mattingly
Contraband Detection Technology

Sandia National Laboratories
P.O. Box 5800
Albuquerque, New Mexico 87185-0782

Abstract

Numerous benchmark measurements have been performed to enable developers of neutron transport models and codes to evaluate the accuracy of their calculations. In particular, for criticality safety applications, the International Criticality Safety Benchmark Experiment Program (ICSBEP) annually publishes a handbook of critical and subcritical benchmarks. Relatively fewer benchmark measurements have been performed to validate photon transport models and codes, and unlike the ICSBEP, there is no program dedicated to the evaluation and publication of photon benchmarks. Even fewer coupled neutron-photon benchmarks have been performed. This report documents a coupled neutron-photon benchmark for plutonium metal reflected by polyethylene. A 4.5-kg sphere of α -phase, weapons-grade plutonium metal was measured in six reflected configurations:

- Bare
- Reflected by 0.5 inch of high density polyethylene (HDPE)
- Reflected by 1.0 inch of HDPE
- Reflected by 1.5 inches of HDPE
- Reflected by 3.0 inches of HDPE
- Reflected by 6.0 inches of HDPE

Neutron and photon emissions from the plutonium sphere were measured using three instruments:

- A gross neutron counter
- A neutron multiplicity counter
- A high-resolution gamma spectrometer

This report documents the experimental conditions and results in detail sufficient to permit developers of radiation transport models and codes to construct models of the experiments and to compare their calculations to the measurements. All of the data acquired during this series of experiments are available upon request.

Acronyms and Nomenclature

BeRP	Beryllium-Reflected Plutonium
cps	counts per second
DAF	Device Assembly Facility
HDPE	high density polyethylene
HPGe	high purity germanium
ICSBEP	International Criticality Safety Benchmark Experiment Program
LANL	Los Alamos National Laboratory
MCA	multichannel analyzer
MCNP	Monte Carlo N-Particle
NIM	nuclear instrumentation module
NIST	National Institute for Standards
NPOD	neutron pod
NTS	Nevada Test Site
ppm	parts per million
SNAP	shielded neutron assay probe

Contents

1	Introduction	11
2	Plutonium Source.....	11
3	Polyethylene Reflectors	15
4	Instruments.....	25
4.1	Gross Neutron Counter	25
4.1.1	Description	25
4.1.2	Operation	29
4.2	Neutron Multiplicity Counter.....	29
4.2.1	Description	29
4.2.2	Operation	33
4.3	Gamma Spectrometer.....	35
4.3.1	Description	35
4.3.2	Operation	39
5	Instrument Configuration	39
6	Instrument Calibration.....	44
6.1	Neutron Calibration Source and Moderators	44
6.2	Gross Neutron Counter Calibration	51
6.3	Neutron Multiplicity Counter Calibration	53
6.4	Gamma Spectrometer Neutron Response Calibration	58
6.5	Gamma Calibration Sources.....	60
6.6	Gamma Spectrometer Photon Response Calibration	61
6.7	Photon Background Measurements	63
7	Benchmark Measurements.....	64
7.1	Gross Neutron Counting Measurements	65
7.2	Neutron Multiplicity Counting Measurements.....	66
7.3	Gamma Spectrometry Measurements	71
8	Other Measurements.....	73
8.1	Neutron Multiplicity Counter Response versus Polyethylene Reflector Temperature	73
8.2	Gross Neutron Counter Response with Neutron Multiplicity Counter Absent	75
8.3	Comparison of SNL Reflectors to LANL Reflectors.....	76
8.3.1	Gross Neutron Counting Measurements	77
8.3.2	Neutron Multiplicity Counting Measurements	78
8.3.3	Gamma Spectrometry Measurements	79
8.4	Californium Source in Polyethylene Reflectors.....	81
8.4.1	Gross Neutron Counting Measurements	81
8.4.2	Neutron Multiplicity Counting Measurements	82
8.4.3	Gamma Spectrometry Measurements	85
9	Summary.....	85
	Acknowledgements.....	86
	References	86

Appendix A: LANL Documentation of Plutonium Source Construction.....	87
Appendix B: Polyethylene Reflector Density Measurements and Uncertainty Analysis.....	96
Appendix C: MCNP Model of the LANL SNAP-3 Detector.....	97
Appendix D: MCNP Model of the LANL NPOD-3 Detector.....	98
Appendix E: MCNP Model of 140% HPGe Detector.....	99
Distribution (Electronic).....	100

Figures

Figure 1: The plutonium metal sphere and its steel cladding.....	12
Figure 2: Plutonium source in six different reflected configurations	16
Figure 3: Photograph of the plutonium source in the nested HDPE hemisHELLS	17
Figure 4: Bare plutonium source and aluminum support stand.....	18
Figure 5: 4-inch (approximate) outside diameter HDPE reflector and aluminum support stand	19
Figure 6: 5-inch (approximate) outside diameter HDPE reflector and aluminum support stand	20
Figure 7: 6-inch (approximate) outside diameter HDPE reflector and aluminum support stand	21
Figure 8: 9-inch (approximate) outside diameter HDPE reflector and aluminum support stand	22
Figure 9: 15-inch (approximate) outside diameter HDPE reflector and aluminum support stand	23
Figure 10: Schematic of the LANL SNAP-3 gross neutron counter showing the assembly of the instrument's components.....	26
Figure 11: Schematic of the LANL SNAP-3 gross neutron counter showing the assembled instrument; dimensions are in inches.....	27
Figure 12: The LANL SNAP gross neutron counter with the front cover on (left) and off (right)	28
Figure 13: Aluminum support stand used to vertically align the SNAP with the center of the plutonium source; dimensions are in inches	28
Figure 14: Schematic of the LANL NPOD-3 neutron multiplicity counter showing the assembly of the instrument's components.....	30
Figure 15: Schematic of the LANL NPOD-3 neutron multiplicity counter showing the assembled instrument; dimensions are in inches.....	31
Figure 16: Schematic of the LANL NPOD-3 polyethylene moderator block showing the positioning of the helium-3 proportional counters; all dimensions are in inches	32
Figure 17: Photograph of the LANL NPOD-3 neutron multiplicity counter	33
Figure 18: Neutron multiplicity measurement exhibiting "drop-outs" in NPOD data acquisition; the spurious segments should be discarded.....	34
Figure 19: Schematic of the HPGe gamma spectrometer showing the assembly of the instrument's components	37
Figure 20: Schematic of the bismuth shield showing the assembly of the shield's subcomponents; dimensions are in inches.....	38
Figure 21: Photographs of the HPGe gamma spectrometer with the bismuth shield on (left) and off (right)	39
Figure 22: Photograph of the bismuth shield	39
Figure 23: Schematic illustrating the positioning of the instruments relative to the plutonium source ...	40

Figure 24: Photograph showing the positioning of the instruments relative to the plutonium source.....	40
Figure 25: Plan view showing the positions of the instruments relative to the plutonium source.....	41
Figure 26: Elevation views showing the positions of the instruments relative to the plutonium source and the floor	42
Figure 27: Schematic of the steel cart used as a work surface; three identical carts were used.....	43
Figure 28: Diagram showing the position of the plutonium source relative to the two nearest walls; the other walls (not shown) were more than 20 feet away from the source.....	43
Figure 29: Schematic showing the construction of the californium neutron calibration source; all dimensions are in inches.....	44
Figure 30: 2-cm thick HDPE neutron moderator and aluminum support stand; dimensions are in inches	46
Figure 31: 4-cm thick HDPE neutron moderator and aluminum support stand; dimensions are in inches	47
Figure 32: 8-cm thick HDPE neutron moderator and aluminum support stand; dimensions are in inches	48
Figure 33: 8-cm thick borated polyethylene neutron moderator and aluminum support stand; dimensions are in inches.....	49
Figure 34: Aluminum source holders for the 14-cm diameter moderators, the 20-cm diameter moderators, and the bare californium calibration source; dimensions are in inches.....	50
Figure 35: Gross neutron counter count rate versus californium source moderation.....	52
Figure 36: Neutron multiplicity counter count rate versus californium source moderation	55
Figure 37: Neutron multiplicity distribution measured for the bare californium source; the coincidence gate width was 4096 μ s	56
Figure 38: Rossi- α distribution measured for the bare californium source.....	57
Figure 39: Gamma spectrum versus californium source moderation; the NPOD and SNAP were present	59
Figure 40: Gamma spectrum versus californium source moderation; the NPOD and SNAP were not present	59
Figure 41: Schematic of the Eckert & Ziegler Isotope Products Type D gamma standard	60
Figure 42: Schematic of the NIST uranium-232 source disk	61
Figure 43: Aluminum mounting fixture for the NIST uranium-232 source.....	61
Figure 44: Gamma spectrum vs. gamma calibration source; the NPOD and SNAP were present	62
Figure 45: Gamma spectrum vs. gamma calibration source; the NPOD and SNAP were not present.....	62
Figure 46: Composite photon background spectrum accumulated from 25 hours of background measurements	63
Figure 47: Gross neutron counter count rate vs. polyethylene reflector thickness.....	66
Figure 48: Neutron multiplicity counter count rate versus polyethylene reflector thickness	68
Figure 49: Neutron multiplicity distribution versus polyethylene reflector thickness	69
Figure 50: Neutron multiplicity distribution versus polyethylene reflector thickness; the coincidence gate width is 1024 μ s	70
Figure 51: Feynman-Y versus polyethylene reflector thickness	70
Figure 52: Rossi- α distribution versus polyethylene reflector thickness.....	71

Figure 53: Gamma spectrum versus polyethylene moderator thickness; the inset shows the region between 0 and 2500 keV. These measurements were performed with the NPOD and SNAP present.....	72
Figure 54: Gamma spectrum versus polyethylene moderator thickness; the inset shows the region between 0 and 2500 keV. These measurements were performed with the NPOD and SNAP absent.....	73
Figure 55: Feynman-Y versus surface temperature of 1.0-inch thick polyethylene moderator	74
Figure 56: Gross neutron counter response with neutron multiplicity counter present and absent	76
Figure 57: Polyethylene reflectors constructed by LANL.....	77
Figure 58: Gross neutron counter response for LANL and SNL reflectors	78
Figure 59: Comparison of the Feynman-Y for the LANL and SNL reflectors	79
Figure 60: Gamma spectrum versus LANL polyethylene reflector thickness; the inset shows the region between 0 and 2500 keV	80
Figure 61: Gamma spectrum versus SNL polyethylene reflector thickness; the inset shows the region between 0 and 2500 keV	81
Figure 62: Gross neutron counter count rate versus polyethylene reflector thickness.....	82
Figure 63: Neutron multiplicity counter count rate versus polyethylene reflector thickness	83
Figure 64: Neutron multiplicity distribution measured with the californium calibration source inside the 1.0-inch thick polyethylene reflector; the coincidence gate width is 4096 μ s	84
Figure 65: Neutron multiplicity distribution mean and variance versus polyethylene reflector thickness; the coincidence gate width is 4096 μ s.....	84
Figure 66: Gamma spectrum versus polyethylene reflector thickness; the inset shows the height of the 2223 keV photopeak from hydrogen neutron capture	85

Tables

Table 1: Nominal composition of the steel cladding	12
Table 2: Chemical composition of the plutonium metal. The composition was measured by analytical chemistry between 24 September 1980 and 3 October 1980.....	13
Table 3: Isotopic composition of the plutonium. The composition was measured by mass spectrometry on 29 September 1980, except the content of americium-241, which was measured by radioanalysis on 23 September 1980.....	13
Table 4: Estimated composition of the plutonium metal on 6 January 2009.....	14
Table 5: Measured mass, volume, and density for the polyethylene reflector hemisHELLS; uncertainties represent one standard deviation	24
Table 6: Nominal composition of aluminum alloy 6061	24
Table 7: Composition of the helium-3 proportional counter fill gas	25
Table 8: Composition of the lithium-6 carbonate/silicone neutron absorber	36
Table 9: Initial composition of the californium neutron calibration source on 9 June 2003.....	45
Table 10: Composition of the californium neutron calibration source on 6 January 2009	45
Table 11: Composition of the borated polyethylene neutron moderator	51
Table 12: Measured mass, calculated volume, and calculated density of each neutron moderator	51

Table 13: Gross neutron counter calibration measurements.....	52
Table 14: Gross neutron counter count rate versus californium source moderation; uncertainties represent one standard deviation	52
Table 15: Neutron multiplicity counter calibration measurements	54
Table 16: Neutron multiplicity counter run time and number of counts collected versus californium source moderation.....	54
Table 17: Neutron multiplicity counter count rate versus californium source moderation; uncertainties represent one standard deviation	55
Table 18: Gamma spectrometer neutron calibration measurements.....	58
Table 19: Gamma calibration sources.....	60
Table 20: Gamma spectrometer photon calibration measurements.....	61
Table 21: Photon background measurements; the real-time for each measurement was 1 hour	63
Table 22: Gross neutron counting benchmark measurements	65
Table 23: Gross neutron counter count rate versus polyethylene reflector thickness; uncertainties represent one standard deviation	66
Table 24: Neutron multiplicity counter benchmark measurements	67
Table 25: Neutron multiplicity counter count rate versus polyethylene reflector thickness; uncertainties represent one standard deviation	67
Table 26: High-resolution gamma spectrometry benchmark measurements.....	71
Table 27: Neutron multiplicity counting measurements taken versus the surface temperature of the 1.0 inch thick polyethylene reflector	74
Table 28: Gross neutron counter response with neutron multiplicity counter present and absent; uncertainties represent one standard deviation	75
Table 29: Gross neutron counter response for LANL and SNL reflectors; uncertainties represent one standard deviation	77
Table 30: Neutron multiplicity measurements comparing LANL and SNL reflectors	78
Table 31: Gamma spectrometry measurements comparing LANL and SNL reflectors	80
Table 32: Gross neutron counter count rate versus polyethylene reflector thickness	82
Table 33: Neutron multiplicity measurements with the californium calibration source placed inside the polyethylene reflectors	83
Table 34: Gamma spectrometry measurements where the californium calibration source was placed inside the polyethylene reflectors	85

1 Introduction

Subcritical experiments were conducted with an α -phase, weapons-grade plutonium metal sphere in the Nevada Test Site (NTS) Device Assembly Facility (DAF) from 6 January 2009 to 15 January 2009. The purpose of this series of experiments was to acquire data to test and evaluate coupled neutron-photon transport calculations. Neutron and photon emissions from the plutonium sphere were measured using three instruments:

- A gross neutron counter
- A neutron multiplicity counter
- A high-resolution gamma spectrometer

The plutonium sphere was measured in six different configurations:

- Bare
- Reflected by 0.5 inch of HDPE
- Reflected by 1.0 inch of HDPE
- Reflected by 1.5 inches of HDPE
- Reflected by 3.0 inches of HDPE
- Reflected by 6.0 inches of HDPE

The intent of this report is to document the experimental conditions and results in detail sufficient to permit developers of radiation transport models and codes to construct models of the experiments and to compare their calculations to the measurements. All of the data acquired during this series of experiments are available upon request.

2 Plutonium Source

The plutonium source for this series of experiments was the BeRP Ball, a 4.5-kg sphere of α -phase, weapons-grade plutonium fabricated by Los Alamos National Laboratory (LANL) in October 1980.¹ The sphere is clad in stainless steel as shown in Figure 1.

The BeRP ball was cast and machined to a mean radius of 3.7938 cm. The theoretical density of α -phase plutonium metal is 19.655 g/cm³. However, the measured mass of the plutonium sphere was 4483.884 g, and the volume of the sphere was 228.72 cm³ (based on the mean diameter). Consequently, the calculated density of the plutonium sphere is 19.604 g/cm³. LANL documentation describing the assembly of the BeRP ball indicates the plutonium sphere was partially immersed in Freon to shrink it just prior to its final assembly in the steel cladding. The dimensions of the plutonium sphere following this Freon bath were not recorded by LANL. As a result, the actual density of the plutonium sphere may be higher than its calculated density if the Freon bath permanently reduced the volume of the sphere by changing the grain structure of the metal.

¹ One of the first experiments conducted with this source was a critical benchmark using a beryllium metal reflector, so the source became known as the “beryllium-reflected plutonium” ball, or BeRP ball.

The BeRP ball was encased in a cladding of stainless steel 304 that is nominally 0.0305 cm thick. The nominal composition of the steel cladding is listed in Table 1. Its nominal density is 7.62 g/cm³. As shown in Figure 1, the cladding was constructed from two hemispheres, each with a nominal inside radius of 3.8278 cm and a nominal outside radius of 3.8583 cm. Each hemishell also had a 4.3764-cm radius, 0.0457-cm thick flange. When the plutonium sphere was assembled in the cladding, the two hemishells were electron-beam-welded together at this flange. Because the outside of the radius of the plutonium sphere is smaller than the inside radius of the cladding by 0.0340 cm, there is a gap between the plutonium sphere and the cladding that is nominally 0.0680 cm at its widest point.

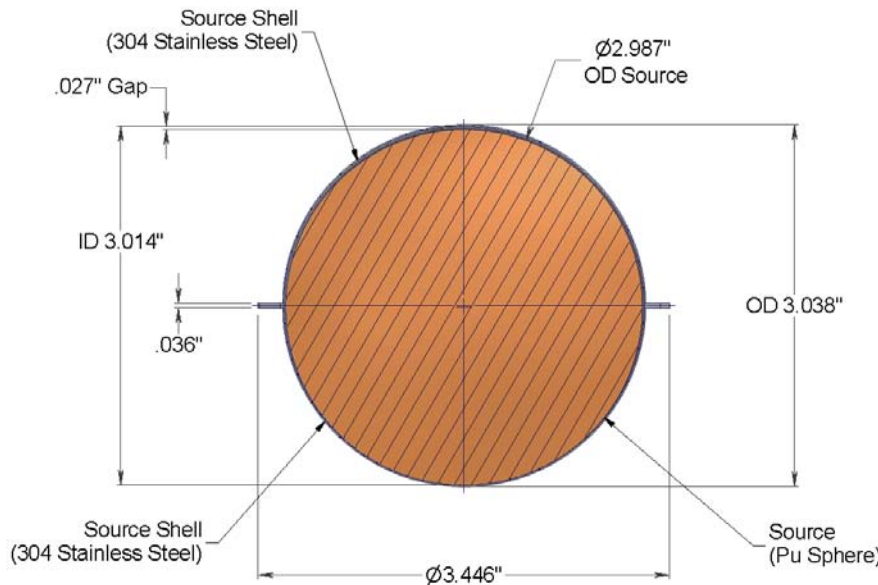


Figure 1: The plutonium metal sphere and its steel cladding

Table 1: Nominal composition of the steel cladding

Constituent	Mass Fraction
Iron	69.5%
Chromium	19%
Nickel	9.5%
Manganese	2%

LANL performed analytical chemistry measurements of the plutonium source material to estimate the content of gallium, iron, carbon, and other elements in the metal. From these measurements, LANL estimated that the composition of the metal was

- 99.58% plutonium
- 335 ppm gallium
- 239 ppm carbon
- 10 ppm iron

All quantities above are *mass* fractions. As shown in Table 2, LANL was also able to estimate and/or bound the content of several other elements in the metal. The analytical chemistry measurements were performed between 24 September 1980 and 3 October 1980. Note that approximately 0.34% of the metal is unaccounted for.

Table 2: Chemical composition of the plutonium metal. The composition was measured by analytical chemistry between 24 September 1980 and 3 October 1980.

Constituent	Mass Fraction	Constituent	Mass Fraction
Pu	99.58%	Cr	< 5 ppm
Ga	335 ppm	Ni	< 5 ppm
C	230 ppm	Zn	< 5 ppm
Fe	10 ppm	Sn	< 5 ppm
Mo	9 ppm	Pb	< 5 ppm
Ca	3 ppm	Be	< 1 ppm
Zr	< 100 ppm	B	< 1 ppm
Na	< 50 ppm	Mg	< 1 ppm
Cd	< 10 ppm	Cu	< 1 ppm
Al	< 5 ppm	Ag	< 1 ppm
Si	< 5 ppm	Bi	< 1 ppm
Balance		≥ 3412 ppm	

LANL also performed radioanalysis of the plutonium source material to estimate its americium content. The americium content was estimated to be 557 ppm by mass on 23 September 1980.² LANL documentation does not indicate the isotopic composition of the americium. It is assumed to be entirely americium-241.

Finally, LANL performed mass spectrometry measurements of the plutonium source material to estimate the plutonium isotopic composition. The estimated isotopic composition on 29 September 1980 is listed in Table 3.³

Table 3: Isotopic composition of the plutonium. The composition was measured by mass spectrometry on 29 September 1980, except the content of americium-241, which was measured by radioanalysis on 23 September 1980.

Isotope	Mass Fraction
Pu238	0.020%
Pu239	93.74%
Pu240	5.95%
Pu241	0.269%
Pu242	0.028%
Am241	557 ppm

² Note that LANL records do not indicate if this quantity is the americium content of the plutonium or the metal (which is 99.58% plutonium by mass). Consequently, the americium content of the plutonium may have been between 557 ppm and 559 ppm.

³ Note that Table 2 lists the isotopic composition of the *plutonium*, which itself comprised 99.58% of the metal. To obtain the mass fraction of a given isotope in the *metal*, multiply the quantity in Table 2 by 99.58%.

Table 4 lists the estimated composition of the plutonium metal on 6 January 2009, the first day of this series of experiments. This composition includes the constituents listed in Table 2 and Table 3. Constituents from Table 2 whose quantity was only bounded by analytical chemistry were treated as if they were present at that upper bound. Radioactive constituents have been aged from the date of their initial assay to 6 January 2009, the first day of this series of experiments. Constituents below 0.1 ppm have been excluded.

Table 4: Estimated composition of the plutonium metal on 6 January 2009

Constituent	Mass Fraction	Constituent	Mass Fraction
Pu238	0.016%	Mo98	2.2 ppm
Pu239	93.265%	Mo96	1.5 ppm
Pu240	5.907%	Zn66	1.4 ppm
Pu241	0.068%	Mo92	1.3 ppm
Pu242	0.028%	Cd111	1.3 ppm
Am241	2472.4 ppm	Cd110	1.2 ppm
Ga	335 ppm	Cd113	1.2 ppm
C	230 ppm	Pb206	1.2 ppm
U235	746.9 ppm	Pb207	1.1 ppm
U236	174.1 ppm	Be	1 ppm
Zr	100 ppm	B	1 ppm
Np237	77.8 ppm	Mg	1 ppm
Na	50 ppm	Cu	1 ppm
U234	39.2 ppm	Ag	1 ppm
Fe	10 ppm	Bi	1 ppm
Al	5 ppm	Zn68	0.97 ppm
Si	5 ppm	Mo100	0.90 ppm
Ni	5 ppm	Mo97	0.87 ppm
Sn	5 ppm	Mo94	0.81 ppm
Cr52	4.2 ppm	Cd116	0.77 ppm
Ca40	2.9 ppm	Cr53	0.48 ppm
Cd114	2.9 ppm	Cr50	0.21 ppm
Pb208	2.6 ppm	Zn67	0.21 ppm
Zn64	2.4 ppm	Cr54	0.12 ppm
Cd112	2.4 ppm	Cd106	0.12 ppm
		Balance	2860.3 ppm

Documents from LANL that record the results of the analytical chemistry, radioanalysis, and mass spectrometry measurements are provided in Appendix A.

3 Polyethylene Reflectors

The plutonium source was measured in six different reflected configurations:

- Bare
- Reflected by 0.5 inch of HDPE
- Reflected by 1.0 inch of HDPE
- Reflected by 1.5 inches of HDPE
- Reflected by 3.0 inches of HDPE
- Reflected by 6.0 inches of HDPE

Figure 2 illustrates the six different reflector configurations. The polyethylene reflectors were constructed as a series of five nesting spherical shells. Each individual shell was constructed of two mating hemishells. Figure 3 is a photograph of the plutonium source in the nested hemishells.

The mating surfaces of the hemishells were stepped to eliminate any streaming path. Each shell was supported by its own aluminum support stand. The stands were designed to keep the center of the plutonium source 8.3 inches above the work surface (which is subsequently described in the section “Instrument Configuration”). Figure 4 through Figure 9 provide the dimensions of the reflectors and support stands used for each configuration.

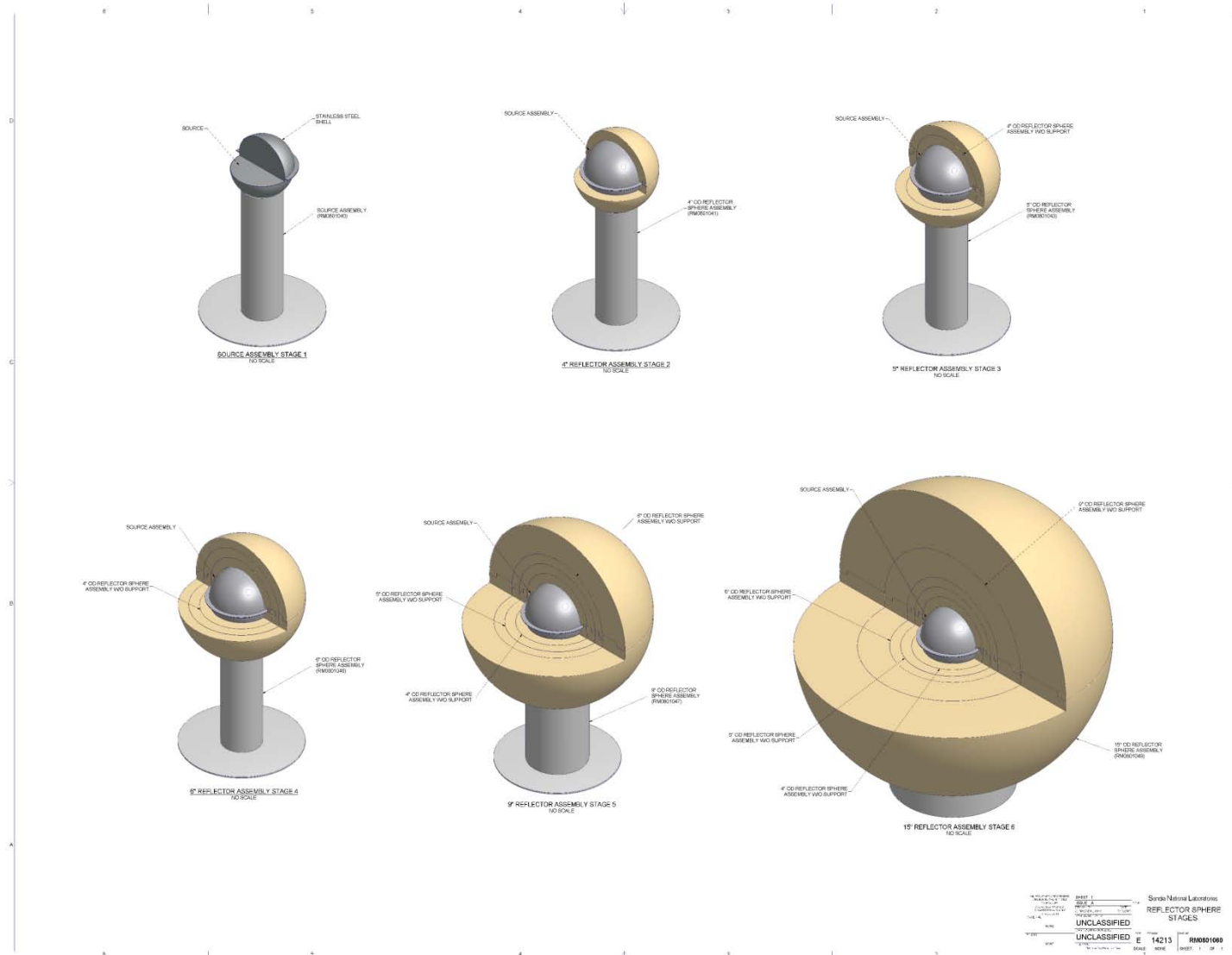


Figure 2: Plutonium source in six different reflected configurations



Figure 3: Photograph of the plutonium source in the nested HDPE hemishells

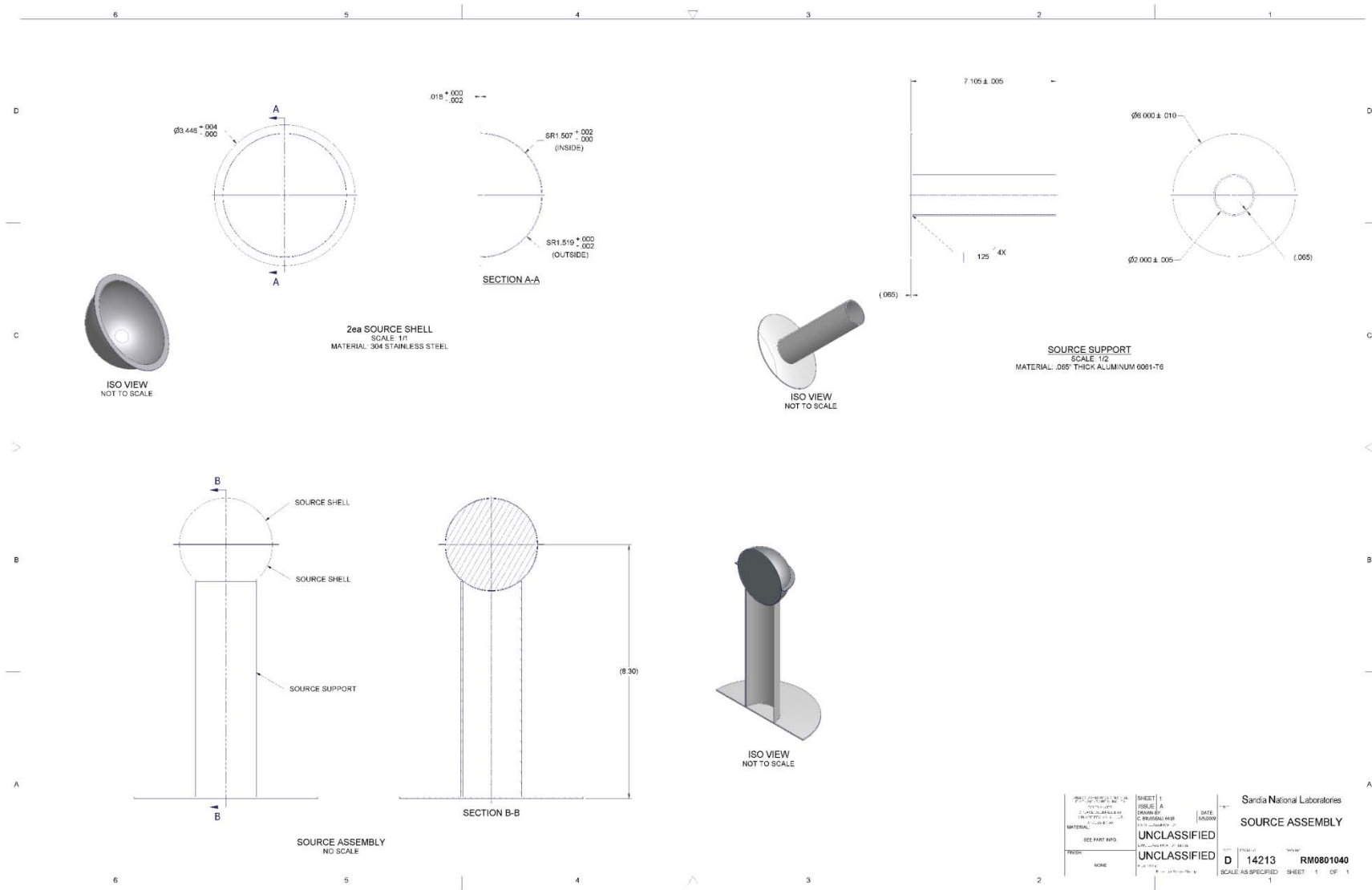


Figure 4: Bare plutonium source and aluminum support stand

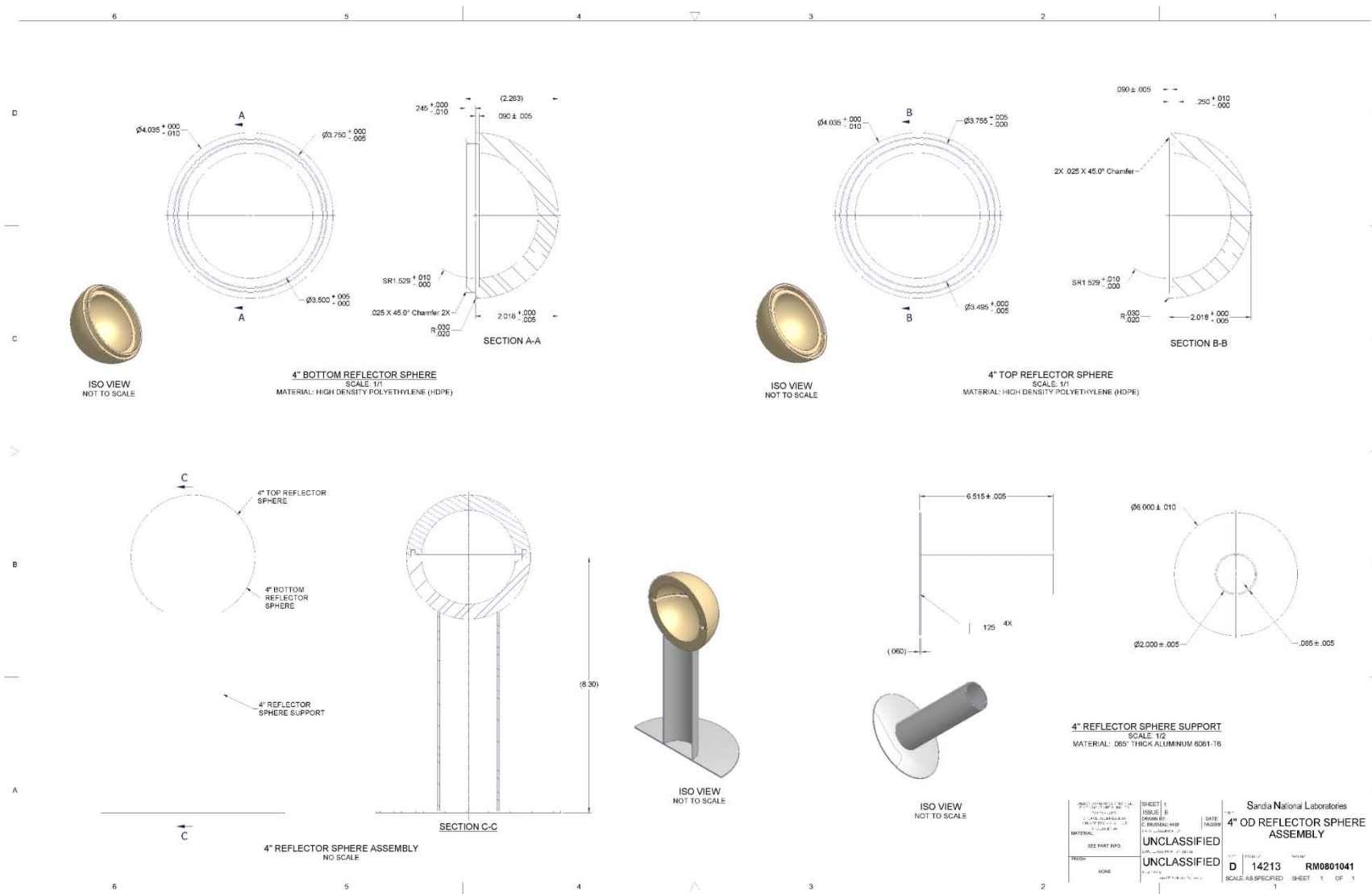


Figure 5: 4-inch (approximate) outside diameter HDPE reflector and aluminum support stand

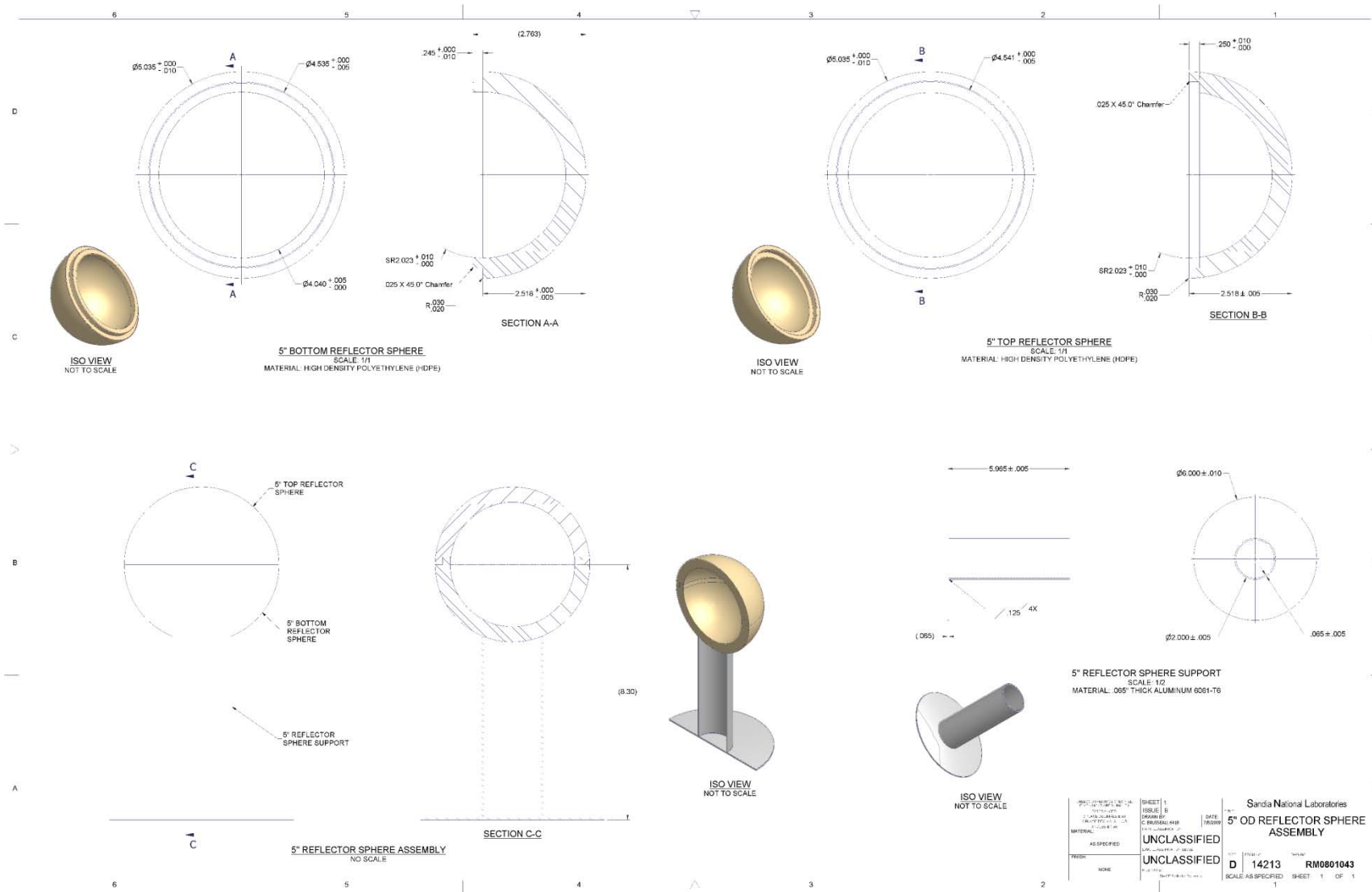


Figure 6: 5-inch (approximate) outside diameter HDPE reflector and aluminum support stand

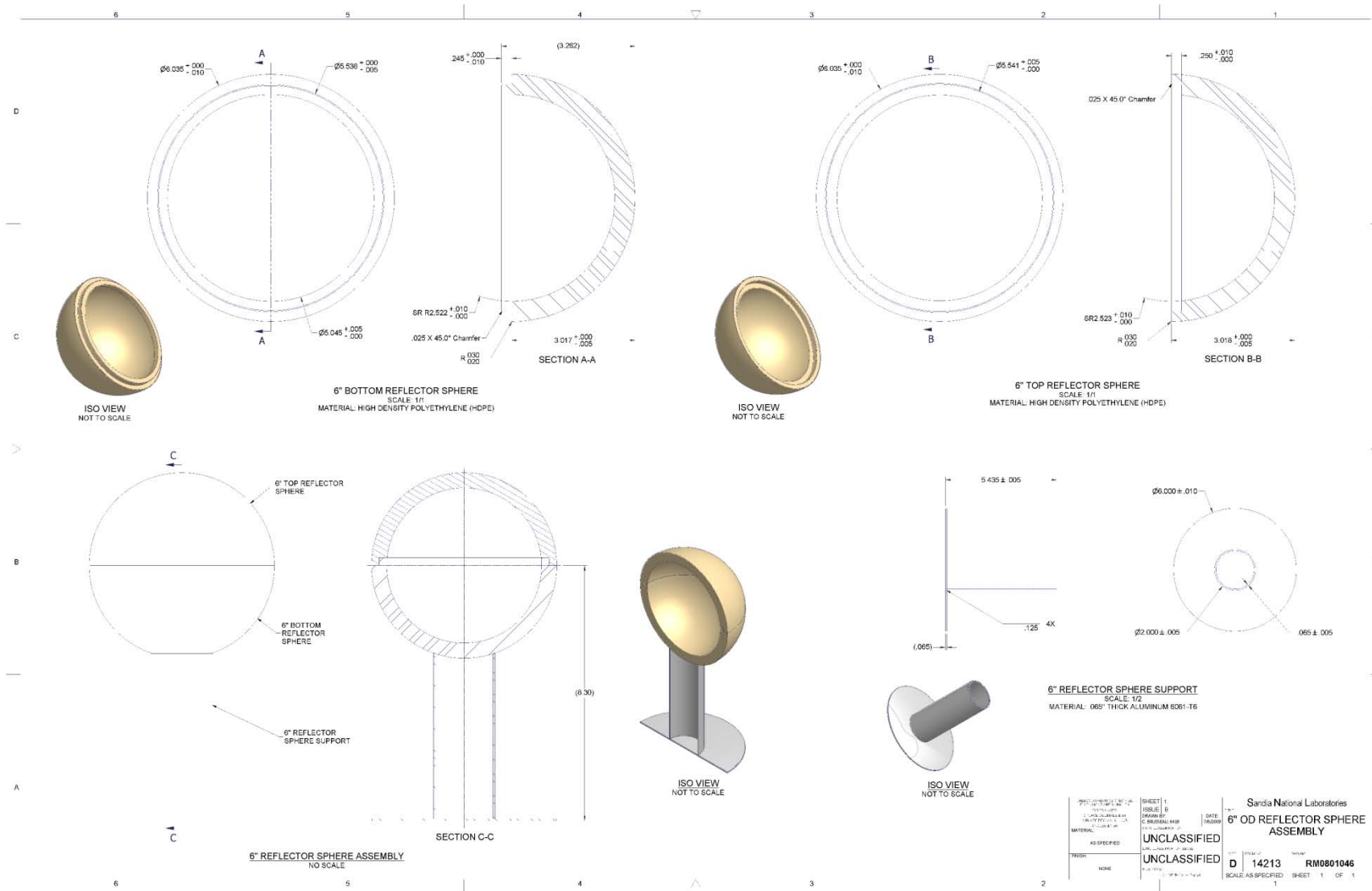


Figure 7: 6-inch (approximate) outside diameter HDPE reflector and aluminum support stand

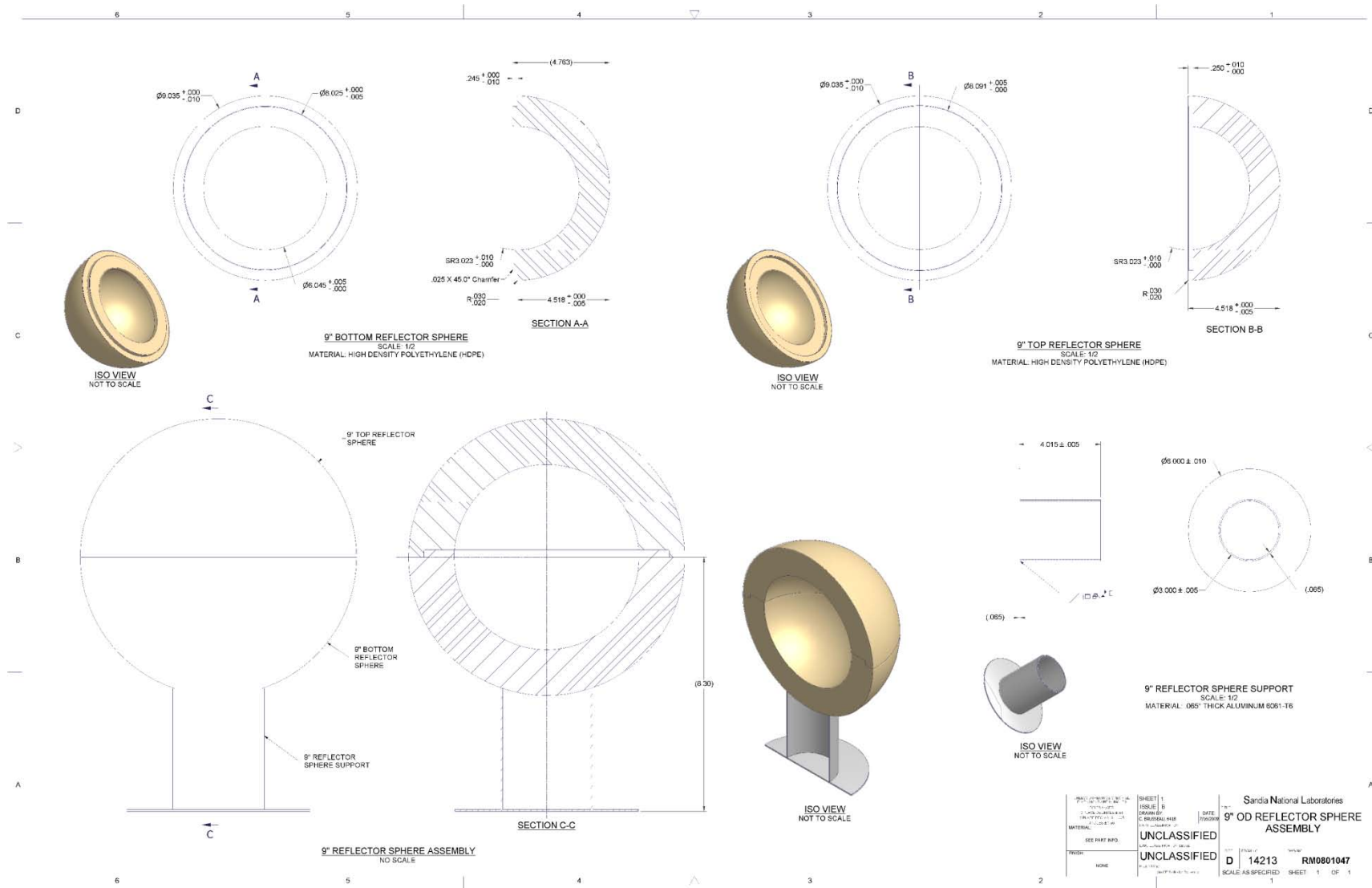


Figure 8: 9-inch (approximate) outside diameter HDPE reflector and aluminum support stand

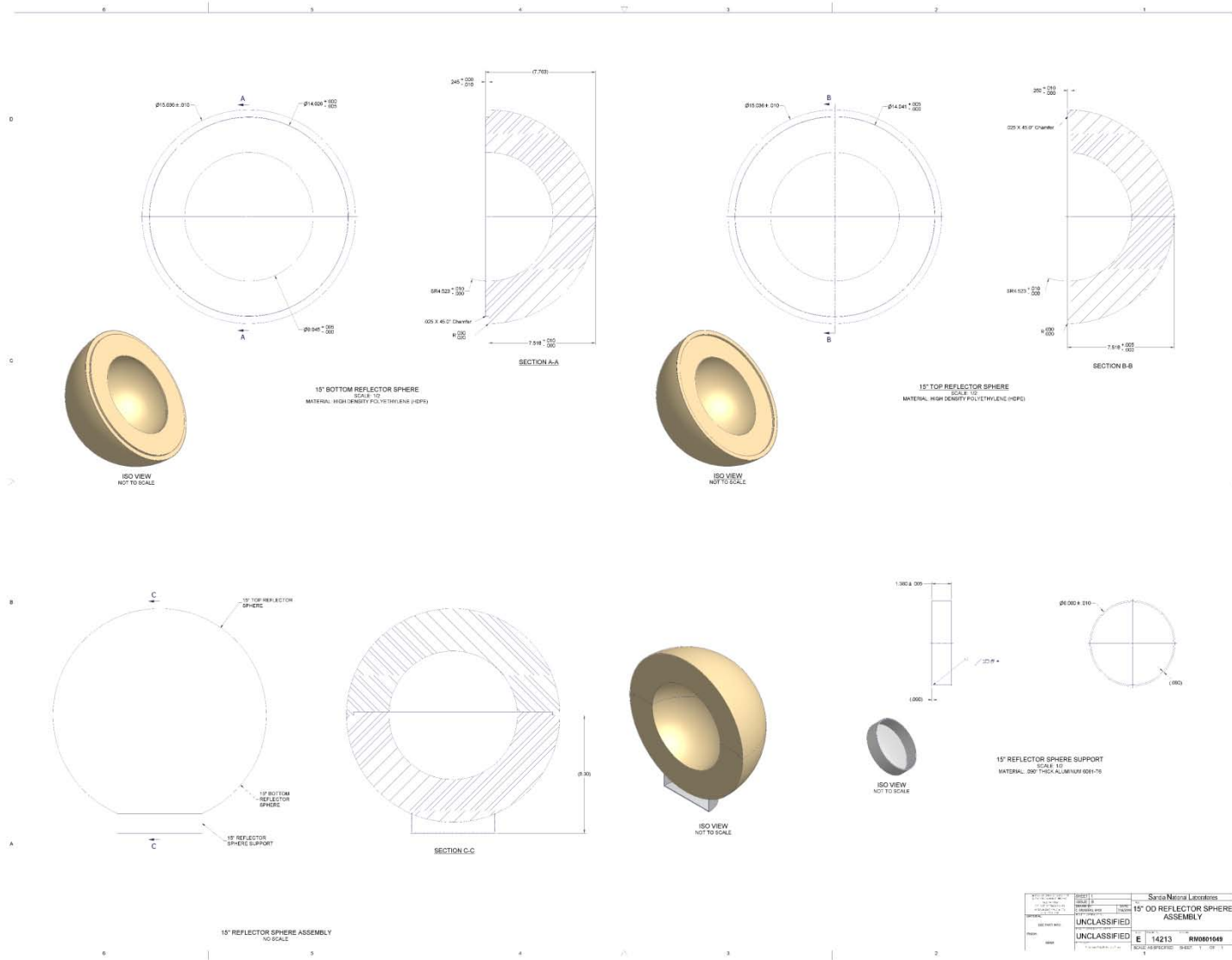


Figure 9: 15-inch (approximate) outside diameter HDPE reflector and aluminum support stand

The reflectors were machined from pure polyethylene (CH₂), which has a nominal density of approximately 0.95 g/cm³. However, the reflectors were fabricated using at least three different batches of HDPE, so some variation in density was observed. Table 5 lists the measured mass, volume, and density for each HDPE hemishell. The quantities listed in Table 5 were estimated from a combination of mass and dimensional measurements. These measurements, and the uncertainty analysis, are described in Appendix B.

Table 5: Measured mass, volume, and density for the polyethylene reflector hemishells; uncertainties represent one standard deviation

Approx. Shell Outside Diameter	Mass (g)		Volume (cm ³)		Density (g/cm ³)	
	Bottom Hemishell	Top Hemishell	Bottom Hemishell	Top Hemishell	Bottom Hemishell	Top Hemishell
15 inches	11271.213	10562.548	11739.45	11042.89	0.9601	0.9565
	± 0.0431	± 0.0203	± 24	± 20	± 0.0020	± 0.0017
9 inches	2207.478	2036.980	2303.17	2125.60	0.9585	0.9583
	± 0.0080	± 0.0040	± 7.8	± 3.8	± 0.0032	± 0.0017
6 inches	389.333	357.785	409.93	375.00	0.9498	0.9541
	± 0.0040	± 0.0050	± 4.4	± 4.2	± 0.0102	± 0.0107
5 inches	259.801	235.948	270.85	246.32	0.9592	0.9579
	± 0.0035	± 0.0030	± 3.6	± 3.0	± 0.0127	± 0.0117
4 inches	152.641	140.608	159.69	146.28	0.9559	0.9612
	± 0.0009	± 0.0019	± 0.82	± 1.60	± 0.0049	± 0.0105

The aluminum support stands were fabricated from aluminum alloy 6061. The nominal density of the alloy is 2.7 g/cm³. The nominal composition of the alloy is listed in Table 6.⁴

Table 6: Nominal composition of aluminum alloy 6061

Constituent	Mass Fraction	
	Minimum	Maximum
Mg	0.8%	1.2%
Si	0.40%	0.8%
Fe	N/A	0.7%
Cu	0.15%	0.40%
Mn	N/A	0.15%
Cr	0.04%	0.35%
Zn	N/A	0.25%
Ti	N/A	0.15%
Other	N/A	0.15%
Al	Balance	

⁴ The nominal density and composition were obtained from the Alcoa data sheet for aluminum alloy 6061; see http://www.alcoa.com/adip/catalog/pdf/Extruded_Alloy_6061.pdf.

4 Instruments

The purpose of this series of experiments was to acquire data to test and evaluate coupled neutron-photon transport calculations. Neutron and photon emissions from the plutonium source were measured using three instruments:

- A gross neutron counter
- A neutron multiplicity counter
- A high-resolution gamma spectrometer

4.1 Gross Neutron Counter

The LANL SNAP-3 was used as a gross neutron counter.⁵ Schematics of the instrument are shown in Figure 10 and Figure 11. Photographs of the instrument are shown in Figure 12. The SNAP used in this series of experiments was serial number NI05, LANL property number 1144519.

4.1.1 Description

The SNAP uses a single 1-inch diameter, 4-inch sensitive length helium-3 proportional counter for neutron detection. The counter's fill gas is a mixture of helium-3 with 2% CO₂ as a quench gas. The composition of the fill gas is listed in Table 7. The partial pressure of helium-3 is 10 atm. Based on the ideal gas law, at 293.6 K the density of the fill gas is 2.55×10^{-4} atoms/b·cm. The proportional counter walls are constructed from 1/32-inch thick aluminum with a nominal density of 2.7 g/cm³.

Table 7: Composition of the helium-3 proportional counter fill gas

Constituent	Partial Pressure (atm)	Atomic Abundance	Atomic Density (atoms/ b·cm)
He3	10.0	98.0%	2.4996E-4
CO ₂	0.2	2.0%	5.1013E-6

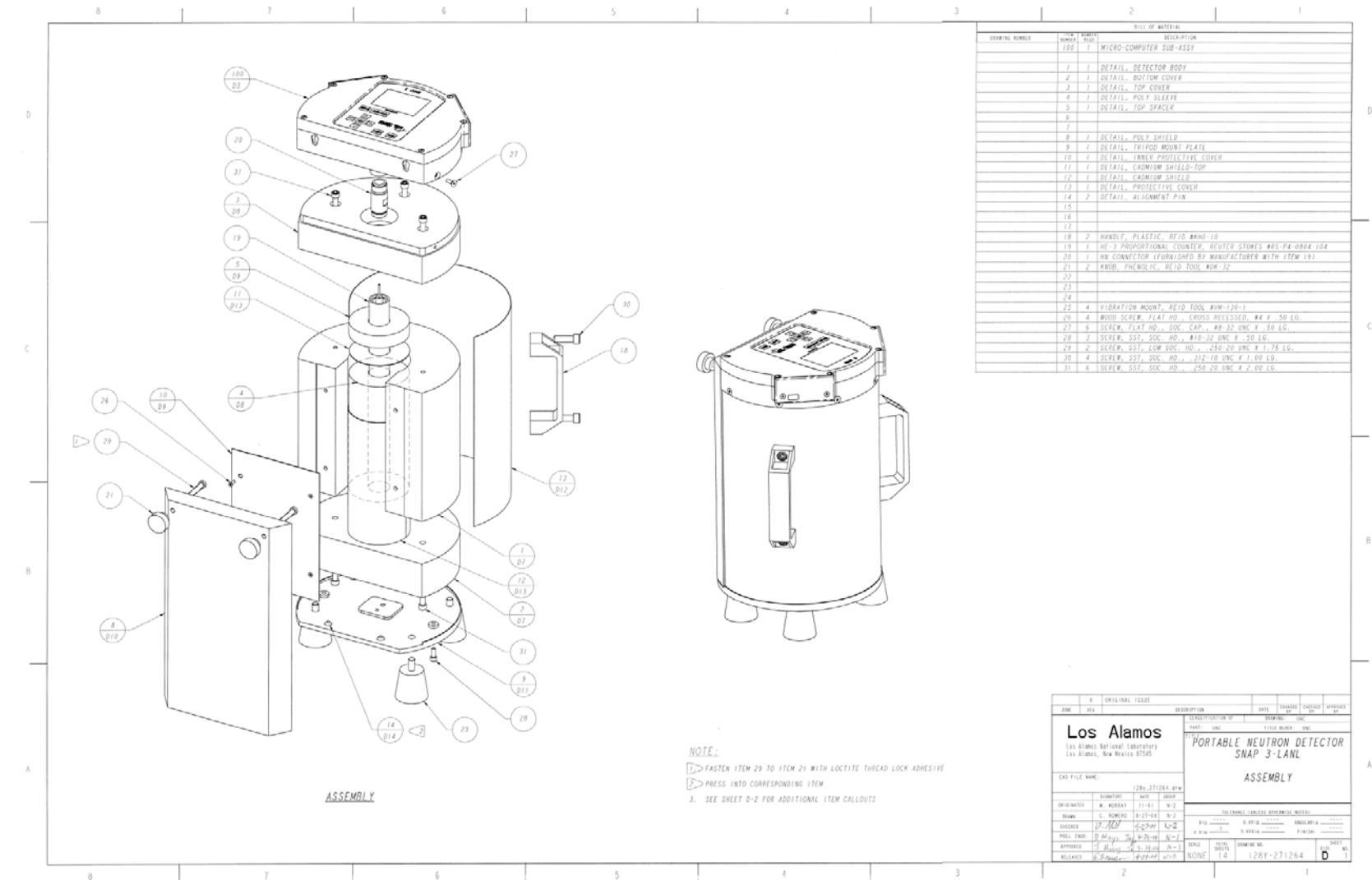
The proportional counter is surrounded by a 1-1/16-inch inside diameter, 3-inch outside diameter, 6-5/8-inch long HDPE annulus that serves as a neutron moderator. This moderator is wrapped in 1/32-inch thick cadmium on its radial surface and on its upper surface.

Outside the neutron absorber is a second annulus of HDPE with a 3-1/8-inch inside diameter and an 8-inch outside diameter that is 7-3/8 inches long. This outer moderator has a front face that is flat; the plane of the flat face is 1-7/8 inches from the axis of the annulus.

Above and below the outer moderator are 1-inch thick HDPE disks; each has a flat face that matches the front face of the outer moderator.

Finally, the SNAP has a 1-inch thick removable HDPE slab on its front face. With the front cover removed, the SNAP preferentially counts slower neutrons; with the cover on, it preferentially counts faster neutrons. All of the HDPE parts have a nominal density of 0.962 g/cm³. The cadmium shield is constructed from cadmium metal with a nominal density of 8.65 g/cm³.

⁵ SNAP-3 stands for shielded neutron assay probe, model 3.



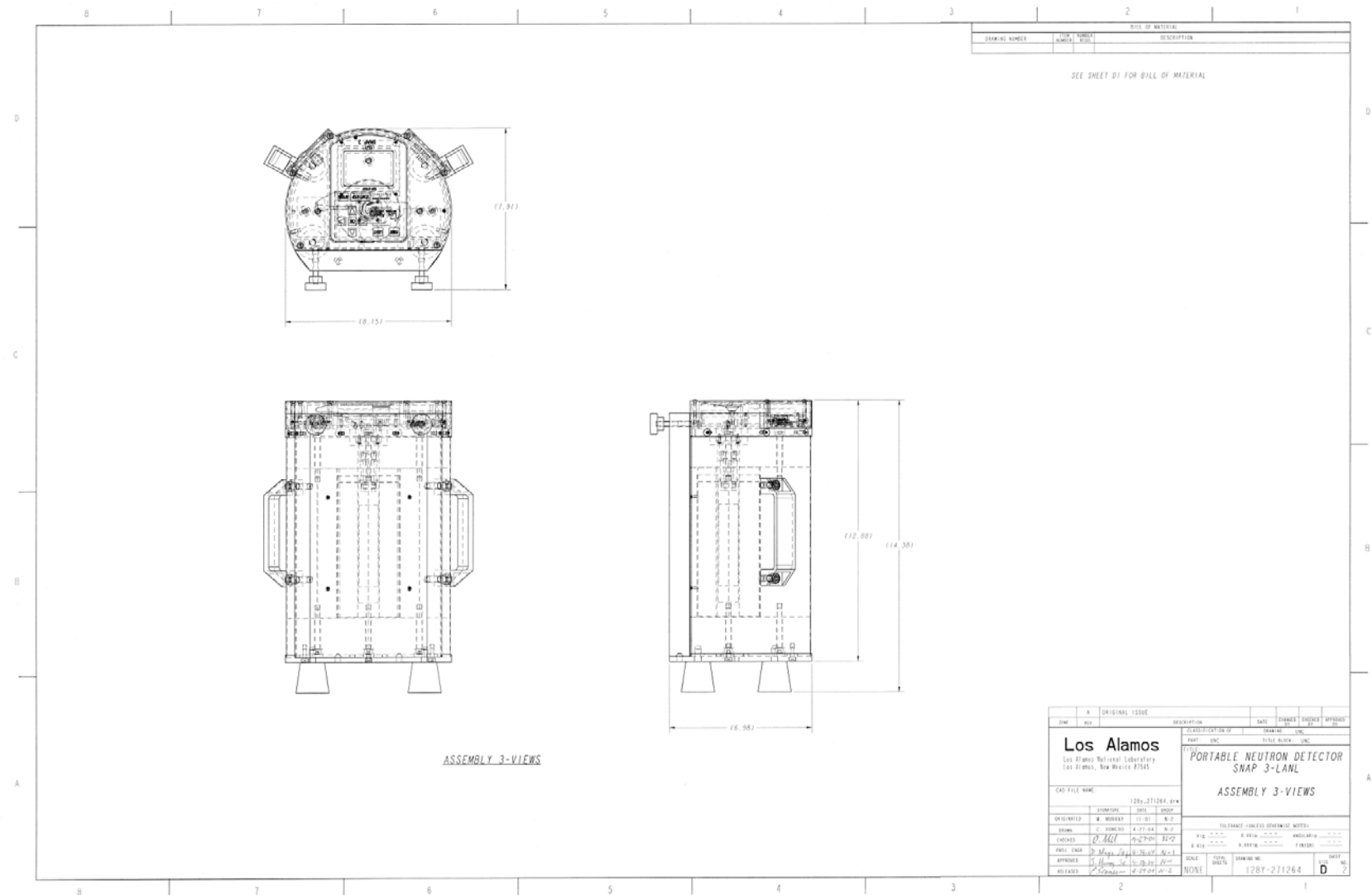


Figure 11: Schematic of the LANL SNAP-3 gross neutron counter showing the assembled instrument; dimensions are in inches

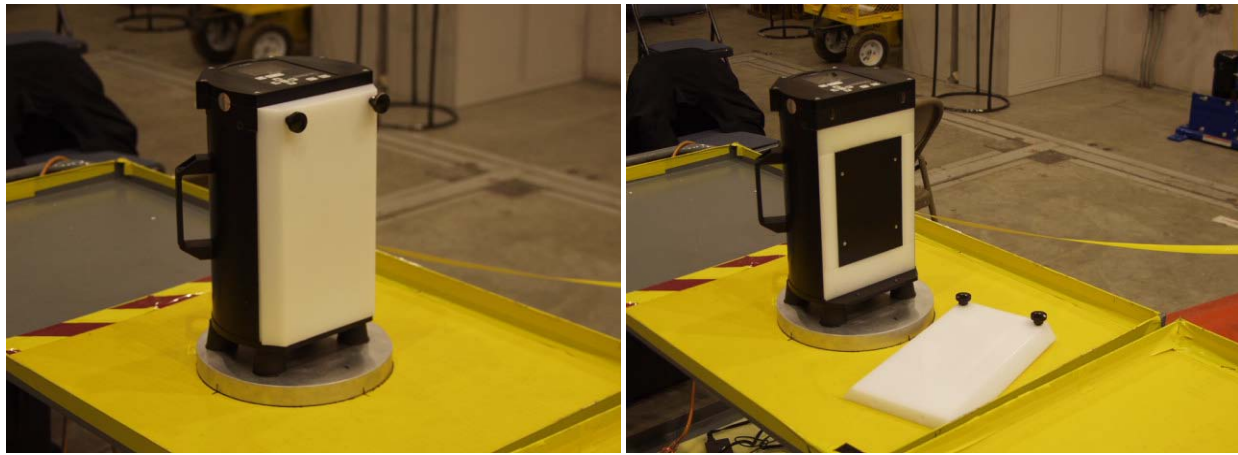


Figure 12: The LANL SNAP gross neutron counter with the front cover on (left) and off (right)

The vertical centerline of the SNAP was aligned with the center of the plutonium source by placing the instrument on the aluminum support stand shown in Figure 13. The SNAP vertical axis was coaxial with the support stand vertical axis.

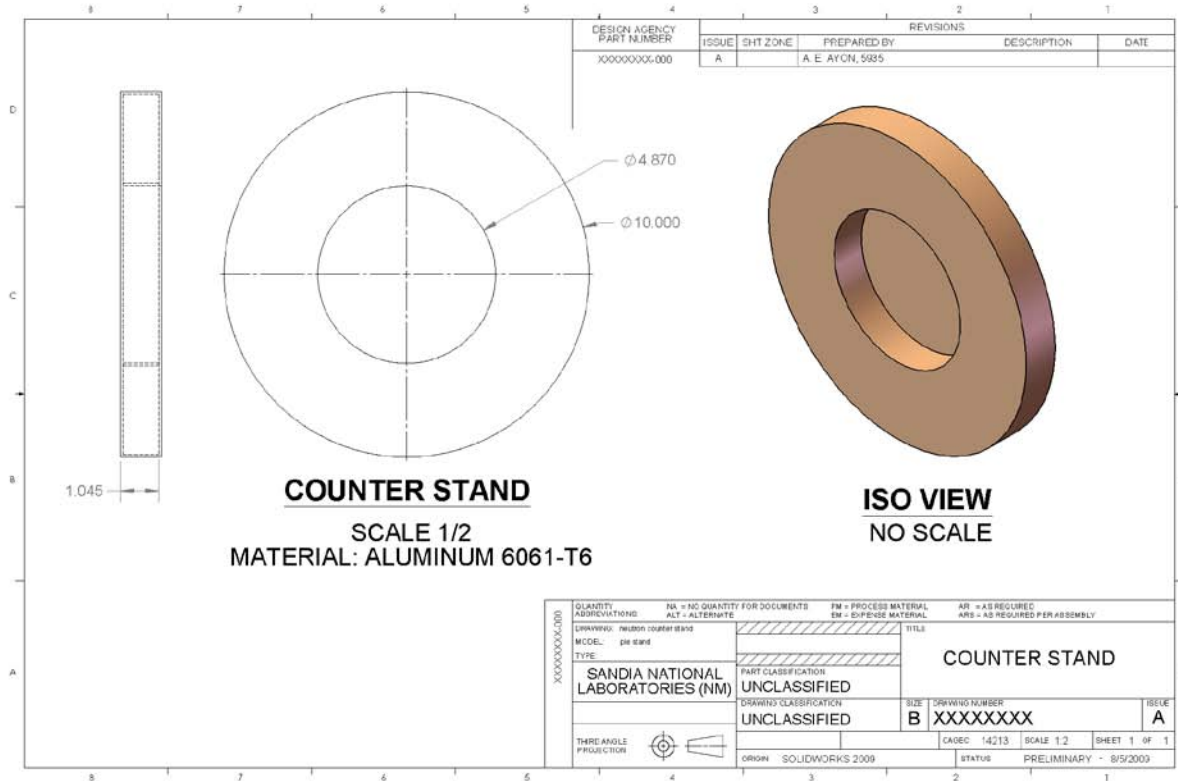


Figure 13: Aluminum support stand used to vertically align the SNAP with the center of the plutonium source; dimensions are in inches

An MCNP model of the SNAP-3 is provided in Appendix C.

4.1.2 Operation

The SNAP was operated using a standard NIM bin counter/timer.⁶ For each reflected configuration of the plutonium source, the SNAP count rate was recorded with the front cover on and off. Counts were typically collected for 300 seconds or more, and most measurements were repeated 3 times. In every case, at least one of those repeated measurements was performed on a different day from the other measurements.

4.2 Neutron Multiplicity Counter

The LANL NPOD-3 was used as a neutron multiplicity counter.⁷ Schematics of the instrument are shown in Figure 14, Figure 15, and Figure 16. A photograph of the instrument is shown in Figure 17. The NPOD used in this series of experiments was serial number 1246/1247.⁸

4.2.1 Description

The NPOD uses 15 1-inch diameter, 15-inch sensitive length helium-3 proportional counters for neutron detection. The counters' fill gas is a mixture of helium-3 with 2% CO₂ as a quench gas. The composition of the fill gas is the same as the composition listed in Table 7 for the SNAP. The partial pressure of helium-3 is 10 atm. Based on the ideal gas law, at 293.6 K the density of the fill gas is 2.55×10^{-4} atoms/b·cm. The proportional counter walls are constructed from 1/32 inch thick aluminum with a nominal density of 2.7 g/cm³.

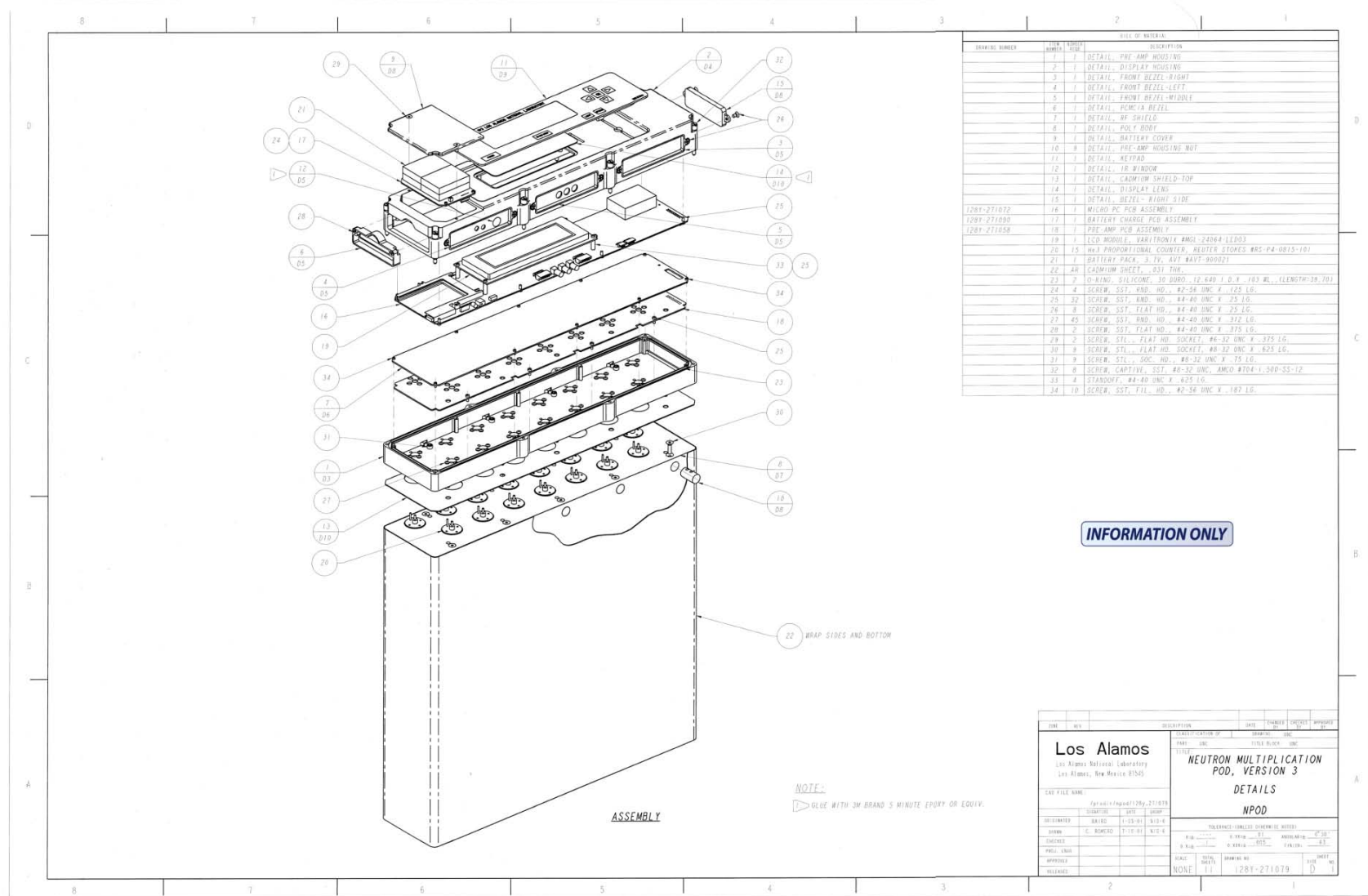
Refer to Figure 16. The proportional counters are embedded in two rows in an HDPE moderator with a nominal density of 0.962 g/cm³. The moderator "block" is 16.6 inches tall, 16-30/32 inches wide, and 4 inches deep. The front row of 8 counters is set 0.75 inch back from the front face of the moderator, and the back row of 7 counters is set 1.6 inches back from the front face of the moderator. The nominal density of the HDPE is 0.962 g/cm³. The moderator is wrapped on all six sides in 1/32-inch thick cadmium metal with a nominal density of 8.65 g/cm³.

Note that the vertical centerline of the NPOD's HDPE moderator block is 8.3 inches above the top of the lower cadmium shield. The aluminum support stands for the plutonium source (described in the preceding section, "Plutonium Source") were designed to place the center of the plutonium source 8.3 inches above the work surface.

⁶ NIM stands for nuclear instrumentation module.

⁷ NPOD-3 stands for neutron pod model 3.

⁸ The first serial number identifies the data acquisition and control box, a.k.a., the "head", and the second serial number identifies the helium-3 proportional counter set.



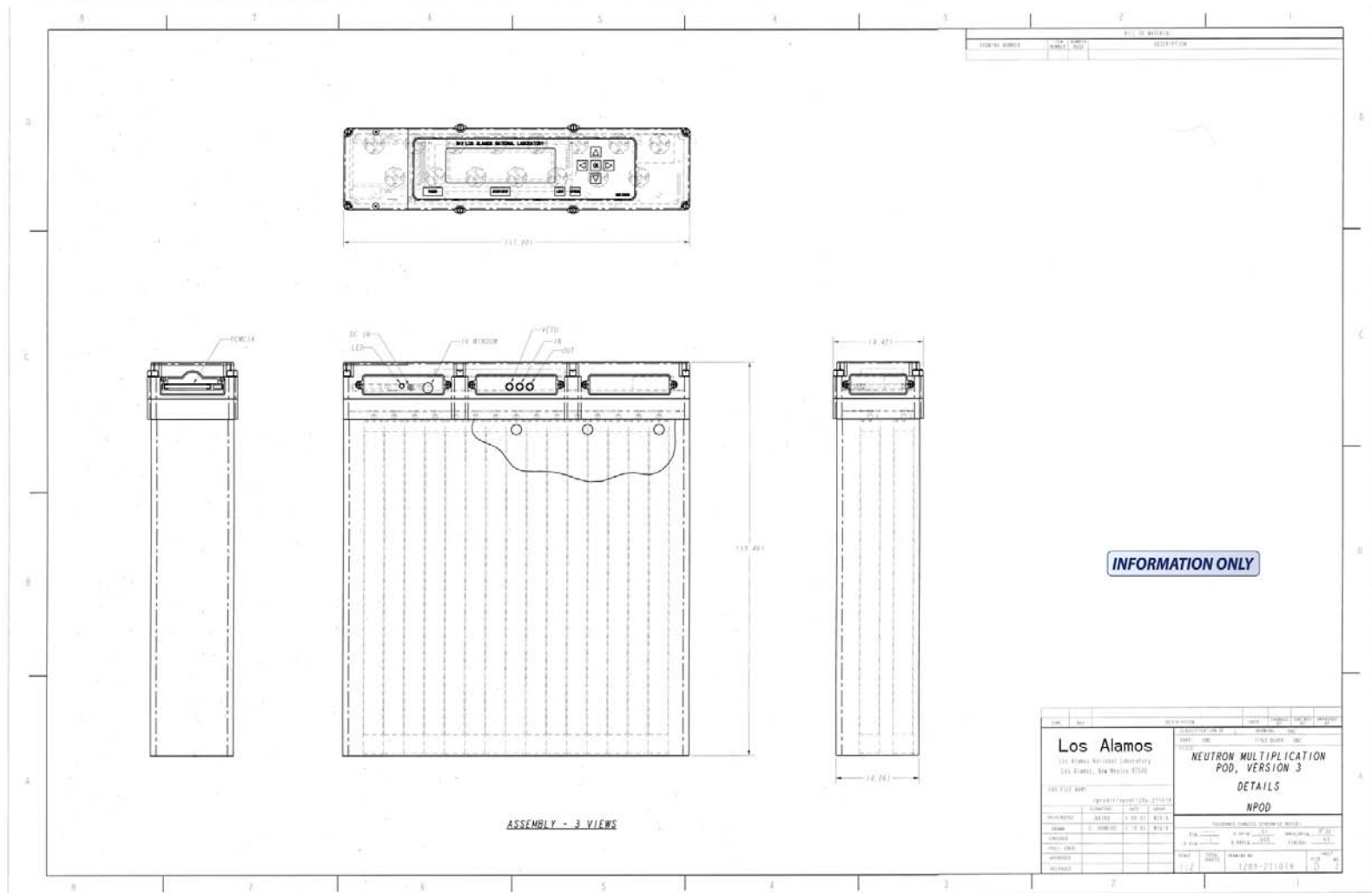


Figure 15: Schematic of the LANL NPOD-3 neutron multiplicity counter showing the assembled instrument; dimensions are in inches

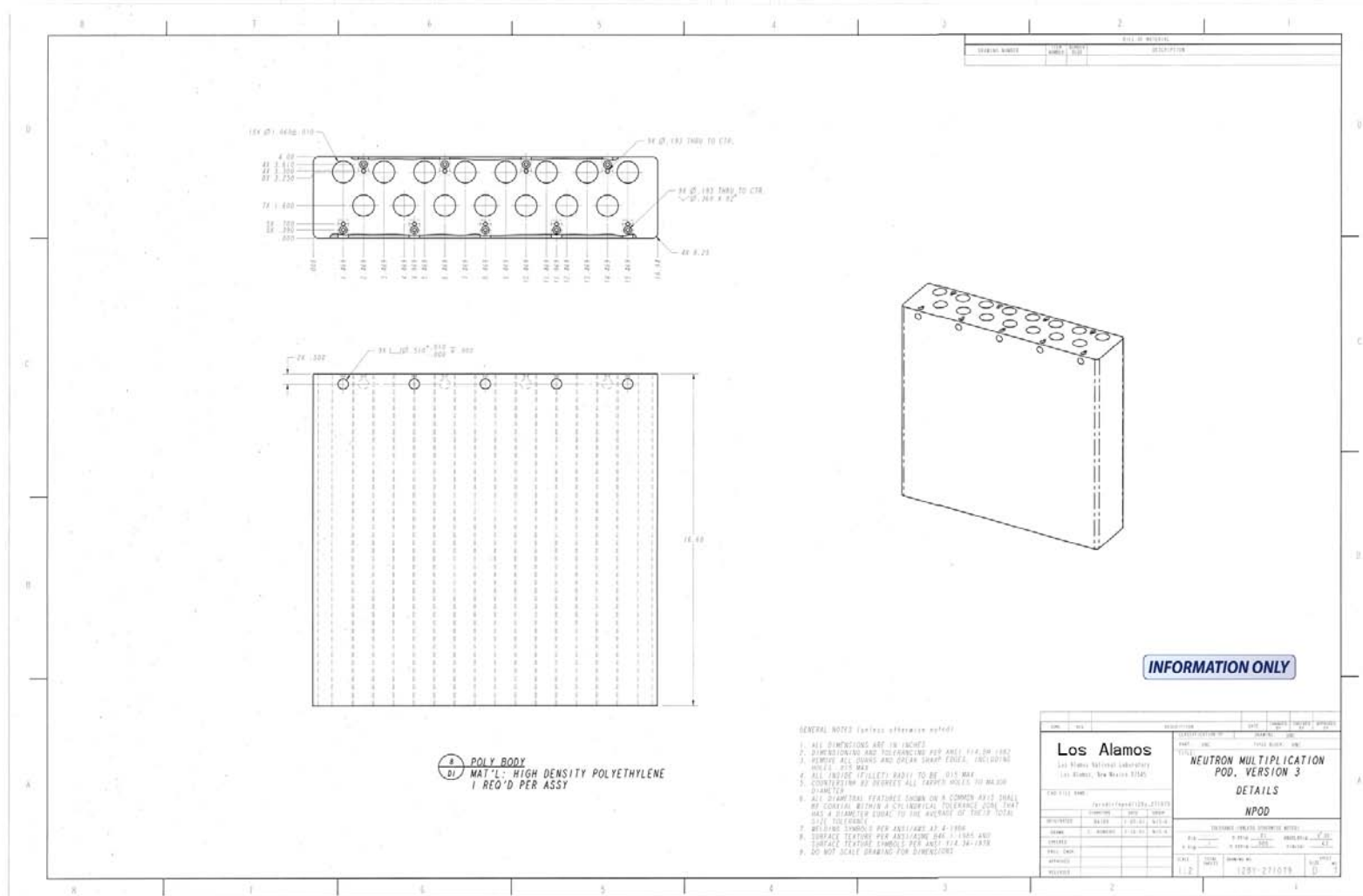


Figure 16: Schematic of the LANL NPOD-3 polyethylene moderator block showing the positioning of the helium-3 proportional counters; all dimensions are in inches

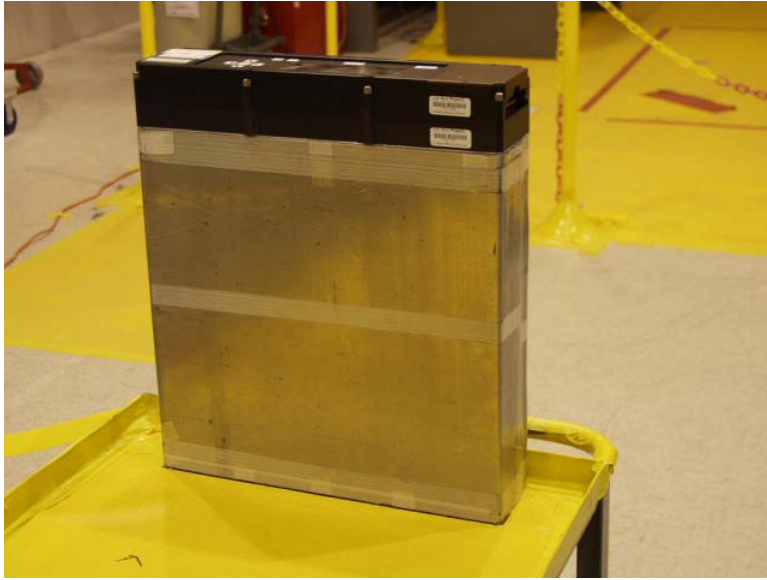


Figure 17: Photograph of the LANL NPOD-3 neutron multiplicity counter

An MCNP model of the NPOD is provided in Appendix D.

4.2.2 Operation

The NPOD data acquisition system records neutron detection events by streaming them to a list-mode file. Each detection event in the file specifies a time-stamp for the event, and it records which of the 15 proportional counters registered a neutron detection. Time-stamps are recorded in one microsecond increments. This mode of data acquisition permits a variety of neutron multiplicity metrics to be accumulated in post-processing. This report focuses on four neutron multiplicity metrics:

- The neutron multiplicity distribution, i.e., the distribution of neutron detection events over the number of coincident events (i.e., the multiplicity of the event) and the width of the coincidence gate
- The neutron count rate, i.e., the mean of the multiplicity distribution
- The Feynman-Y, which is the ratio of the variance in the multiplicity distribution to the mean of the distribution; the Feynman-Y is computed versus coincidence gate width (DeHoffman 1949)
- The Rossi- α , which is the distribution of the number of coincident pairs of events over the time between events

For each reflected configuration of the plutonium source, the NPOD collected between 1.8×10^7 and 4.1×10^7 neutron detection events. These events were collected in three or four repeated measurements for each source configuration, and in every case at least one of those repeated measurements was performed on a different day from the other measurements.

The NPOD streams events to a list-mode file in groups of events referred to as segments. Segments contain 83,168 events. Each event uses a 4-byte unsigned integer to record the number of one-microsecond clock ticks since the beginning of the segment. The clock tick is recorded in “big-endian” order, with the two high-order bytes first and the two low-order bytes second. Each event also uses a 2-byte unsigned integer to record which channels registered a detection. This “channel mask” is

recorded in normal byte order. The high-order bit (bit 16) is a channel reserved for a veto signal. The end of each segment is marked by a single event in which the veto bit is set, and none of the other bits are set.

Nominally, the first event in the file recorded by the NPOD is the beginning of the first segment, and segments are normally terminated by the veto bit every 83,168 events. However, the NPOD firmware exhibits some errors that must be handled by further data processing. This processing includes:

- The first few events in a segment with a clock tick less than 5 microseconds should be discarded.
- The last event in the segment where the veto bit is set should be discarded.
- Sometimes, in two consecutive events, the second event will have a clock tick that is smaller than the preceding event, i.e., there is a “backward clock tick.” In that case, the segment should be terminated at the preceding event, and all events to the end of the segment should be discarded.
- Sometimes, the NPOD will record an event where none of the channel mask bits are set, i.e., there is a “null event.” In that case, the entire segment should be discarded.

In addition, during post-processing and analysis of the data acquired in this experiment, it was observed that occasionally the NPOD will record a segment of very short duration containing very few events, i.e., a “drop-out” in data acquisition was observed. These spurious segments may terminate normally (i.e., by setting the veto bit), or they may terminate with a backwards clock tick or a null event. One measurement exhibiting this behavior is shown in Figure 18. These spurious segments should be discarded.

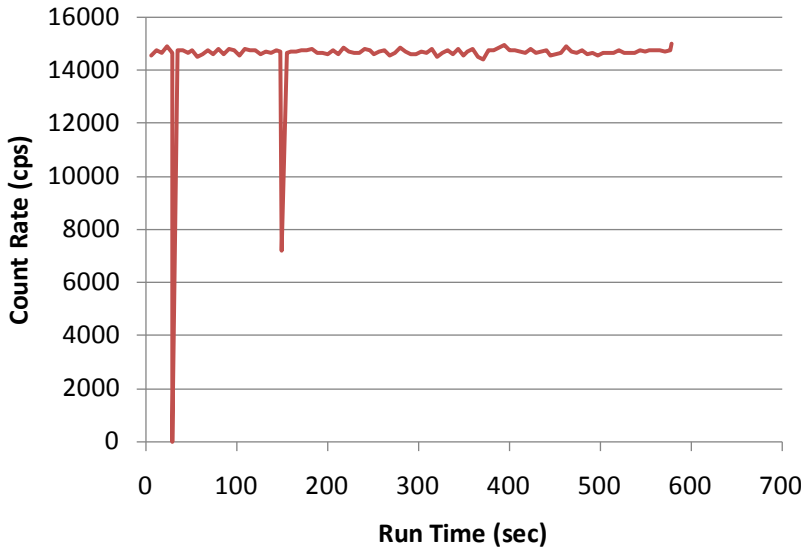


Figure 18: Neutron multiplicity measurement exhibiting “drop-outs” in NPOD data acquisition; the spurious segments should be discarded

Finally, NPOD data acquisition is manually started and stopped by manipulating the controls on the control box. Consequently, at the beginning and end of each measurement, a human body is in close

proximity to the instrument. The presence of this extraneous hydrogenous material can affect neutron interactions observed by the instrument by creating an albedo source of neutrons. Even though the NPOD is designed to be relatively insensitive to thermal neutrons (recall it is wrapped in cadmium), the first and last minute of data acquisition in each measurement should still be discarded.

The preceding logic for processing the measurements was used to accumulate all the neutron multiplicity metrics presented in this report.

4.3 Gamma Spectrometer

A high purity germanium (HPGe) photon detector was used as a gamma spectrometer. Schematics of the instrument are shown in Figure 19 and Figure 20. Photographs of the instrument are shown in Figure 21 and Figure 22. The HPGe detector was an Ortec Model GEM-140195-P-S p-type coaxial detector with a nominal efficiency of 148%.⁹ The detector had a PopTop cryostat and a 3-liter liquid nitrogen (LN₂) dewar.¹⁰ The detector's serial number was 42-TP41172A.

4.3.1 Description

The germanium crystal has a nominal density of 5.33 g/cm³ and is 110.7 mm long and has a diameter of 88.6 mm. The surface of the crystal has a layer of insensitive germanium approximately 700 μ m thick. The crystal is enclosed in a cryostat made of aluminum that has an outside diameter of 108 mm and is 323 mm long. The front face of the cryostat is 1.5 mm thick, and the radial wall of the cryostat is 1.3 mm thick.

The cryostat is attached to an aluminum dewar with an outside diameter of 8-3/4 inches and a length of 10-1/2 inches. The dewar outer walls are nominally 3/32 inches thick. The dewar has an inner vessel that is coaxial with the outer walls. The inner vessel has an outside diameter of 7-3/4 inches and is 14-7/8 inches long. The inner vessel radial wall is nominally 3/32 inch thick, and the two axial walls are nominally 3/16 inches thick. The space between the two vessels is evacuated.

All aluminum components have a nominal density of 2.7 g/cm³.

The dewar was filled with LN₂ daily, which gradually evaporated over the course of time. Typically, the majority of the LN₂ evaporated in a 24-hour period, so in the course of a normal 8-hour work day, the inner vessel contained between 2 and 3 liters of LN₂. The nominal density of LN₂ is 0.81 g/cm³.

The instrument was equipped with a bismuth shield to minimize the detector's response to photon radiation originating from outside its forward field of view. Figure 20 provides a schematic of the shield, and a photograph of the shield is shown in Figure 22. The shield is constructed from an annulus of pure bismuth with a nominal density of 9.78 g/cm³. The annulus has an inside diameter of 4.35 inches, an outside diameter of 6.35 inches, and a length of 6 inches.

The shield also contains a thermal neutron absorber to reduce thermal neutron capture interactions in the germanium. Thermal capture tends to increase the high energy continuum component of the

⁹ 148% is the efficiency for counting 1332 keV photons relative to the efficiency of a 3-inch diameter, 3-inch long sodium iodide detector for the same energy photon.

¹⁰ "PopTop" is Ortec's brand name for a particular cryostat design.

gamma spectrum, which can obscure some weak photopeaks. The absorber is an elastomer composed of silicone (poly dimethyl siloxane $(CH_3)_2SiO$) containing 39% lithium carbonate (Li_2CO_3) by mass. The lithium in the carbonate is 95% lithium-6 by atomic abundance. The composition of the elastomer is listed in Table 8. The density of the elastomers is approximately 1.4 g/cm^3 .

Table 8: Composition of the lithium-6 carbonate/silicone neutron absorber

Constituent	Atomic Abundance	Mass Fraction
H	43.03%	4.97%
Li6	8.96%	6.18%
Li7	0.47%	0.38%
C	19.06%	26.25%
O	21.31%	39.11%
Si	7.17%	23.10%

This neutron absorber is wrapped around the outer radial surface of the bismuth annulus, and a disk of the elastomer is placed over the front face of the annulus. The thickness of the elastomer is $1/8$ inch, and the diameter of the front elastomer disk is 6.60 inches.

The outermost layer of the shield is constructed of tin, which serves to attenuate low energy gammas and X rays. This tin filter is 0.05 inches thick. The tin is wrapped around the outer radial surface of the neutron absorber, and a disk of tin is placed on the front face of the shield, outside the neutron absorber. The diameter of the tin disk is 6.70 inches.

The central axis of the HPGe detector was approximately aligned with the center of the plutonium source by placing the detector on a support pad of two-pound polyurethane ($C_{25}H_{42}N_2O_6$) foam.¹¹ The density of the foam is 0.026 g/cm^3 . The foam support was $13\text{-}1/2$ inches wide, $19\text{-}7/8$ inches long, and 2 inches thick. This support placed the central axis of the HPGe detector 6.5 inches above the work surface.

¹¹ Two-pound foam has a nominal density of approximately 2 lb/ft^3 .

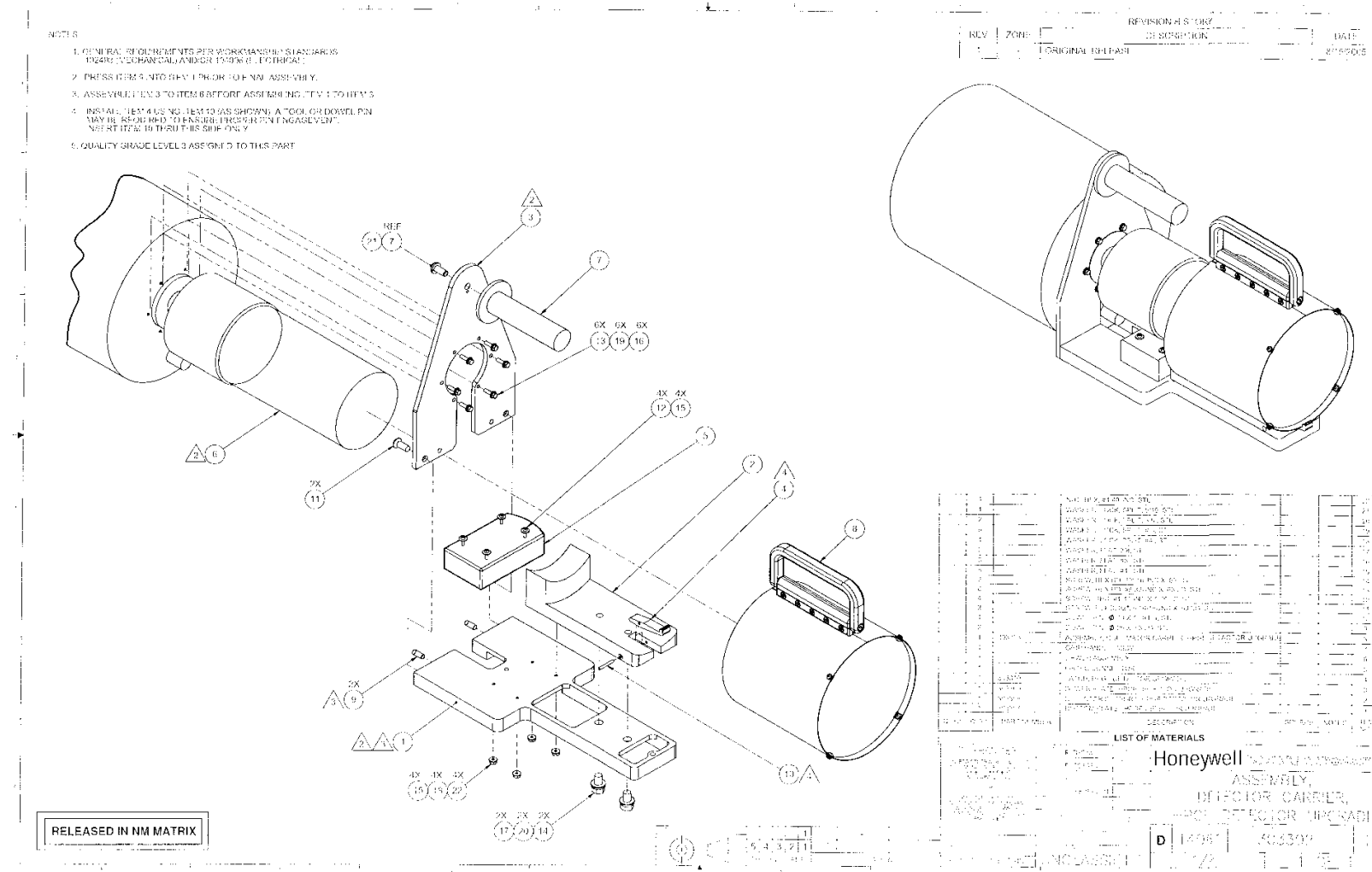


Figure 19: Schematic of the HPGe gamma spectrometer showing the assembly of the instrument's components

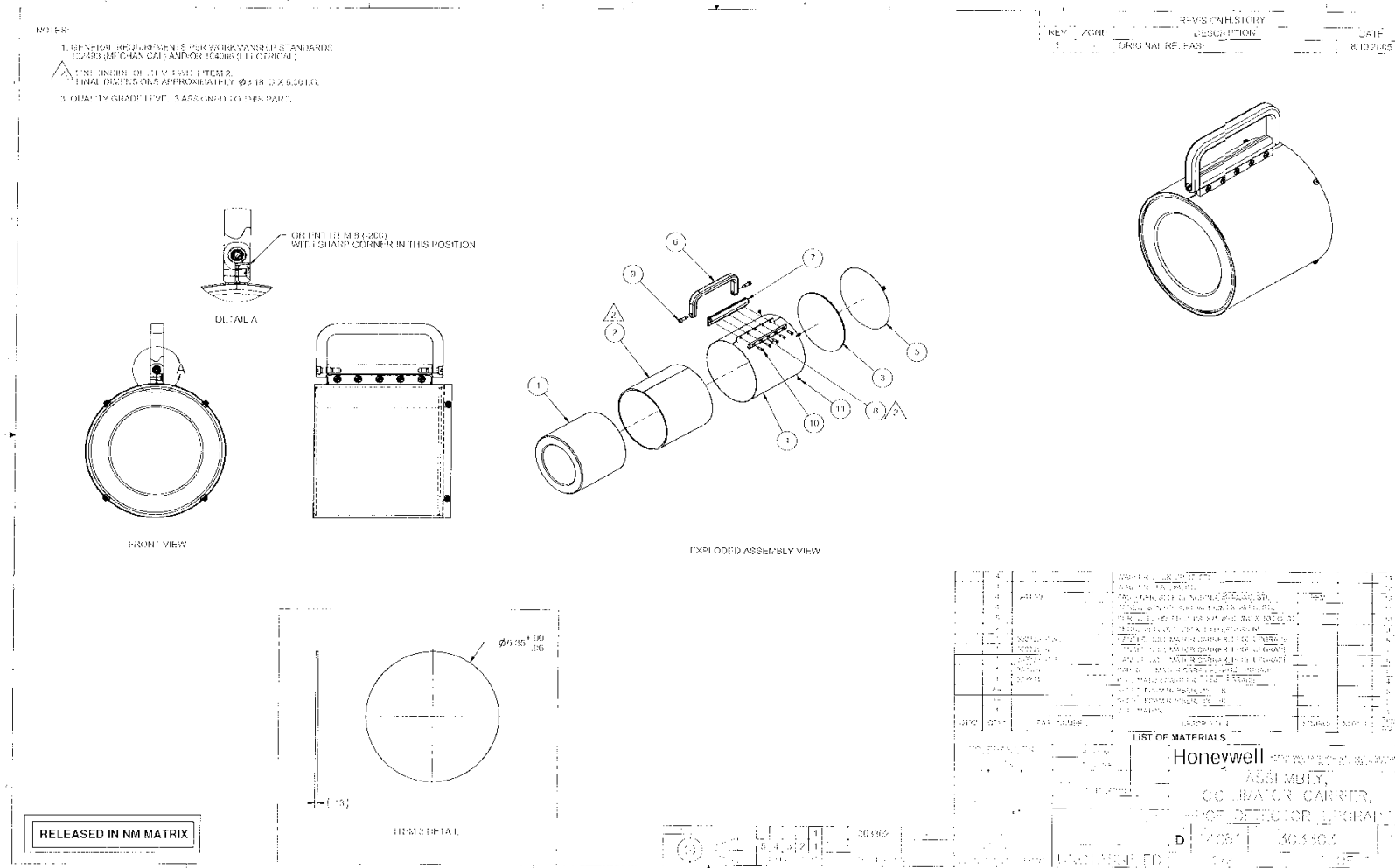


Figure 20: Schematic of the bismuth shield showing the assembly of the shield's subcomponents; dimensions are in inches

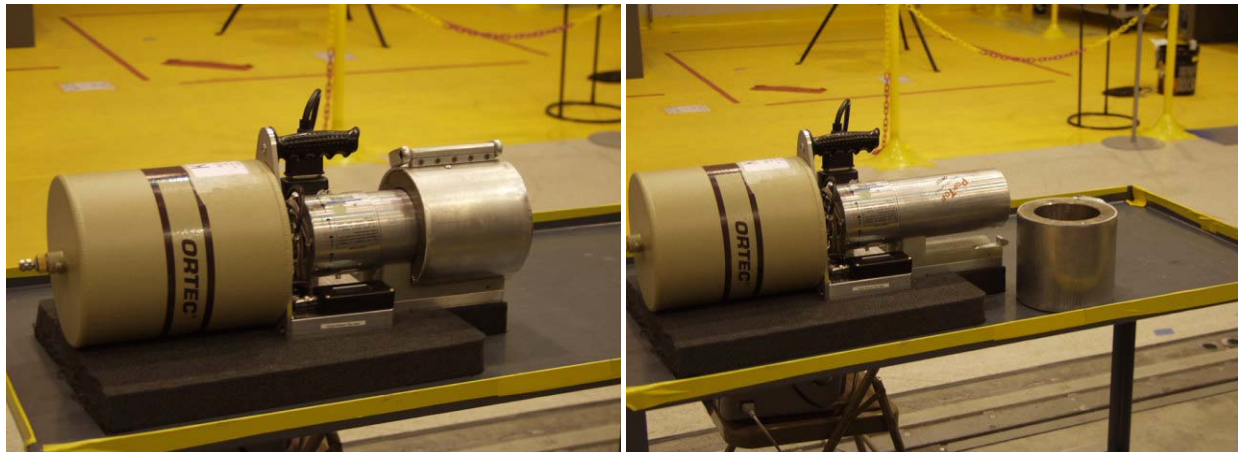


Figure 21: Photographs of the HPGe gamma spectrometer with the bismuth shield on (left) and off (right)



Figure 22: Photograph of the bismuth shield

An MCNP model of the HPGe detector is provided in Appendix E.

4.3.2 Operation

Gamma spectra were acquired using an Ortec DigiDart multichannel analyzer (MCA). The MCA was controlled using custom software developed by LANL. All spectra were saved in Ortec's floating point ".chn" format. Gamma spectra were collected for 10-minute, 20-minute, and 60-minute dwell times. For a given reflected configuration of the plutonium source, typically all gamma spectra were collected either on the same day or on consecutive days.

5 Instrument Configuration

For each reflected configuration of the plutonium source, the three instruments were positioned as illustrated by Figure 23. Figure 24 is a photograph of one of the measurements showing the positioning of the instruments.

Dimensioned views of the instrument configuration are shown in Figure 25 and Figure 26. The distance from the front face of the SNAP (with the cover on) to the center of the plutonium source was 1 meter. The distance from the cadmium front face of the NPOD to the plutonium source was 0.5 meter. The distance from the tin front face of the HPGe shield to the plutonium source was 2 meters.

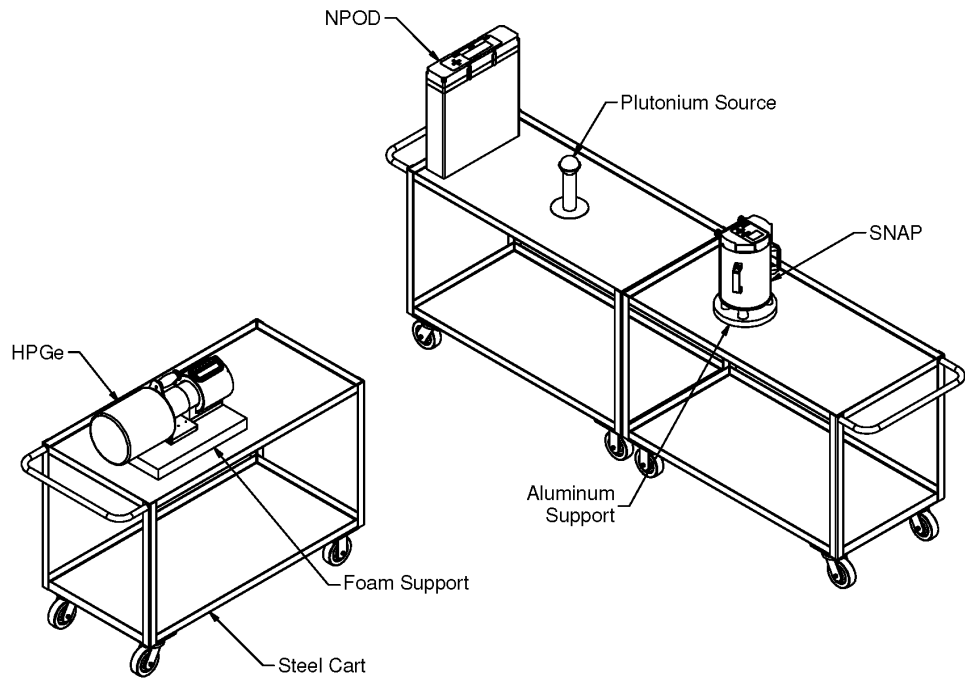


Figure 23: Schematic illustrating the positioning of the instruments relative to the plutonium source

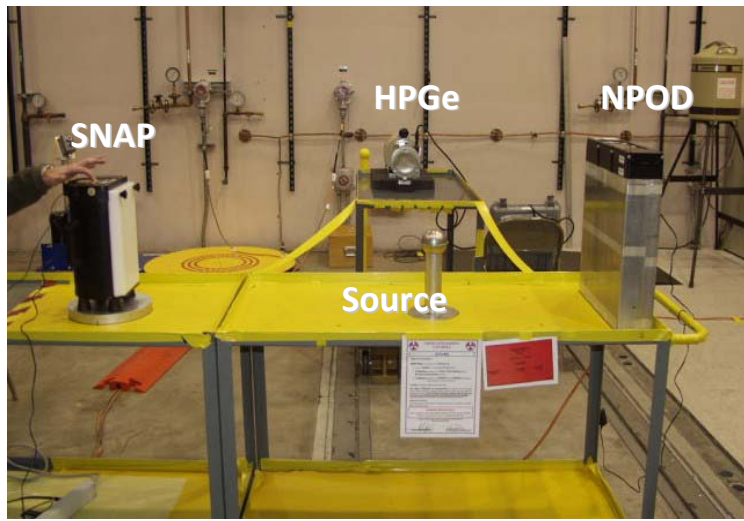


Figure 24: Photograph showing the positioning of the instruments relative to the plutonium source

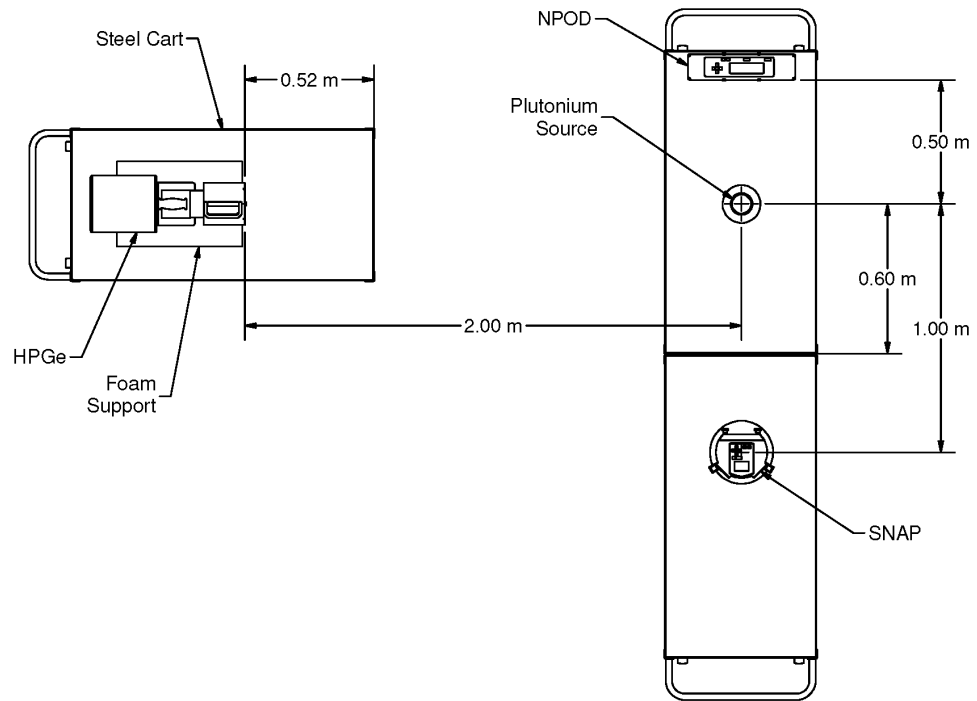


Figure 25: Plan view showing the positions of the instruments relative to the plutonium source

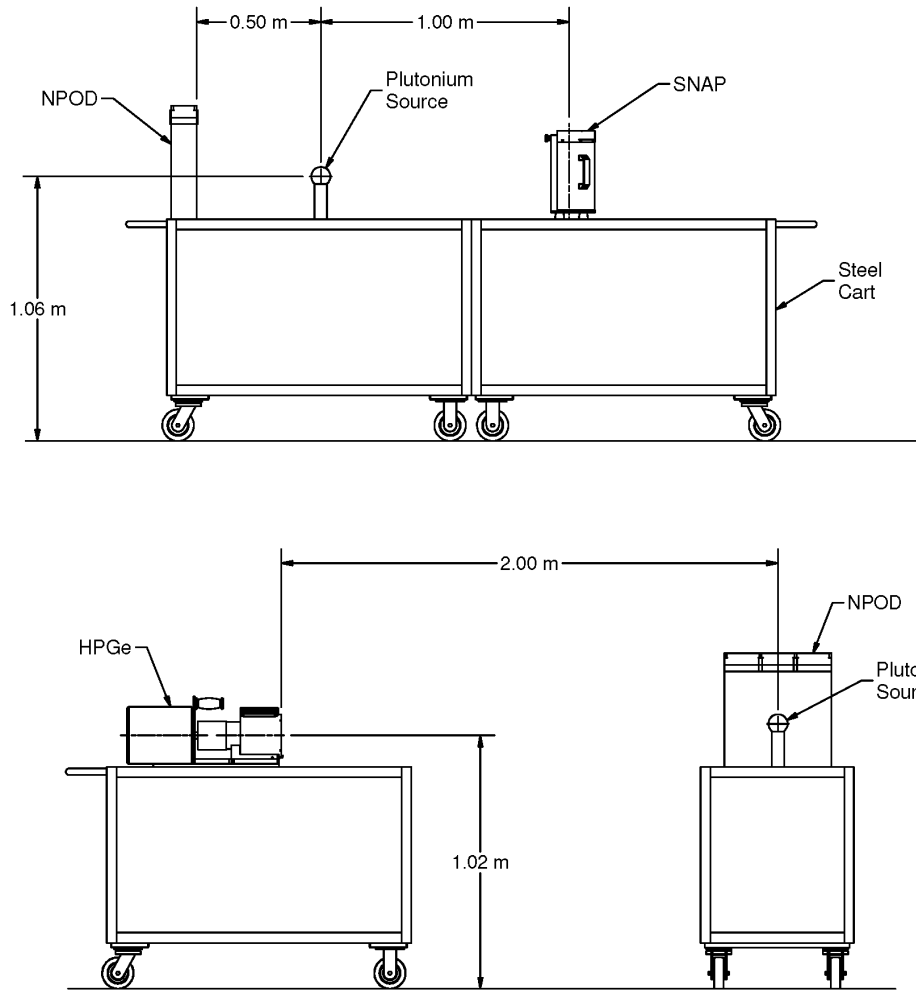


Figure 26: Elevation views showing the positions of the instruments relative to the plutonium source and the floor

Three steel carts were used as the work surfaces. All three carts were of identical construction. A schematic showing the cart construction is provided in Figure 27. The carts are made of carbon steel, which is 99.5% iron and 0.5% carbon by mass, with a nominal density of 7.82 g/cm^3 . Each cart has an upper and lower shelf constructed of 12-gauge steel, which is nominally 0.1046 inches thick. Both shelves are 24 inches wide by 48 inches long. The distance between the shelves is 25 inches. Each shelf has a 1.5-inch tall vertical lip that is also constructed of 12-gauge steel. Each cart has four 3/16" thick legs constructed from angle brackets. Each side of the angle bracket is 1-1/2 inches wide, and each leg is 25 inches long. Each cart has four 5-inch diameter polyurethane wheels. The distance from the top of the upper shelf's lip to the floor is 35 inches. Consequently, the distance from the floor to the center of the plutonium source is 41.8 inches.

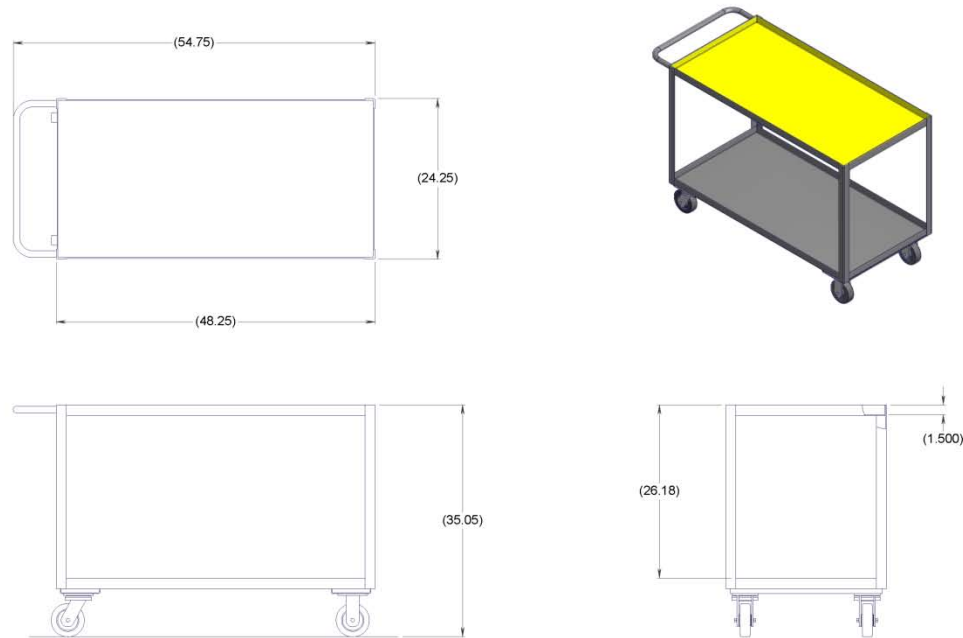


Figure 27: Schematic of the steel cart used as a work surface; three identical carts were used

The floor was constructed of concrete approximately 30 inches thick. The space below the floor was empty for approximately 16 feet. Figure 28 is a diagram showing the placement of the source relative to the walls. As shown, the source was positioned in the center of the room with the nearest two walls 15 feet from the center of the source. The other walls were more than 20 feet from the source. The ceiling was over 30 feet from the center of the source. The exact thicknesses of the walls and ceiling are unknown; it is only known they are more than 30 inches thick. Also, the exact composition of the concrete is unknown. The room is underground, so thick compacted soil is exterior to the walls. The roof is overlaid with thick gravel.

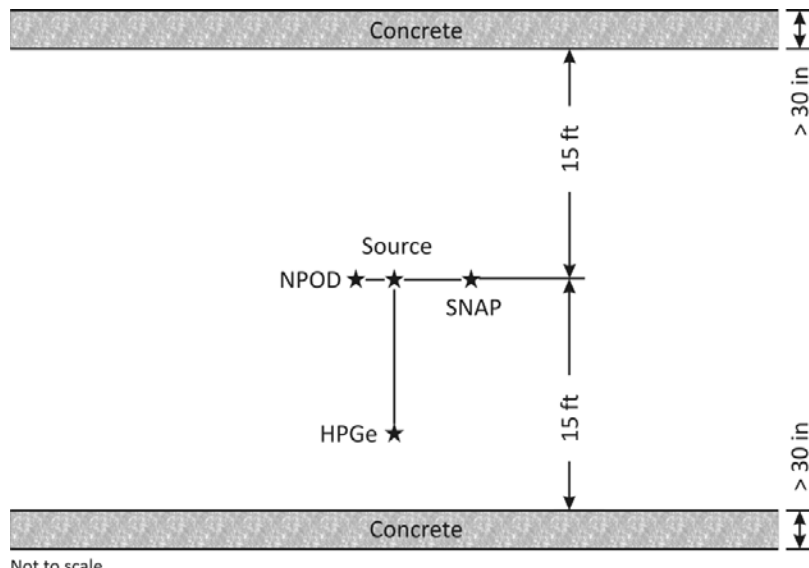


Figure 28: Diagram showing the position of the plutonium source relative to the two nearest walls; the other walls (not shown) were more than 20 feet away from the source

In addition to the preceding instrument configuration, gamma spectrometry measurements were also performed with the gross neutron counter and the neutron multiplicity counter removed (the positioning of the plutonium source and gamma spectrometer were unchanged). These measurements were performed to assess the effect of the neutron instruments on the measured gamma spectrum. In particular, it was expected that the presence of the neutron multiplicity counter, which contains a large polyethylene moderator, would significantly enhance the 2223 keV photopeak resulting from thermal neutron capture in hydrogen.

6 Instrument Calibration

Before commencing the subcritical measurements of the reflected plutonium source, each instrument was calibrated in-situ using radionuclide sources with known activity. The photon response of the gamma spectrometer was measured using four gamma sources. The response of the gross neutron counter and the neutron multiplicity counter, and the neutron response of the gamma spectrometer were measured using a spontaneous fission neutron source in bare and moderated configurations.

These measurements can be used to

- Characterize each instrument's energy-dependent response function for use in point models of the instruments.
- Confirm the accuracy of the calculated response for three dimensional radiation transport models of the instruments.

6.1 Neutron Calibration Source and Moderators

The neutron calibration source was a Frontier Technology Corporation Model 10S sealed californium source; the source's serial number is FTC-CF-2641. A schematic illustrating the source's construction is shown in Figure 29. The source capsule is a cylinder with an outside diameter between 0.217 and 0.218 inches. The capsule is 0.975 inches long.¹²

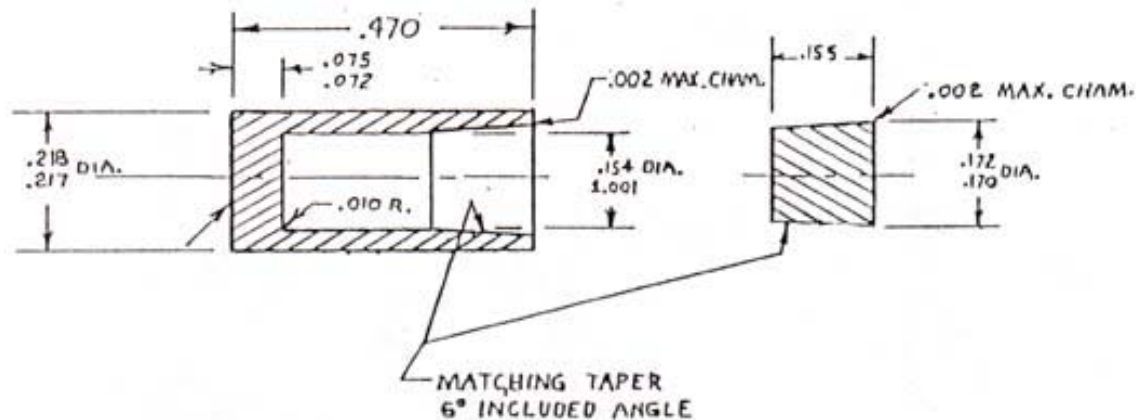


Figure 29: Schematic showing the construction of the californium neutron calibration source; all dimensions are in inches

¹² This schematic of the californium source was obtained from Frontier Technology's product website; see <http://www.frontiertechcorp-cf252.com/sers10.htm>.

The source is primarily composed of californium-252, but it does contain several other californium isotopes. The composition of the source on 9 June 2003 is listed in Table 9; at that time, the californium-252 mass was 0.401 μg (the activity was 215 μCi), and the total neutron emission rate (including neutrons from the spontaneous fission of californium-250) was 9.275×10^5 neutrons per second.

Table 9: Initial composition of the californium neutron calibration source on 9 June 2003

Constituent	Atomic Abundance
Cf249	3.411%
Cf250	8.702%
Cf251	2.600%
Cf252	85.273%
Cf253	0.004%
Cf254	0.001%

Table 10 lists the composition of the source on 6 January 2009, the first day of this series of experiments (note that the californium-253 and -254 constituents have decayed away). On that date, the californium-252 mass was 0.093 μg (the activity was 49.9 μCi). The total neutron emission rate, including spontaneous fission neutrons from californium-250, was 2.151×10^5 neutrons per second.

Table 10: Composition of the californium neutron calibration source on 6 January 2009

Constituent	Atomic Abundance
Cf249	8.985%
Cf250	18.032%
Cf251	6.888%
Cf252	66.094%

The californium source was measured bare and in the four spherical shell moderators shown in Figure 30 through Figure 33. These schematics also show the aluminum support stands that position the californium source at the same height as the plutonium source.

The aluminum source holder that positions the californium source at the center of each moderator is shown in Figure 34. Note that each source holder attaches to its corresponding moderator from the moderator's outer radius. Each moderator has a 13/16 inch diameter through-hole on the top half to permit the source holder to pass through the moderator. Figure 34 also shows the aluminum source holder for the bare source. All of the aluminum parts have the same composition as listed in Table 6.

The first three moderators are constructed from HDPE. The last moderator was constructed from borated polyethylene, i.e., HDPE mixed with 28.6% boric acid (H_3BO_3) by mass. The boron has natural isotopic composition. The composition of the borated polyethylene is listed in Table 11. The calculated density of each moderator is listed in Table 12.

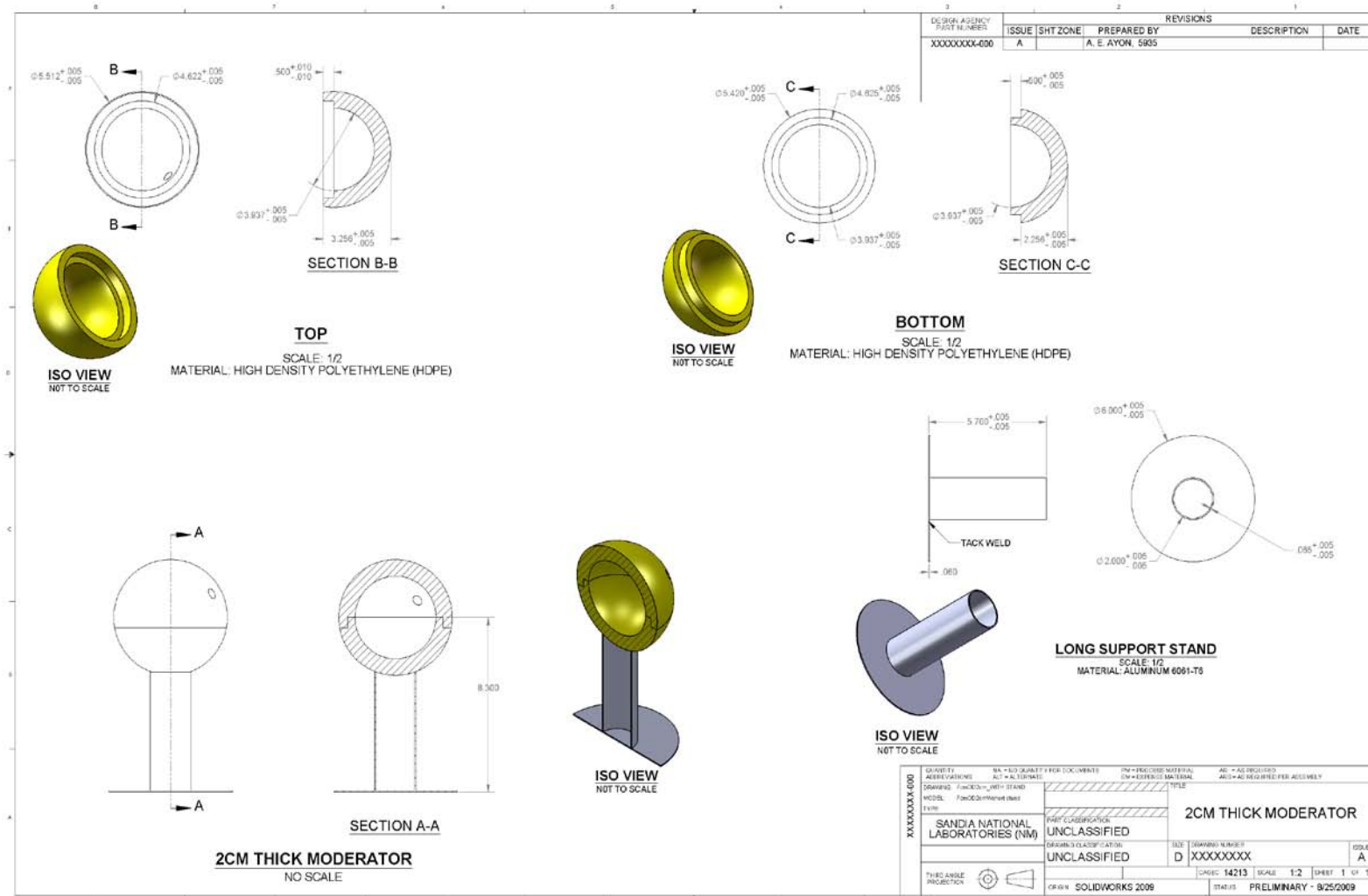


Figure 30: 2-cm thick HDPE neutron moderator and aluminum support stand; dimensions are in inches

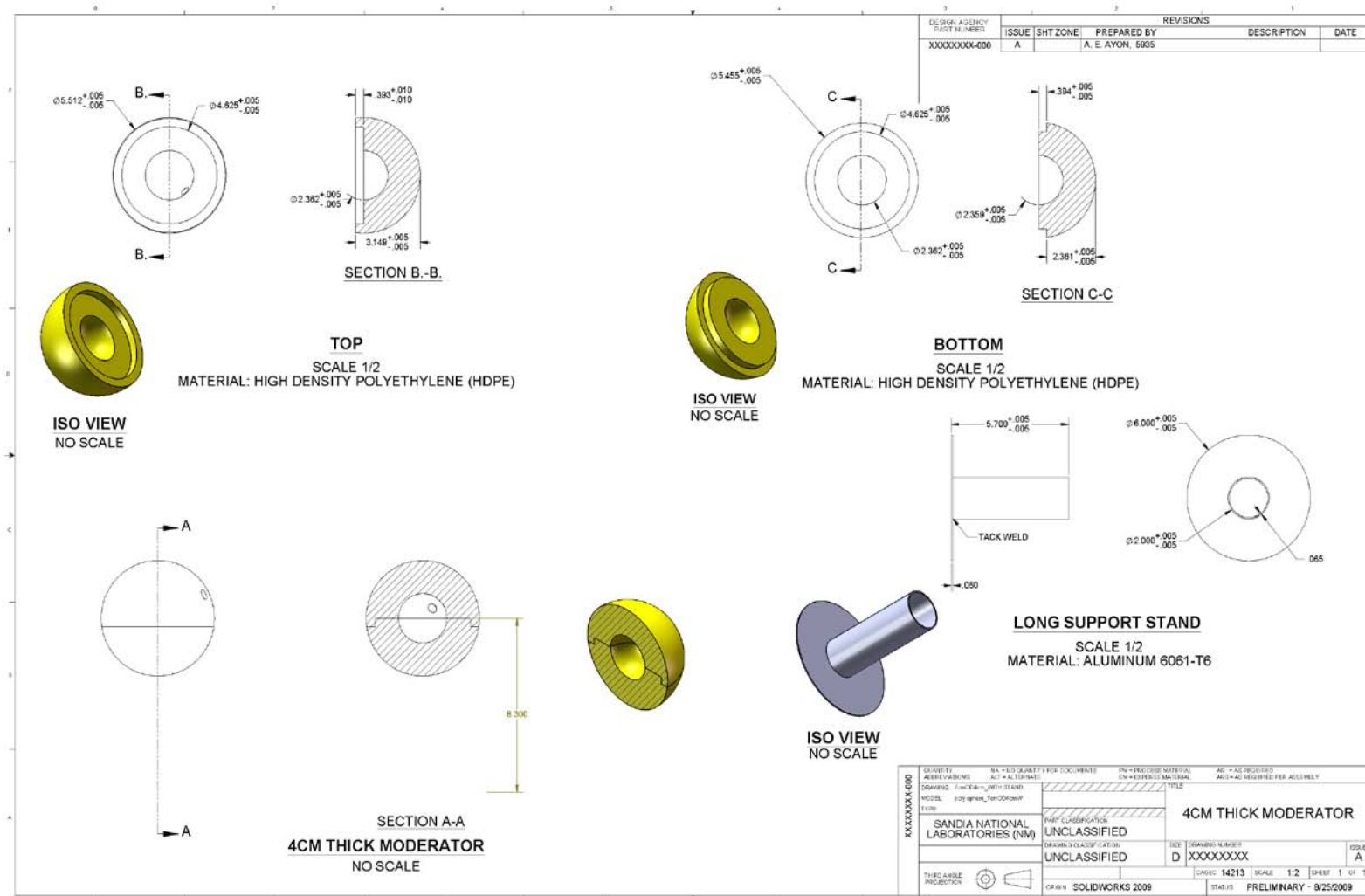


Figure 31: 4-cm thick HDPE neutron moderator and aluminum support stand; dimensions are in inches

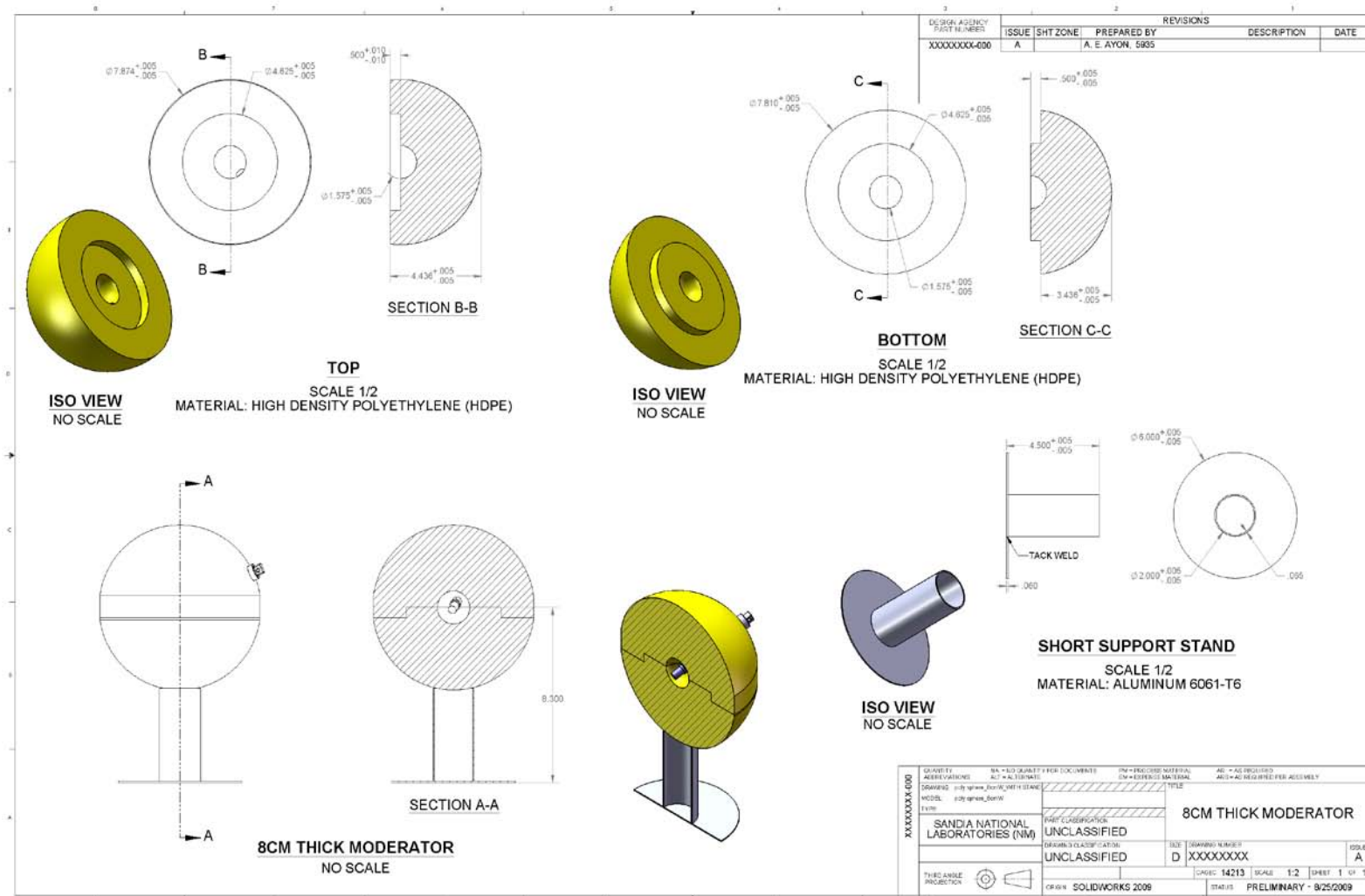


Figure 32: 8-cm thick HDPE neutron moderator and aluminum support stand; dimensions are in inches

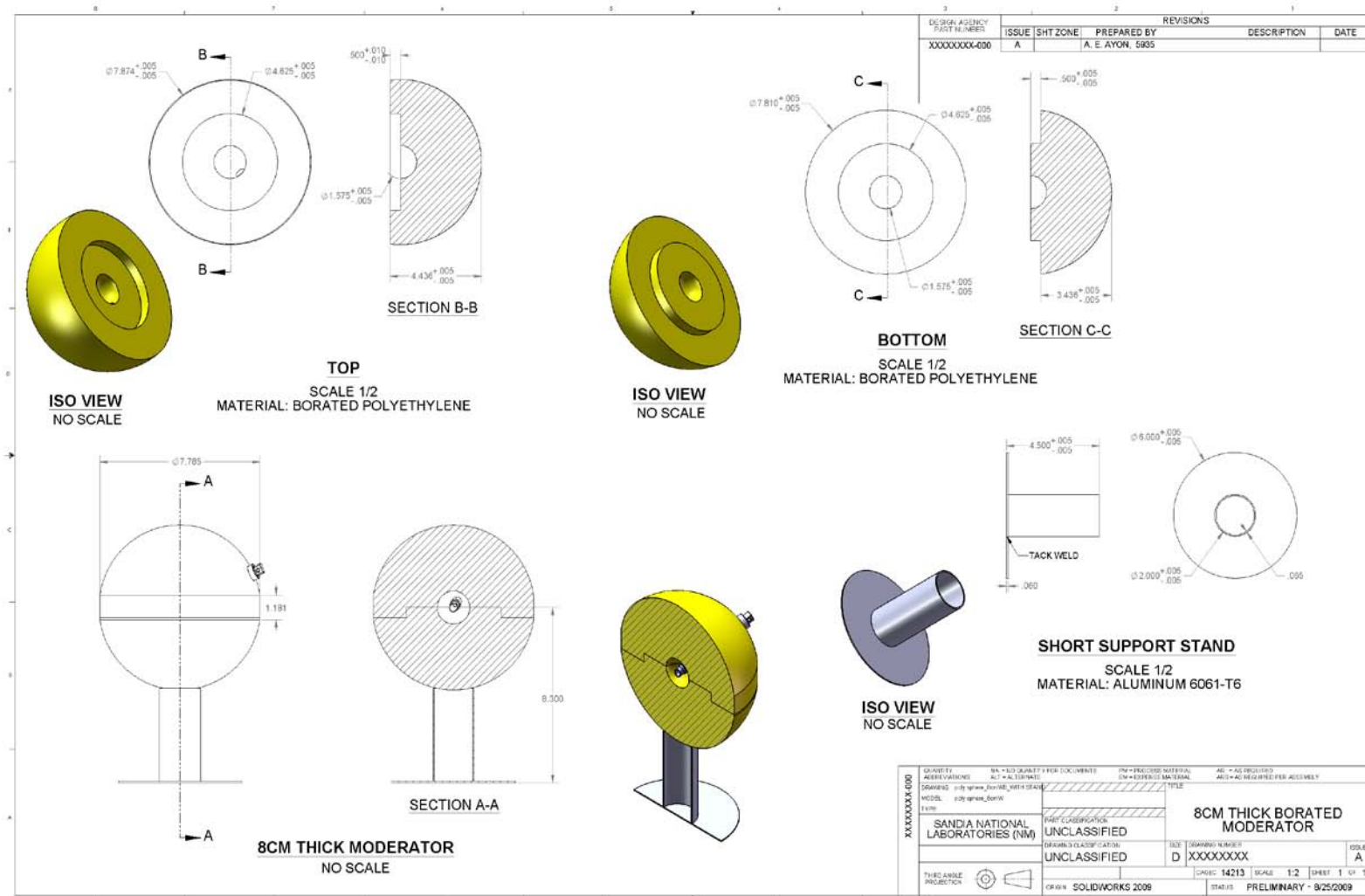


Figure 33: 8-cm thick borated polyethylene neutron moderator and aluminum support stand; dimensions are in inches

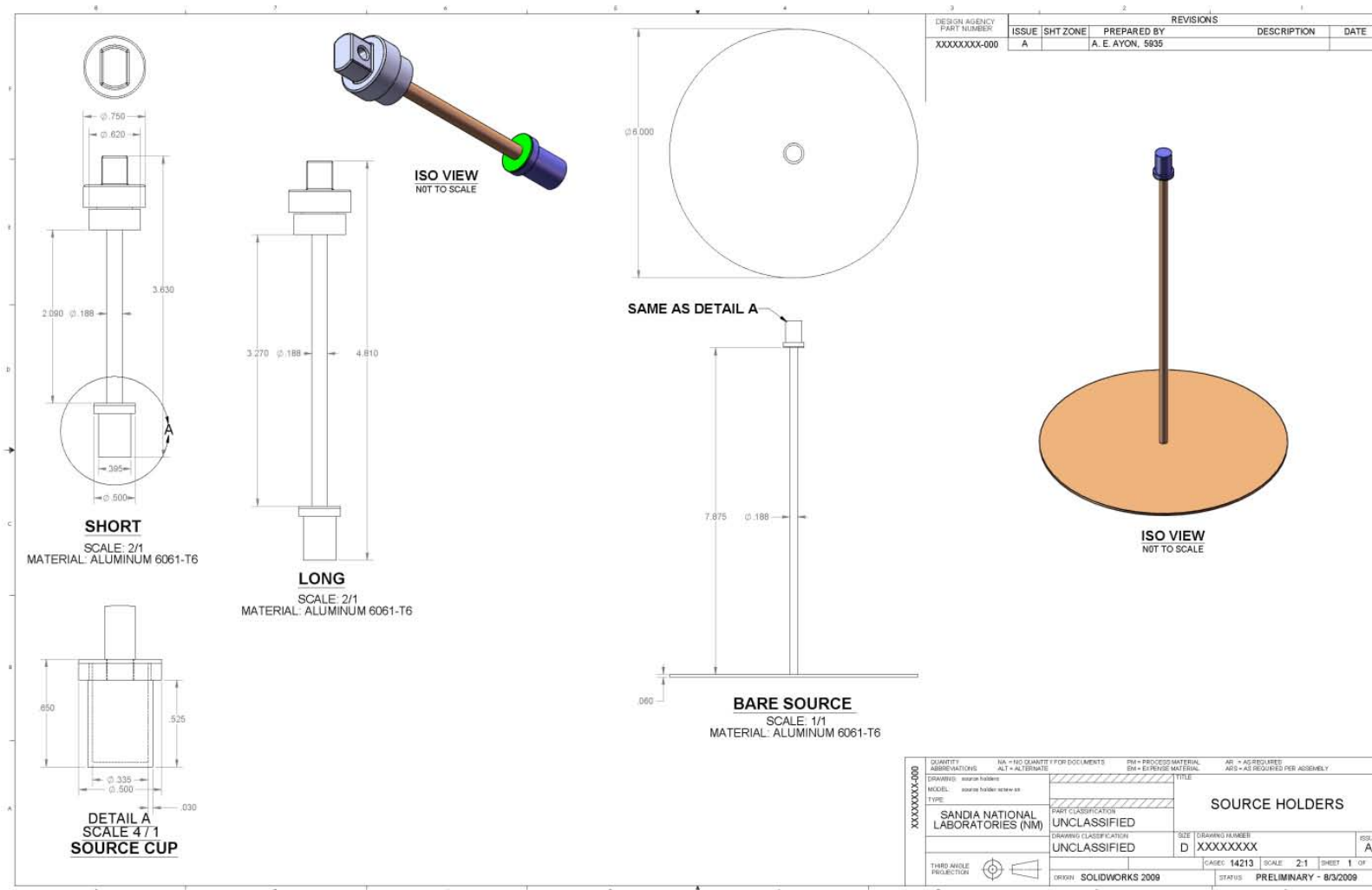


Figure 34: Aluminum source holders for the 14-cm diameter moderators, the 20-cm diameter moderators, and the bare californium calibration source; dimensions are in inches

Table 11: Composition of the borated polyethylene neutron moderator

Constituent	Mass Fraction
H	62.5%
B10	0.5%
B11	2.0%
C	27.5%
O	7.5%

Table 12: Measured mass, calculated volume, and calculated density of each neutron moderator

Moderator	Measured Mass (g)	Calculated Volume (cm ³)	Calculated Density (g/cm ³)
2 cm HDPE	847.9	906.5	0.935
4 cm HDPE	1257.1	1310.3	0.959
8 cm HDPE	3949.7	4128.5	0.957
8 cm borated polyethylene	3851.2	4112.3	0.937

Note that as Figure 33 shows, the borated polyethylene moderator was not perfectly spherical. This was the result of an error the manufacturer made when ordering the material for the moderator. The stock used was too short for the outside diameter of the sphere. Consequently, the moderator is an oblate spheroid with a band of missing material around its equator. The band is approximately 1.2 inches tall and 0.04 inches thick.

For each calibration measurement, the neutron source was placed in the same position as the plutonium source, and the instruments were positioned exactly as described in the preceding section, "Instrument Configuration". The neutron response of the gamma spectrometer was also measured with the gross neutron counter and neutron multiplicity counter removed.

6.2 Gross Neutron Counter Calibration

Individual measurements collected to calibrate the neutron response of the SNAP are listed in Table 13. Table 14 and Figure 35 show the instrument's count rate versus californium source moderation.

Note that the neutron count rate for the borated polyethylene moderator was higher than it was for the same thickness of pure HDPE. The boron does tend to absorb neutrons, but it preferentially absorbs slower neutrons, and the SNAP is relatively insensitive to thermal neutrons. Furthermore, the boric acid mixed with the polyethylene in the borated moderator displaces some of the moderator's hydrogen content. Consequently, the hydrogen density (as well as the overall density) of the borated moderator is lower than it is in the pure HDPE moderator.

Table 13: Gross neutron counter calibration measurements

Front Cover On?	Moderator	Count Time (sec)	Counts
Yes	None	900	10878
	2 cm HDPE	900	9483
	4 cm HDPE	900	7445
	8 cm HDPE	900	4056
	8 cm borated polyethylene	900	5001
No	None	300	4192
	2 cm HDPE	300	5250
	4 cm HDPE	300	4067
	8 cm HDPE	300	2396
	8 cm borated polyethylene	300	2851

Table 14: Gross neutron counter count rate versus californium source moderation; uncertainties represent one standard deviation

Moderator	Front Cover On		Front Cover Off	
	Count Rate (cps)	Uncertainty (cps)	Count Rate (cps)	Uncertainty (cps)
None	12.1	0.1	14.0	0.2
2 cm HDPE	10.5	0.1	17.5	0.2
4 cm HDPE	8.3	0.1	13.6	0.2
8 cm HDPE	4.5	0.1	8.0	0.2
8 cm borated polyethylene	5.6	0.1	9.5	0.2

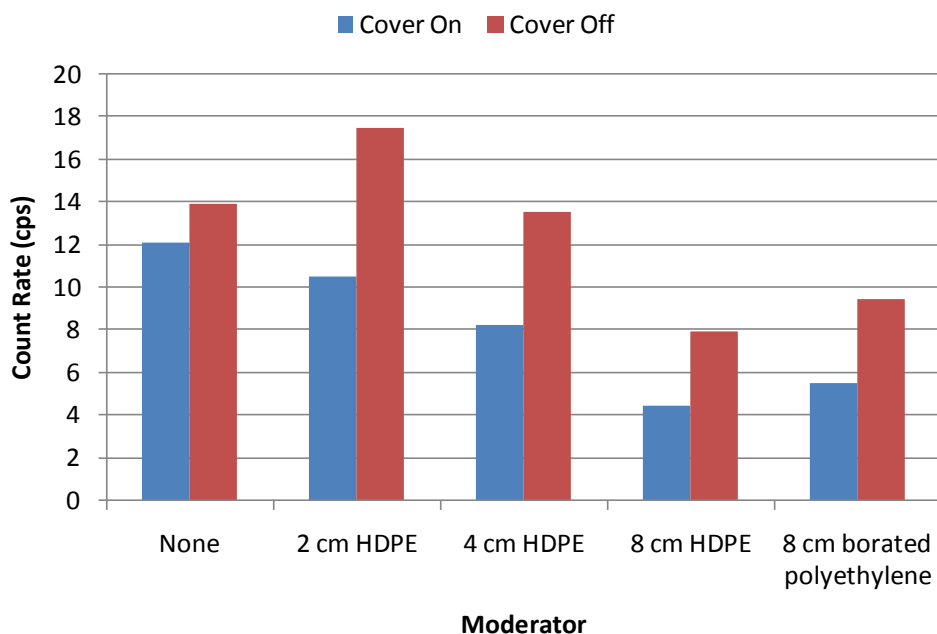


Figure 35: Gross neutron counter count rate versus californium source moderation

An overnight background measurement was also collected using the SNAP. For a 200,000 second count time, only 269 counts were collected. This neutron background rate of 0.0013 counts per second is low enough to be neglected.

6.3 Neutron Multiplicity Counter Calibration

Individual measurements collected to calibrate the neutron response of the NPOD are listed in Table 15.¹³ The run time and the number of counts collected are listed in Table 16.

¹³ The NPOD control software creates files using the naming convention “yyMMddnn.dat” where “yy” is the two-digit year, “MM” is the two-digit month, “dd” is the two-digit day, and “nn” is a two-digit run number that is automatically incremented.

Table 17 and Figure 36 show the instrument's count rate versus californium source moderation.

As was observed during calibration of the SNAP, the neutron count rate in the NPOD was higher for the borated polyethylene moderator than it was for the same thickness of HDPE. This behavior is due to the lower hydrogen content of the borated moderator and the fact that the NPOD is designed to be relatively insensitive to thermal neutrons.

Table 15: Neutron multiplicity counter calibration measurements

Moderator	Segments	File
None	50	09010644.dat
2 cm HDPE	47	09010646.dat
4 cm HDPE	45	09010648.dat
8 cm HDPE	25	09010649.dat
8 cm borated polyethylene	31	09010651.dat

Table 16: Neutron multiplicity counter run time and number of counts collected versus californium source moderation

Moderator	Run Time (sec)	Counts
None	1822.646	3745747
2 cm HDPE	1583.985	3496135
4 cm HDPE	1702.912	3412559
8 cm HDPE	1604.674	1830196
8 cm borated polyethylene	1705.079	2329652

Table 17: Neutron multiplicity counter count rate versus californium source moderation; uncertainties represent one standard deviation

Moderator	Count Rate (cps)	Uncertainty (cps)
None	2055.1	1.1
2 cm HDPE	2207.2	1.2
4 cm HDPE	2004.0	1.1
8 cm HDPE	1140.5	0.8
8 cm borated polyethylene	1366.3	0.9

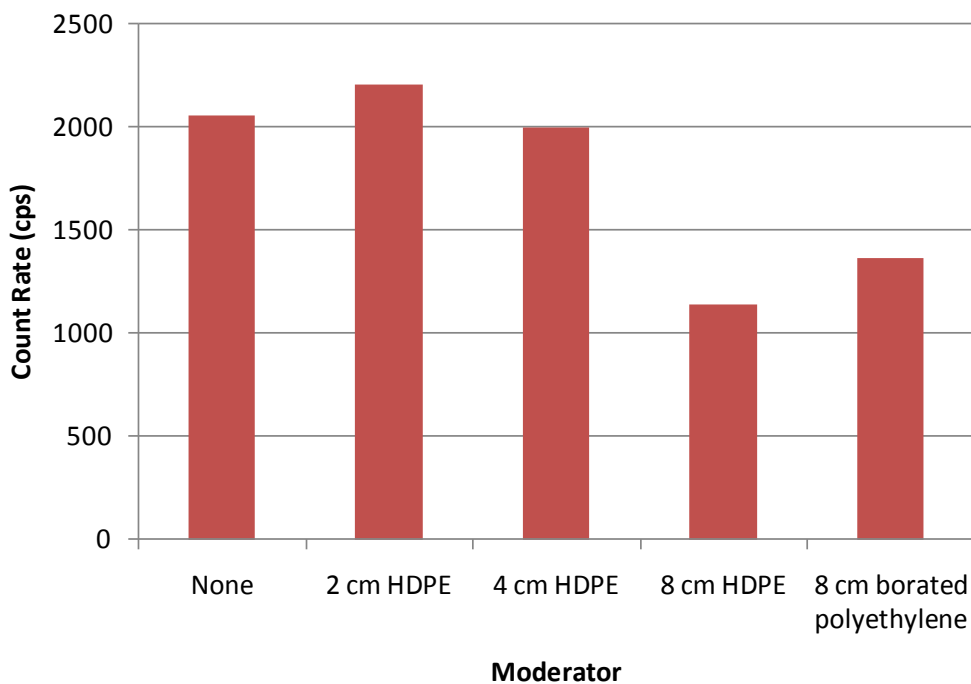


Figure 36: Neutron multiplicity counter count rate versus californium source moderation

These calibration measurements were also used to confirm the correct operation of the NPOD. For a bare spontaneous fission source, the measured neutron multiplicity distribution should be very close to a Poisson distribution.¹⁴ As Figure 37 shows, the multiplicity distribution measured for the bare californium source exhibits a very small excess variance:

$$Y = \frac{\sigma^2}{\mu} - 1 \quad (1)$$

where

- μ is the mean of the distribution (the first moment)
- σ^2 is the variance of the distribution (the second central moment)
- Y is the excess variance; for a Poisson distribution, Y vanishes

¹⁴ The multiplicity distribution is only exactly Poisson for a source that emits only one neutron per decay, e.g., an (α, n) source like americium-beryllium. Such a source was unavailable for this series of experiments.

For the measurement shown in Figure 37, the excess variance Y is only 0.027. If it were substantially larger, such that the measured distribution was much wider than a Poisson distribution, or if it were negative, such that the measured distribution was much narrower, then that would indicate that the NPOD was malfunctioning. It should also be noted the same behavior was observed for each source moderator: the measured multiplicity distribution exhibited a small excess variance relative to a Poisson distribution.

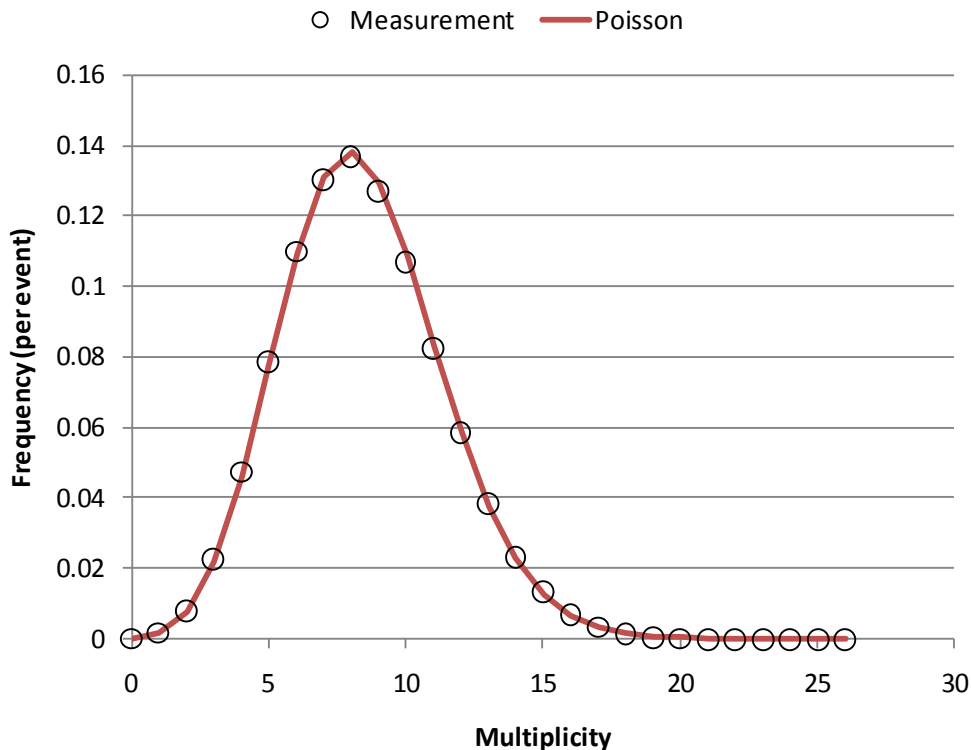


Figure 37: Neutron multiplicity distribution measured for the bare californium source; the coincidence gate width was 4096 μ s

In addition, these calibration measurements were used to characterize the neutron slowing-down time in the NPOD. For a bare spontaneous fission source, the Rossi- α distribution should approximately conform to

$$R \approx Ae^{-\lambda\tau} + B \quad (2)$$

where

- R is the Rossi- α distribution, i.e., the distribution of pairs of coincident events over the time-delay between them
- τ is the time-delay between two coincidence events
- λ is the effective time constant for the multiplicity counter, dictated primarily by the time required for neutrons to slow to thermal speeds
- A is the rate of real coincidence for simultaneous events (a time-delay of zero)
- B is the rate of accidental coincidence

For the measurement shown in Figure 38, the time constant λ is $39.6 \mu\text{s}$. The first ten microseconds of the measured Rossi- α distribution were neglected because they do not conform to equation (2) due to dead-time in the NPOD. It should also be noted that the same behavior was observed for each source moderator: the measured Rossi- α distribution exhibited a time-constant of approximately $40 \mu\text{s}$.

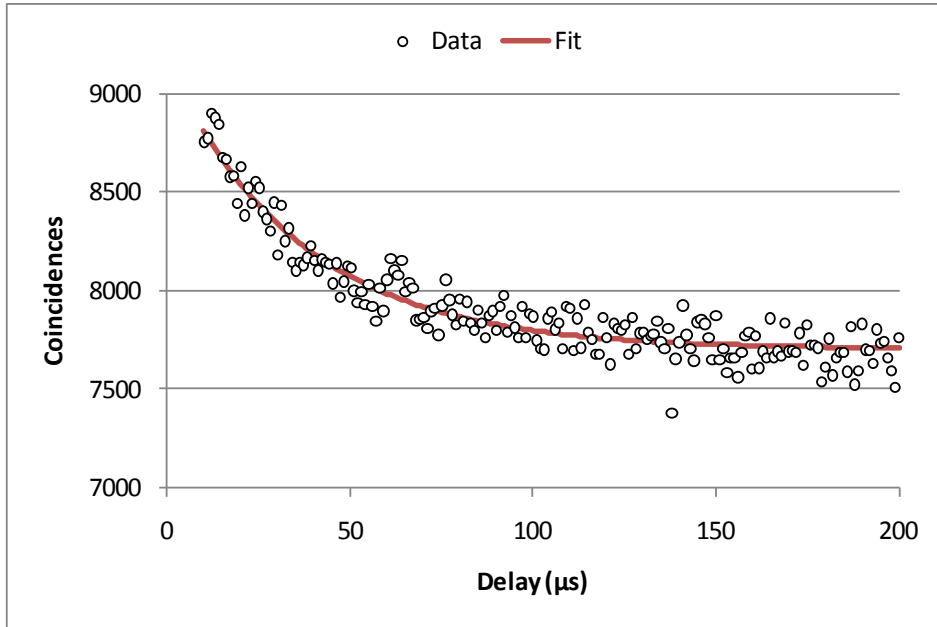


Figure 38: Rossi- α distribution measured for the bare californium source

No background measurements were collected using the NPOD. The instrument's data acquisition and control logic automatically shut it down if the count rate falls below a preset low threshold. However, this indicates that the neutron background rate is low enough to be neglected.

6.4 Gamma Spectrometer Neutron Response Calibration

Individual measurements collected to calibrate the neutron response of the HPGe detector are listed in Table 18.¹⁵ Note that calibration measurements were performed both with the NPOD and SNAP present near the source and with those two instruments removed.

Table 18: Gamma spectrometer neutron calibration measurements

Moderator	NPOD & SNAP Present?	Real Time	File
None	Yes	30 min	06Jan09_110527.chn
2 cm HDPE		30 min	06Jan09_115119.chn
4 cm HDPE		30 min	06Jan09_123116.chn
8 cm HDPE		30 min	06Jan09_131056.chn
8 cm borated polyethylene		30 min	06Jan09_141000.chn
None	No	15 min	06Jan09_155831.chn
2 cm HDPE		15 min	06Jan09_152525.chn
4 cm HDPE		15 min	06Jan09_154215.chn
8 cm HDPE		15 min	06Jan09_150739.chn
8 cm borated polyethylene		15 min	06Jan09_145035.chn

Figure 39 shows the measured gamma spectra when the NPOD and SNAP were present. Note that the background photon spectrum was subtracted from the spectra shown (see the following section “Photon Background Measurements” for information on the photon background measurements). The most noticeable feature is the change in the high-energy photon continuum, which results from the scatter of high-energy photons in the environment and in the detector. Those high-energy photons are primarily created by neutron capture interactions in the environment (e.g., in the iron tables) and in the germanium itself. Figure 40 shows the same series of spectra acquired when the NPOD and SNAP were absent.

¹⁵ The HPGe detector control software creates files using the naming convention “yyMMMdd_hhmmss.chn” where

- “yy” is the two-digit year
- “MMM” is the three-character month abbreviation
- “dd” is the two-digit day
- “hh” is the two-digit hour, in 24-hour format
- “mm” is the two-digit minute
- “ss” is the two-digit second

The time stamp is in universal coordinated time.

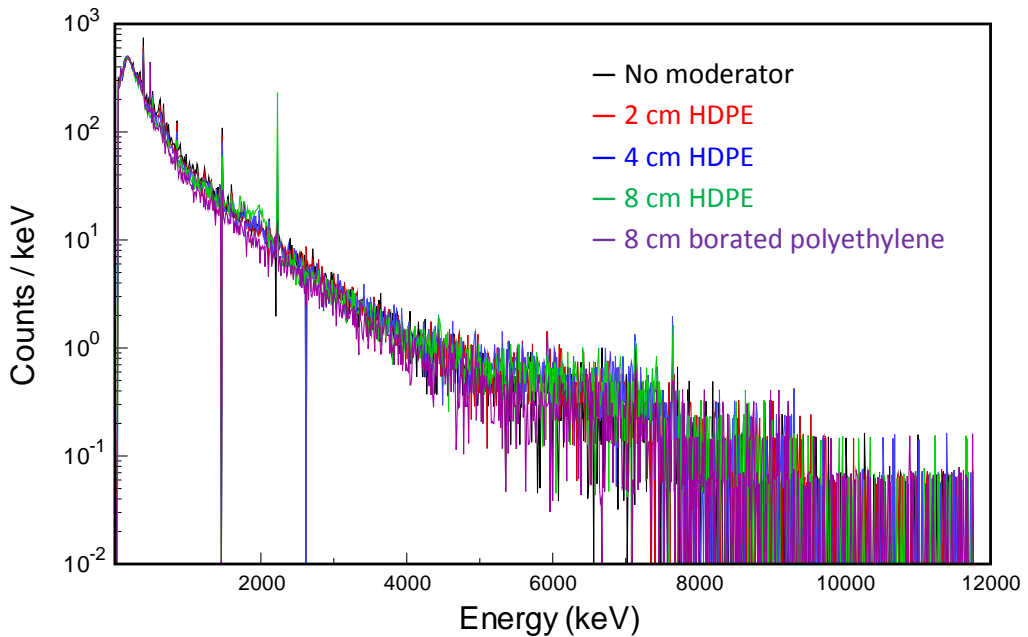


Figure 39: Gamma spectrum versus californium source moderation; the NPOD and SNAP were present

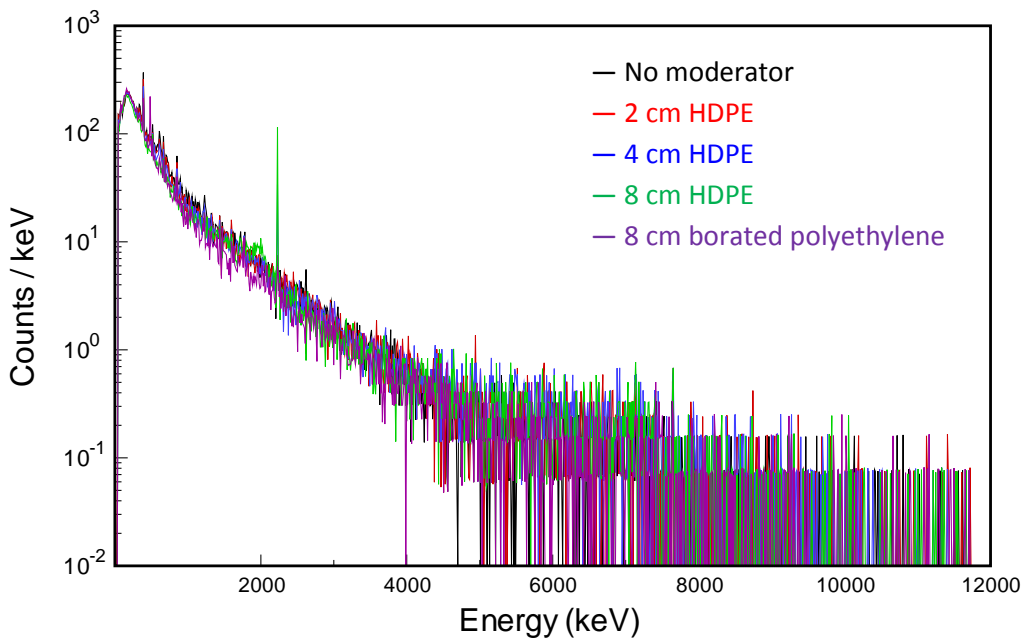


Figure 40: Gamma spectrum versus californium source moderation; the NPOD and SNAP were not present

Two sets of overnight photon background measurements were also collected using the HPGe detector. These measurements are described in the subsequent section “Photon Background Measurements”.

6.5 Gamma Calibration Sources

The gamma calibration sources listed in Table 19 were used to measure the response of the gamma spectrometer.

Table 19: Gamma calibration sources

Nuclide	Activity (μCi)	Reference Date	Manufacturer	Model No.	Serial No.
Ba133	106.51	15 December 2008	Eckert & Ziegler Isotope Products	Type D Gamma Standard	1351-20-1
Cs137	98.19	15 December 2008	Eckert & Ziegler Isotope Products	Type D Gamma Standard	1351-20-2
Co60	100.41	15 December 2008	Eckert & Ziegler Isotope Products	Type D Gamma Standard	1351-20-3
U232	101.5	23 April 2007	NIST	N/A	06-232-8

Each of the sources manufactured by Eckert & Ziegler is a 1-inch diameter, 0.25-inch thick acrylic disk. The radioactive material is deposited in a small spot near the top of the disk as shown in Figure 41.¹⁶

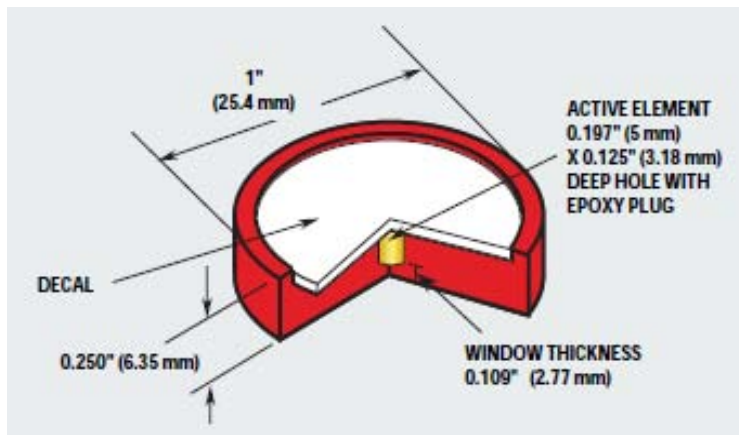


Figure 41: Schematic of the Eckert & Ziegler Isotope Products Type D gamma standard

The uranium-232 source manufactured by the National Institute of Standards and Technology (NIST) is constructed from two 1.5-inch diameter, 0.1-inch thick steel disks welded together with the radioactive material sandwiched between them in a 0.5-inch diameter, 1-mm thick disk as shown in Figure 42. (L. Lucas 2005) The source disk was mounted in a 3.5-inch tall, 2-inch wide, 0.125-inch thick aluminum holder as shown in Figure 43.

¹⁶ The schematic of the Eckert & Ziegler Isotope Products type D gamma standard is from the company's product catalog. See http://www.isotopeproducts.com/pdf/IPL_RefCal_LoRes.pdf.

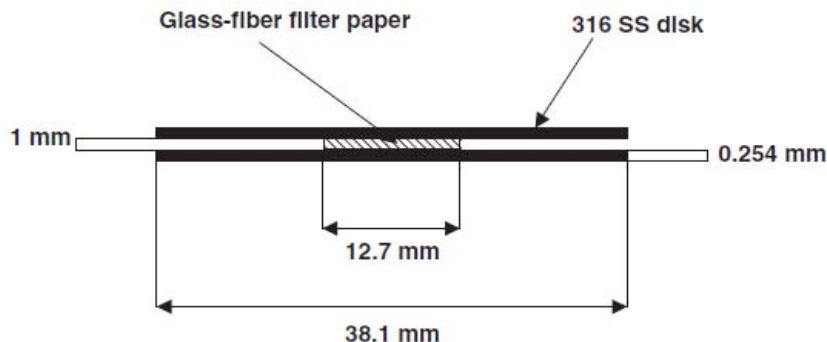


Figure 42: Schematic of the NIST uranium-232 source disk

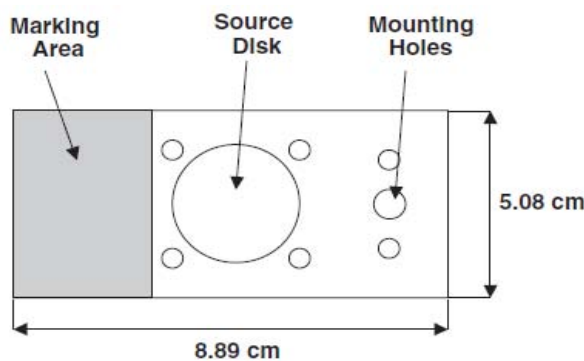


Figure 43: Aluminum mounting fixture for the NIST uranium-232 source

For each calibration measurement, the gamma source was placed in the same position as the plutonium source, and the instruments were positioned exactly as described in the preceding section, “Instrument Configuration”.

6.6 Gamma Spectrometer Photon Response Calibration

Individual measurements collected to calibrate the photon response of the HPGe detector are listed in Table 20. Note that calibration measurements were performed both with the NPOD and SNAP present near the source and with those two instruments removed.

Table 20: Gamma spectrometer photon calibration measurements

Source	NPOD & SNAP Present?	Real Time	File
Ba133	Yes	30 min	06Jan09_173714.chn
Cs137		30 min	07Jan09_110631.chn
Co60		30 min	07Jan09_114443.chn
U232		30 min	12Jan09_164627.chn
Ba133	No	15 min	06Jan09_170206.chn
Cs137		15 min	06Jan09_164323.chn
Co60		15 min	06Jan09_162229.chn
U232		30 min	12Jan09_171753.chn

Figure 44 shows the measured gamma spectra when the NPOD and SNAP were present. Figure 45 shows the measured gamma spectra when the NPOD and SNAP were absent. Note that the background photon spectrum was subtracted from the spectra shown (see the following section “Photon Background Measurements” for information on the photon background measurements).

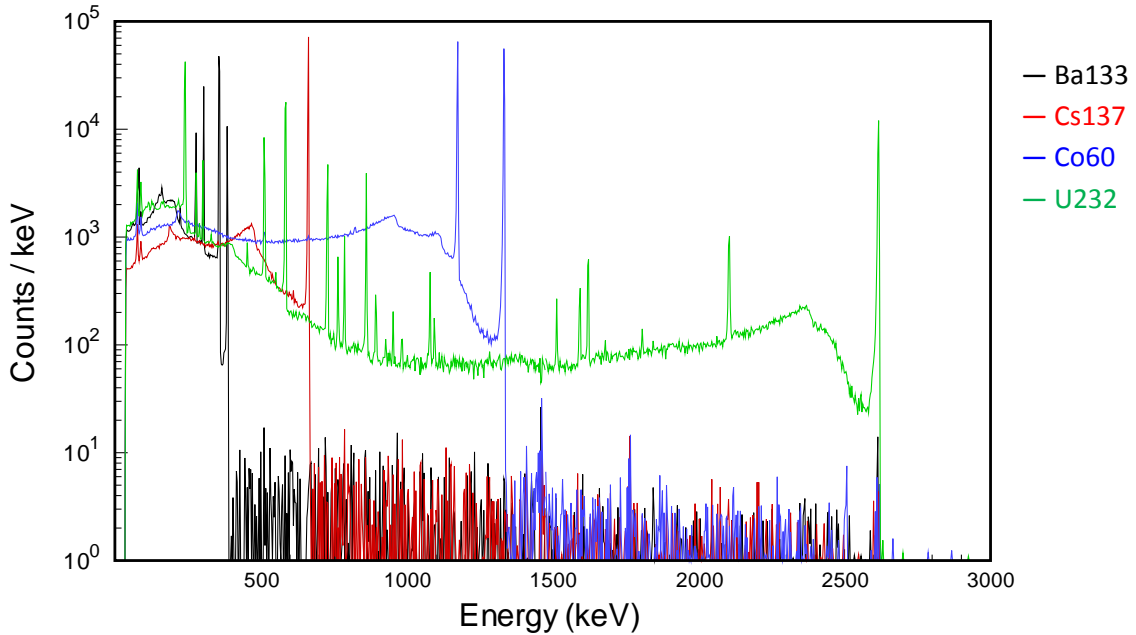


Figure 44: Gamma spectrum vs. gamma calibration source; the NPOD and SNAP were present

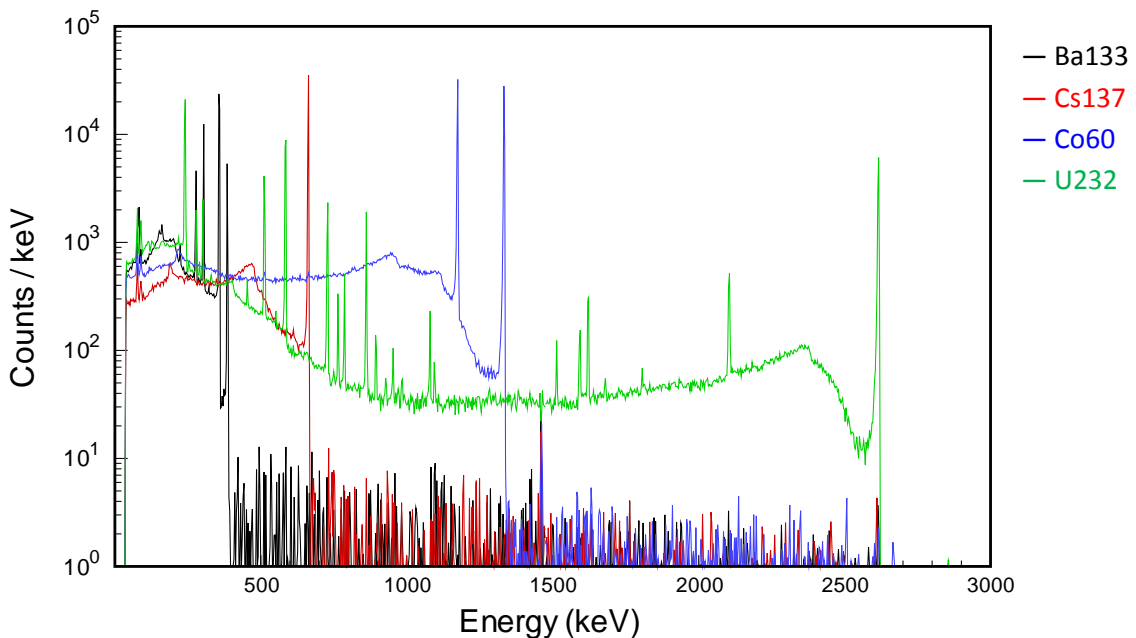


Figure 45: Gamma spectrum vs. gamma calibration source; the NPOD and SNAP were not present

6.7 Photon Background Measurements

Two overnight background measurements were performed; they are listed in Table 21. During those measurements, the photon background spectrum was collected in 1-hour increments. Cross-comparisons of the 25 background measurements did not reveal any significant differences between individual measurements. Consequently, a single cumulative background composed of the sum of the 25 individual measurements can be treated as the effective background for all gamma spectrometry measurements in this series of experiments. This composite background spectrum is shown in Figure 46.

Table 21: Photon background measurements; the real-time for each measurement was 1 hour

File	
7 – 8 January 2009	14 – 15 January 2009
07Jan09_195239.chn	14Jan09_193553.chn
07Jan09_205248.chn	14Jan09_203601.chn
07Jan09_215256.chn	14Jan09_213611.chn
07Jan09_225304.chn	14Jan09_223620.chn
08Jan09_005321.chn	14Jan09_233630.chn
08Jan09_015330.chn	15Jan09_003638.chn
08Jan09_025339.chn	15Jan09_013647.chn
08Jan09_035349.chn	15Jan09_023656.chn
08Jan09_045358.chn	15Jan09_033705.chn
08Jan09_055408.chn	15Jan09_043714.chn
08Jan09_065418.chn	15Jan09_053722.chn
08Jan09_075428.chn	15Jan09_063730.chn
	15Jan09_073741.chn

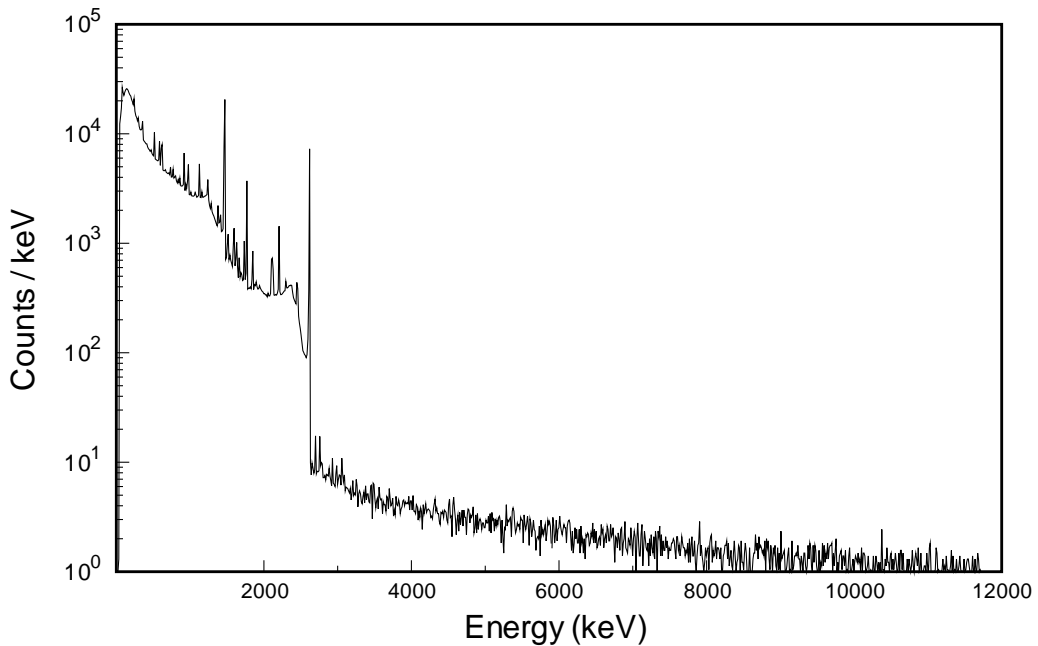


Figure 46: Composite photon background spectrum accumulated from 25 hours of background measurements

7 Benchmark Measurements

Gross neutron counting, neutron multiplicity counting, and gamma spectrometry measurements were performed on the plutonium source in six configurations:

- Bare
- Reflected by 0.5 inch of HDPE
- Reflected by 1.0 inch of HDPE
- Reflected by 1.5 inches of HDPE
- Reflected by 3.0 inches of HDPE
- Reflected by 6.0 inches of HDPE

Gross neutron counting, neutron multiplicity counting, and gamma spectrometry measurements were collected for each of the preceding reflected configurations of the plutonium source. The instruments were configured as described in the section “Instrument Configuration”.

7.1 Gross Neutron Counting Measurements

Gross neutron counting measurements acquired with the LANL SNAP are listed in Table 22.

Measurements were performed with the SNAP polyethylene cover both on and off. Table 23 lists the SNAP neutron count rate and uncertainty versus the thickness of the polyethylene reflector. The measured count rates are plotted in Figure 47.

Table 22: Gross neutron counting benchmark measurements

Reflector	Front Cover On		Front Cover Off	
	Count Time (sec)	Counts	Count Time (sec)	Counts
None	300	14316	300	17237
	300	14367	300	17201
	300	14409	300	17039
	300	13900		
0.5"	300	16500	300	22978
	300	16322	300	22859
	300	16690	300	22588
	300	16310	300	22877
1.0"	300	18555	300	29141
	300	18647	300	29279
	300	18402	300	29452
	300	18448		
1.5"	300	20714	300	35048
	300	20479	300	34681
	300	20601	300	34341
	300	20230		
3.0"	300	16354	300	29271
	300	16429	300	29215
	900	49090	300	28786
	300	15722		
6.0"	300	4458	300	7390
	300	4311	300	7200
	300	4274	300	7373
	300	4238		
	300	4294		

Table 23: Gross neutron counter count rate versus polyethylene reflector thickness; uncertainties represent one standard deviation

Reflector	Front Cover On		Front Cover Off	
	Count Rate (cps)	Uncertainty (cps)	Count Rate (cps)	Uncertainty (cps)
None	47.9	0.2	57.4	0.4
0.5"	55.0	0.2	76.0	0.5
1.0"	61.8	0.3	97.4	0.6
1.5"	68.7	0.3	116.2	0.6
3.0"	54.6	0.2	97.5	0.6
6.0"	14.4	0.1	24.3	0.3

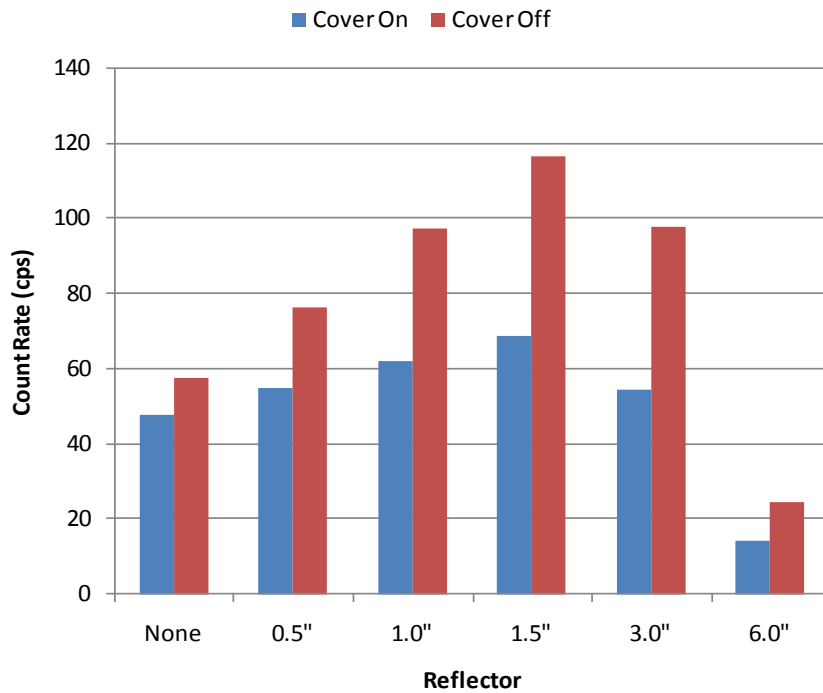


Figure 47: Gross neutron counter count rate vs. polyethylene reflector thickness

7.2 Neutron Multiplicity Counting Measurements

Neutron multiplicity counting measurements acquired with the LANL NPOD are listed in Table 24. The measured count rate and its uncertainty are given in Table 25 versus the thickness of the polyethylene reflector, and the count rate is plotted in Figure 48. Figure 49 shows the entire neutron multiplicity distribution versus coincidence gate width, and Figure 50 shows the measured neutron multiplicity distribution for a coincidence gate width of 1024 μ s. Figure 51 and Figure 52 respectively show the measured Feynman-Y and Rossi- α versus reflector thickness.

Note that both the gross neutron counting measurements and the neutron multiplicity measurements demonstrate competition between

- Increasing neutron multiplication with increasing reflector thickness
- Decreasing neutron leakage with increasing reflector thickness

As a result, most of the neutron metrics are maximized for the 1.5-inch thick reflector, where the product of multiplication and leakage probability are near their maximum.

Table 24: Neutron multiplicity counter benchmark measurements

Reflector	Segments	File
None	98	09010866.dat
	111	09011268.dat
	107	09011269.dat
	90	09011492.dat
0.5"	109	09010861.dat
	170	09010862.dat
	108	09010864.dat
	106	09011493.dat
1.0"	109	09011376.dat
	108	09011377.dat
	102	09011378.dat
	115	09011494.dat
1.5"	103	09011271.dat
	109	09011272.dat
	113	09011273.dat
	129	09011495.dat
3.0"	103	09010753.dat
	102	09010754.dat
	103	09010755.dat
	108	09011496.dat
6.0"	103	09010857.dat
	83	09010860.dat
	38	09011497.dat

Table 25: Neutron multiplicity counter count rate versus polyethylene reflector thickness; uncertainties represent one standard deviation

Reflector	Count Rate (cps)	Uncertainty (cps)
None	8299	26
0.5"	11133	26
1.0"	14439	71
1.5"	17488	70
3.0"	14687	55
6.0"	3646	61

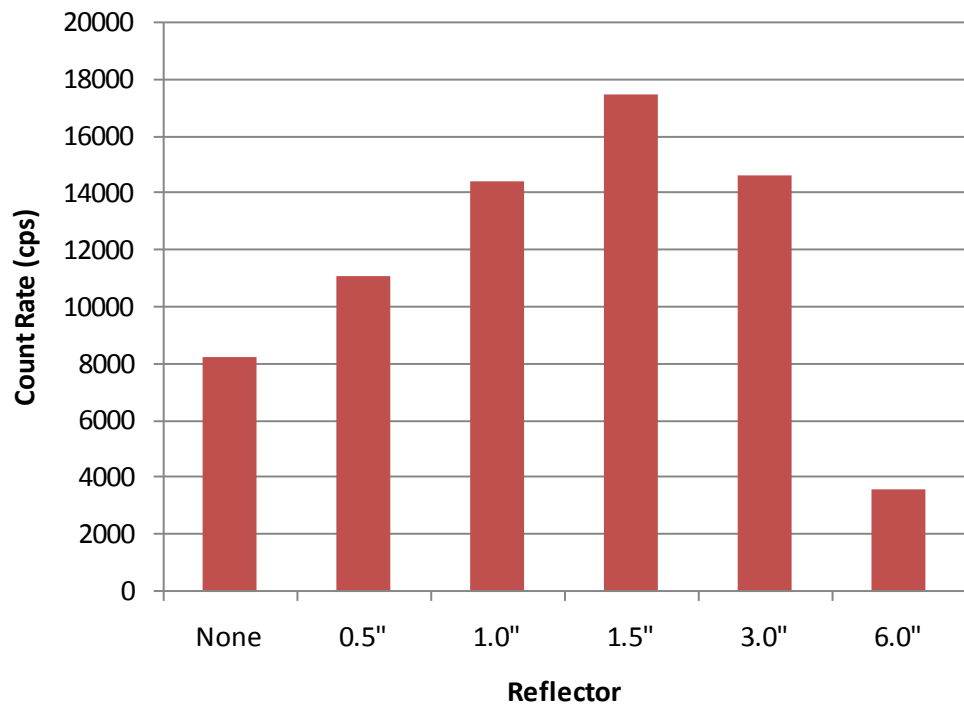


Figure 48: Neutron multiplicity counter count rate versus polyethylene reflector thickness

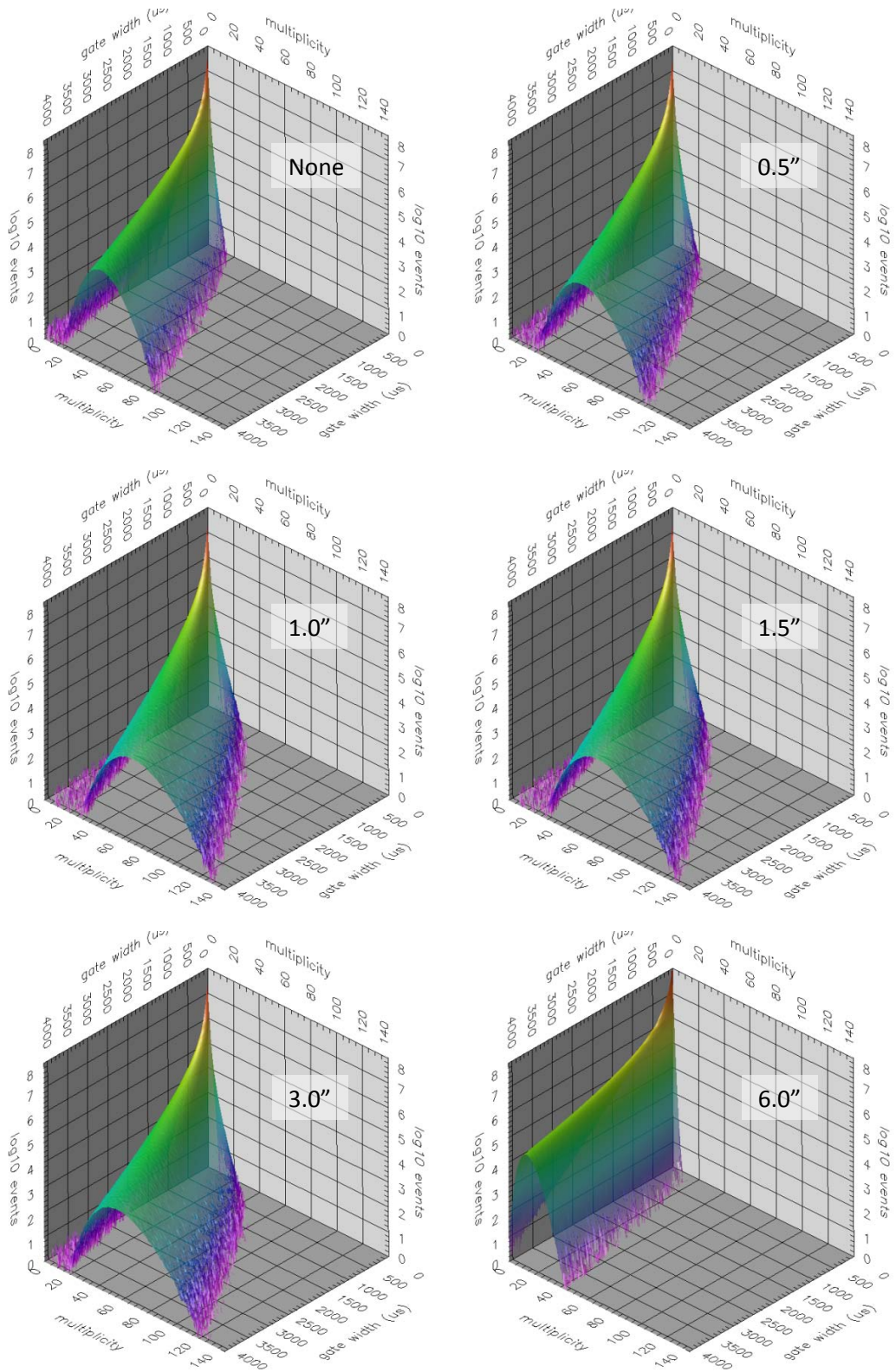


Figure 49: Neutron multiplicity distribution versus polyethylene reflector thickness

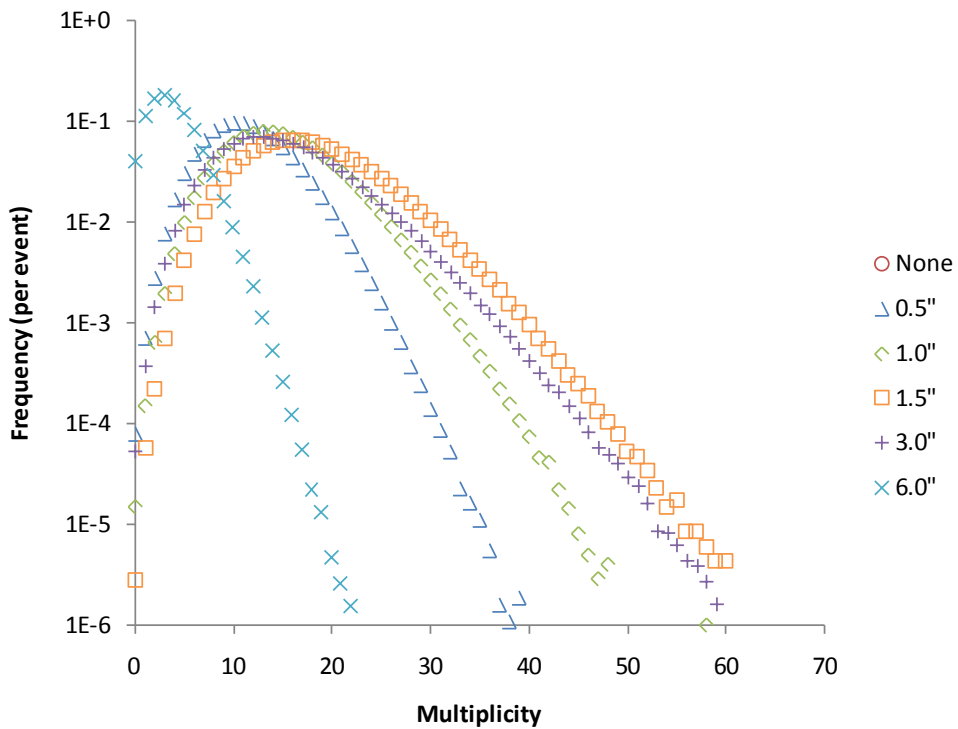


Figure 50: Neutron multiplicity distribution versus polyethylene reflector thickness; the coincidence gate width is 1024 μ s

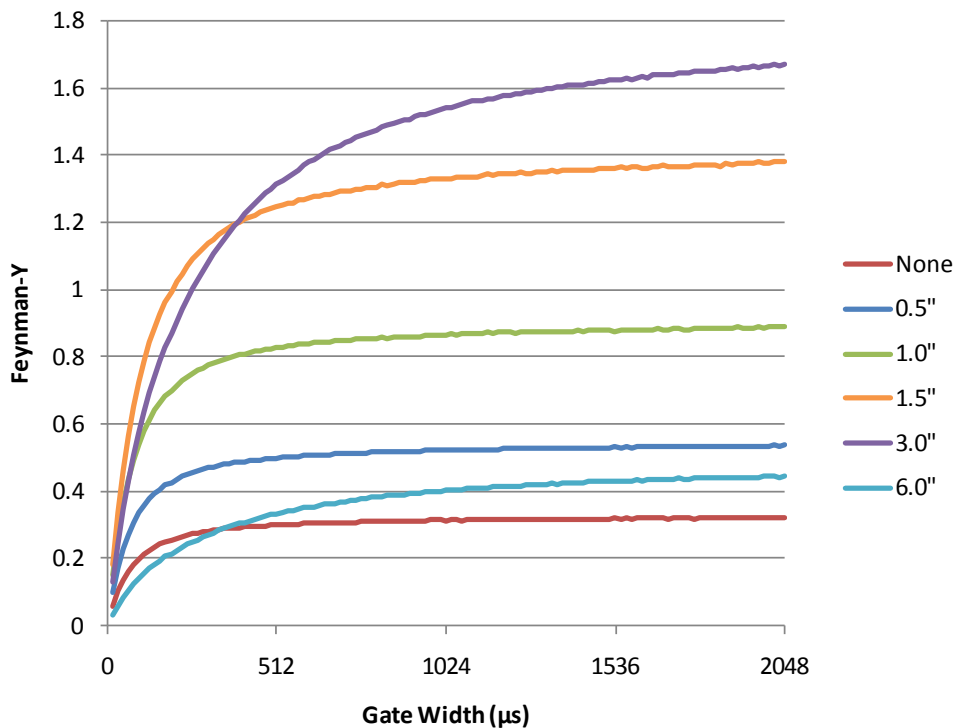


Figure 51: Feynman-Y versus polyethylene reflector thickness

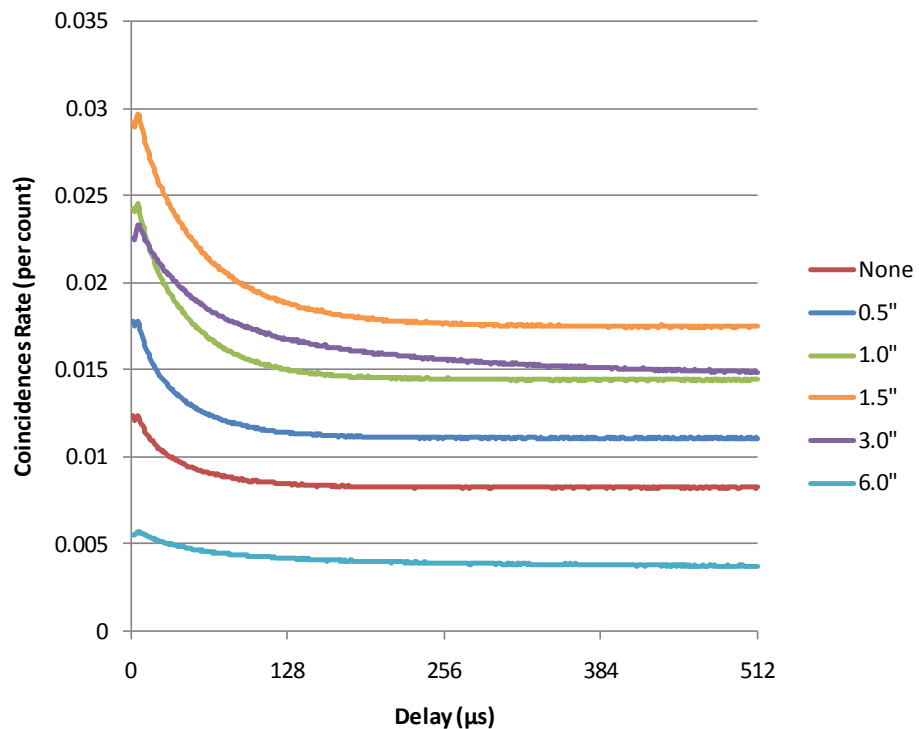


Figure 52: Rossi- α distribution versus polyethylene reflector thickness

7.3 Gamma Spectrometry Measurements

Gamma spectrometry measurements acquired with the HPGe detector are listed in Table 26. Recall that measurements were performed both with and without the NPOD and SNAP present. For each reflected configuration of the plutonium source, gamma spectra were collected for 10, 20, and 60 minutes.

Table 26: High-resolution gamma spectrometry benchmark measurements

Reflector	Real Time	NPOD & SNAP Present?	
		Yes	No
None	10 min	08Jan09_171230.chn	13Jan09_104946.chn
	20 min	08Jan09_173304.chn	13Jan09_111044.chn
	60 min	12Jan09_121406.chn	12Jan09_131539.chn
0.5"	10 min	08Jan09_151731.chn	07Jan09_161934.chn
	20 min	08Jan09_153801.chn	08Jan09_150000.chn
	60 min	08Jan09_165920.chn	07Jan09_172015.chn
1.0"	10 min	13Jan09_123849.chn	13Jan09_160339.chn
	20 min	13Jan09_125915.chn	13Jan09_155258.chn
	60 min	13Jan09_141924.chn	13Jan09_153028.chn
1.5"	10 min	12Jan09_150855.chn	12Jan09_154503.chn
	20 min	12Jan09_145813.chn	12Jan09_153346.chn

	60 min	12Jan09_142626.chn	13Jan09_121850.chn
3.0"	10 min	07Jan09_122733.chn	07Jan09_155511.chn
	20 min	07Jan09_125043.chn	07Jan09_154450.chn
	60 min	07Jan09_141321.chn	07Jan09_152407.chn
6.0"	10 min	08Jan09_122925.chn	08Jan09_124147.chn
	20 min	08Jan09_121708.chn	08Jan09_130240.chn
	60 min	08Jan09_114126.chn	08Jan09_140344.chn

Figure 53 plots the gamma spectra versus the thickness of the polyethylene moderator when the NPOD and SNAP were present. Figure 54 shows the gamma spectra measured when the NPOD and SNAP were absent. In both figures, the inset shows the region between 0 and 2500 keV. Aside from the 2223 keV photopeak from hydrogen neutron capture, other features that change noticeably with polyethylene thickness include the high-energy continuum resulting from

- neutron capture in germanium as well as iron and other structural materials and
- induced fission gammas.

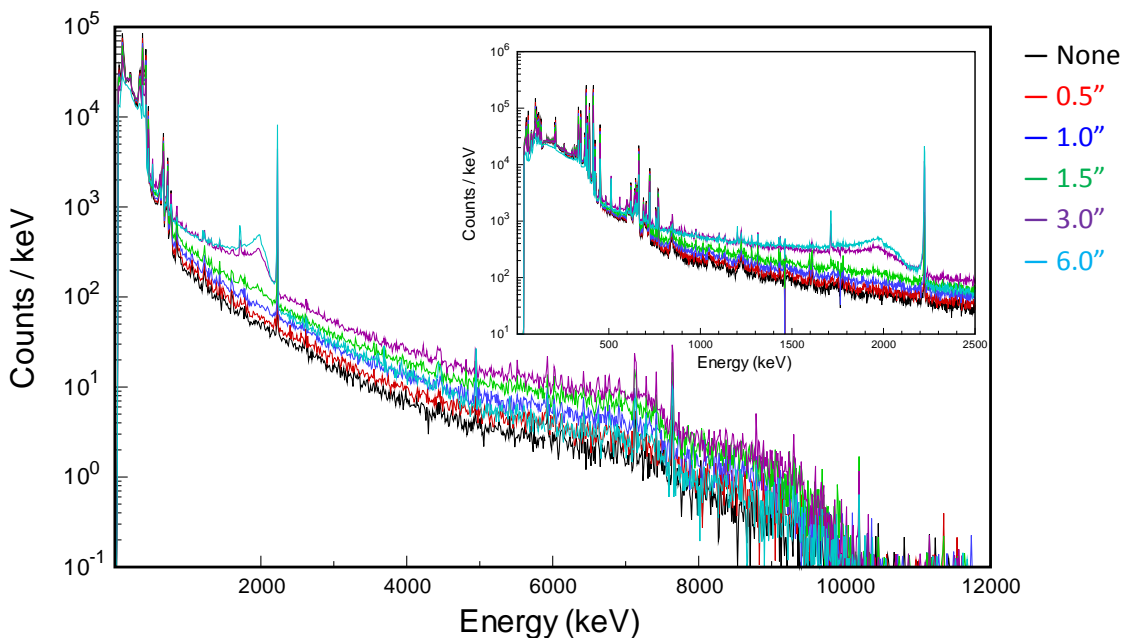


Figure 53: Gamma spectrum versus polyethylene moderator thickness; the inset shows the region between 0 and 2500 keV. These measurements were performed with the NPOD and SNAP present

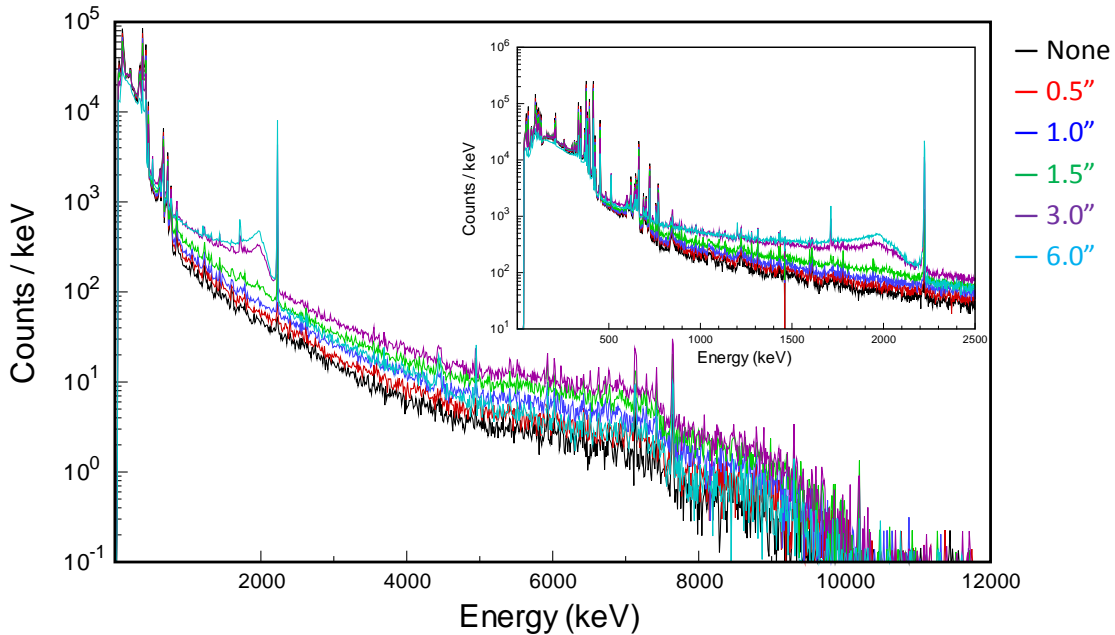


Figure 54: Gamma spectrum versus polyethylene moderator thickness; the inset shows the region between 0 and 2500 keV. These measurements were performed with the NPOD and SNAP absent

8 Other Measurements

In addition to the calibration and benchmark measurements described in preceding sections, several other auxiliary measurements were performed. These measurements were conducted to characterize

- the effect of the polyethylene reflectors' temperature on the response of the neutron multiplicity counter.
- the effect of the neutron multiplicity counter's large moderator on the response of the gross neutron counter.
- the differences between the reflectors constructed by SNL and reflectors constructed at LANL.
- the response of the instruments to the californium neutron calibration source in the polyethylene reflectors.

8.1 Neutron Multiplicity Counter Response versus Polyethylene Reflector Temperature

For an ambient air temperature of 23 – 24 C, the surface temperature of the plutonium source's steel cladding will equilibrate to 44 – 45 C. Consequently, when the source was placed inside one of the polyethylene reflectors, the reflector gradually warmed from ambient temperature. That warming caused the reflector to expand, which in turn reduced its density.

To assess the significance of this gradual temperature transient, neutron multiplicity measurements were collected versus time as the 1.0-inch thick reflector warmed up from ambient temperature. These

measurements are listed in Table 27. Over the course of approximately 50 minutes, the surface temperature of the reflector warmed from 23.8 C to 30.7 C.

Table 27: Neutron multiplicity counting measurements taken versus the surface temperature of the 1.0 inch thick polyethylene reflector

Approximate Time (min)	Reflector Surface Temp. (C)	Segments	File
0	23.8		
10	25.3	102	09011480.dat
20	27.1	79	09011481.dat
30	29.1	120	09011482.dat
40	29.8	100	09011483.dat
50	30.7	129	09011484.dat

Analysis of those measurements indicates that the gradual warming and expansion of the reflector has a negligible effect on the neutron multiplicity metrics. This observation is illustrated by Figure 55: the measured Feynman-Y did not change significantly as the reflector warmed and expanded.

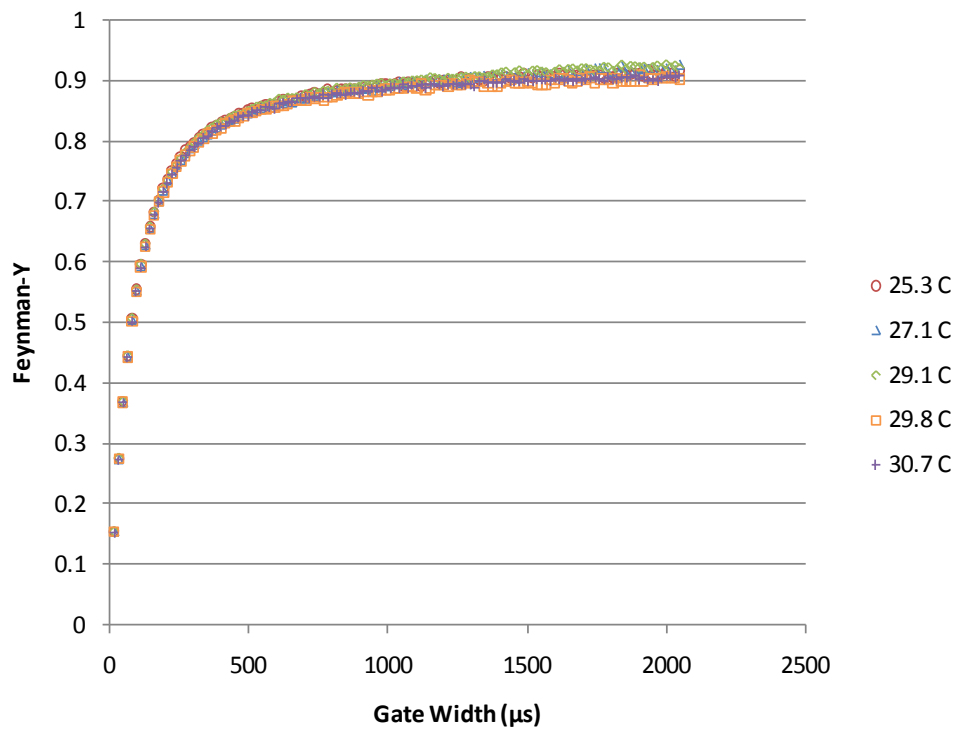


Figure 55: Feynman-Y versus surface temperature of 1.0-inch thick polyethylene moderator

8.2 Gross Neutron Counter Response with Neutron Multiplicity Counter Absent

Recall that the LANL NPOD is constructed with a large polyethylene moderator (approximately 0.5 m × 0.5 m), and that the counter was operated relatively close to the plutonium source (0.5 m).

Consequently, the NPOD was a significant source of neutron reflection.

Gamma spectrometry measurements were performed with the SNAP and NPOD present for each configuration of the plutonium source so that the effect of those detectors on the spectrometer's response can be characterized. In addition, to assess the effect of the NPOD's presence on the SNAP measurements, SNAP measurements were performed both with the NPOD present and absent. Table 28 and Figure 56 provide the SNAP count rate measured with the NPOD present and absent. The effect of neutron reflection by the NPOD is statistically significant, but the NPOD's presence does not induce a large increase in the SNAP count rate.

Table 28: Gross neutron counter response with neutron multiplicity counter present and absent; uncertainties represent one standard deviation

Front Cover On?	Reflector	NPOD Present		NPOD Absent	
		Count Rate (cps)	Uncertainty (cps)	Count Rate (cps)	Uncertainty (cps)
Yes	None	47.9	0.2	46.6	0.4
	0.5"	55.0	0.2	53.9	0.4
	1.0"	61.8	0.3	61.0	0.5
	1.5"	68.7	0.3	68.0	0.5
	3.0"	54.6	0.2	52.9	0.4
	6.0"	14.4	0.1	13.4	0.2
No	None	57.4	0.3	55.7	0.4
	0.5"	76.0	0.3	75.8	0.5
	1.0"	97.4	0.4	95.6	0.6
	1.5"	116.2	0.4	113.6	0.6
	3.0"	97.5	0.4	95.0	0.6
	6.0"	24.3	0.2	23.6	0.3

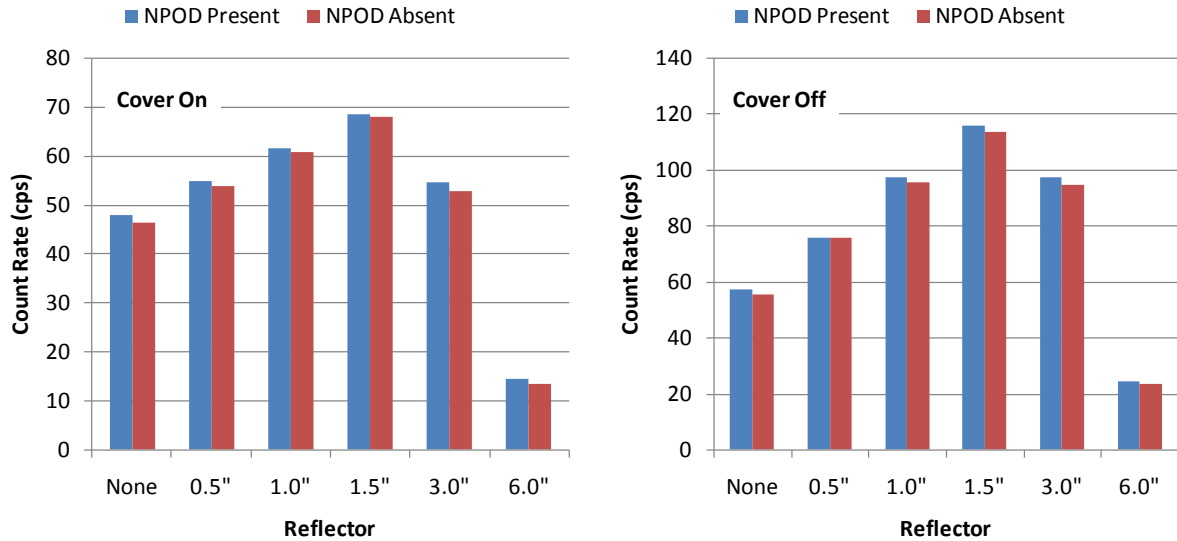


Figure 56: Gross neutron counter response with neutron multiplicity counter present and absent

8.3 Comparison of SNL Reflectors to LANL Reflectors

The polyethylene reflectors used in this series of experiments (see Figure 2) were constructed to be nearly perfectly spherical. In previous similar experiments, different reflectors fabricated by LANL have been used. Figure 57 is a photograph of the LANL reflectors; they are described in detail in (Valentine 2006). As the photograph shows, the reflectors are not perfectly spherical. The innermost reflectors (0.5, 1.0, and 1.5 inches thick) each has a diametral hole in the bottom for an aluminum support stand. The outer two reflectors (3.0 and 6.0 inches thick) are truncated at the bottom. For the 6 inch thick moderator in particular, this geometry results in a significant removal of moderating material.

Experiments were conducted with the LANL reflectors to assess the effect of their geometry relative to the spherical geometry of the SNL reflectors. Note that the stand designed by LANL used to support the plutonium source is different from the stand designed by SNL, so even the measurements of the bare plutonium source exhibited differences.



Figure 57: Polyethylene reflectors constructed by LANL

8.3.1 Gross Neutron Counting Measurements

Table 29 compares SNAP neutron count rates measured for the LANL and SNL reflectors. These count rates are also plotted in Figure 58. The count rates measured for the SNL reflectors were consistently lower than those measured for the LANL reflectors. This difference is statistically significant in each case. Since neutron multiplication is lower for the LANL reflectors, the effect observed is probably primarily due to higher leakage probability. The neutron spectrum is probably slightly harder for the LANL reflectors as well.

Table 29: Gross neutron counter response for LANL and SNL reflectors; uncertainties represent one standard deviation

Front Cover On?	Reflector	LANL Reflector		SNL Reflector	
		Count Rate (cps)	Uncertainty (cps)	Count Rate (cps)	Uncertainty (cps)
Yes	None	48.3	0.4	46.3	0.4
	0.5"	54.8	0.4	54.4	0.4
	1.0"	62.7	0.5	61.5	0.5
	1.5"	68.6	0.5	67.4	0.5
	3.0"	54.7	0.4	52.4	0.4
	6.0"	16.3	0.2	14.3	0.2
No	None	56.9	0.4	56.8	0.4
	0.5"	77.1	0.5	76.3	0.5
	1.0"	99.5	0.6	98.2	0.6
	1.5"	117.6	0.6	114.5	0.6
	3.0"	99.1	0.6	96.0	0.6
	6.0"	27.6	0.3	24.6	0.3

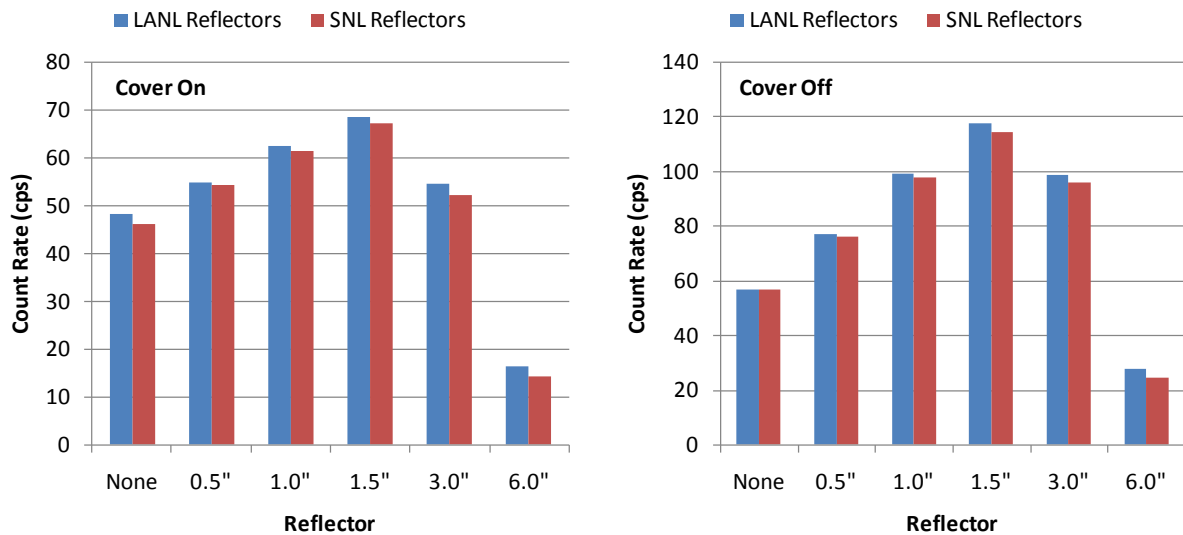


Figure 58: Gross neutron counter response for LANL and SNL reflectors

8.3.2 Neutron Multiplicity Counting Measurements

Table 30 lists NPOD measurements performed to compare the LANL and SNL reflectors. As shown in Figure 59, the Feynman-Y was consistently higher for the LANL reflectors. The effect observed is probably also primarily due to higher leakage probability for the LANL reflectors.

Table 30: Neutron multiplicity measurements comparing LANL and SNL reflectors

Reflector	LANL Reflector		SNL Reflector	
	Segments	File	Segments	File
None	93	09011491.dat	90	09011492.dat
0.5"	105	09011489.dat	106	09011493.dat
1.0"	103	09011488.dat	115	09011494.dat
1.5"	103	09011487.dat	129	09011495.dat
3.0"	128	09011486.dat	108	09011496.dat
6.0"	49	09011485.dat	38	09011497.dat

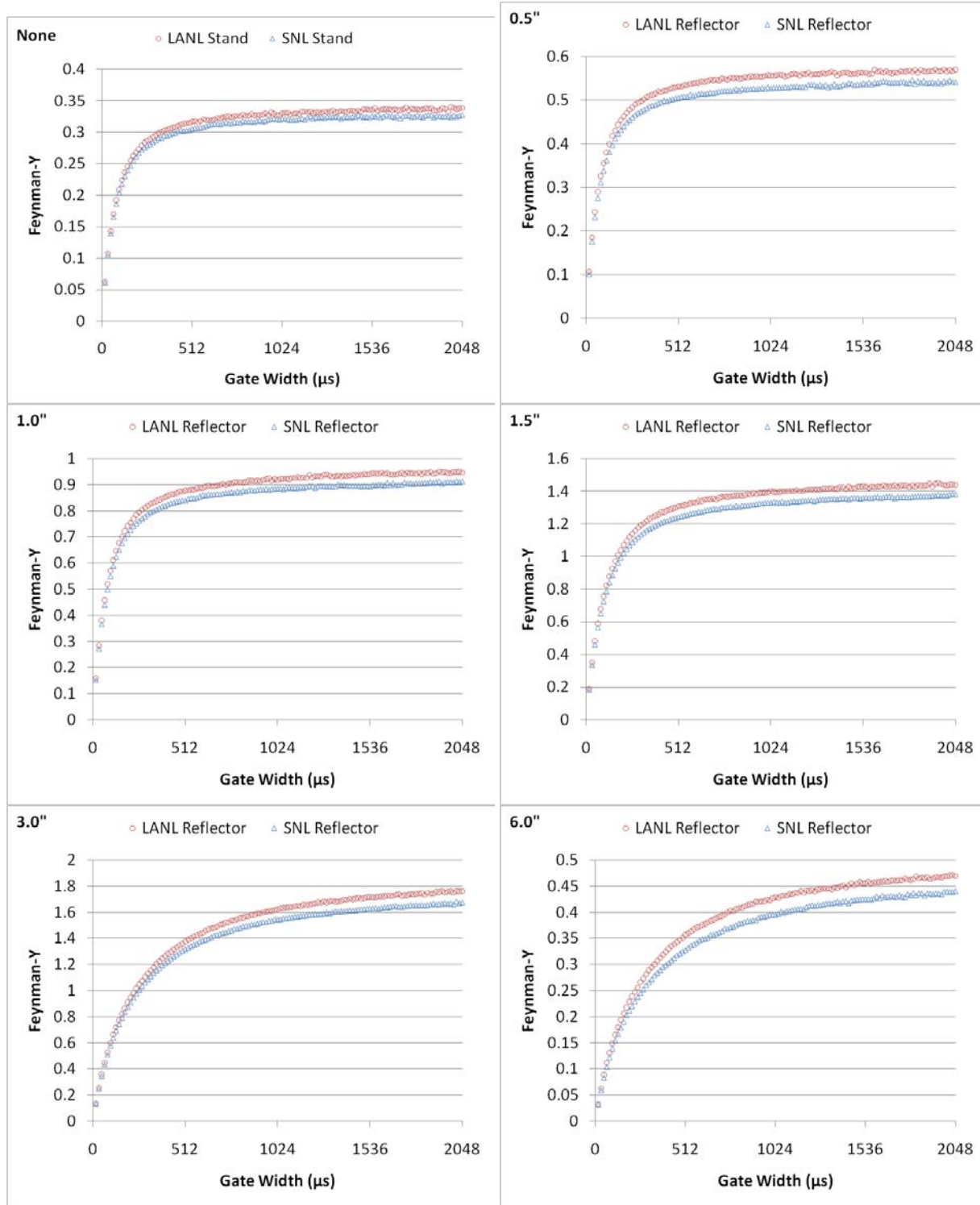


Figure 59: Comparison of the Feynman-Y for the LANL and SNL reflectors

8.3.3 Gamma Spectrometry Measurements

Gamma spectrometry measurements collected to compare the LANL and SNL reflectors are listed in Table 31. Figure 60 and Figure 61 respectively show the gamma spectrum versus reflector thickness for the LANL and SNL reflectors. In both figures, the inset emphasizes the region from 0 to 2500 keV. The

differences observed in the gamma spectrum for the LANL and SNL reflectors are generally much more subtle than the differences observed in the gross neutron counting and neutron multiplicity counting measurements.

Table 31: Gamma spectrometry measurements comparing LANL and SNL reflectors

Reflector	LANL Reflector		SNL Reflector	
	Real Time	File	Real Time	File
None	15 min	14Jan09_152528.chn	15 min	14Jan09_154231.chn
0.5"	15 min	14Jan09_150814.chn	15 min	14Jan09_155854.chn
1.0"	15 min	14Jan09_145129.chn	15 min	14Jan09_161519.chn
1.5"	15 min	14Jan09_130404.chn	15 min	14Jan09_161348.chn
3.0"	15 min	14Jan09_124644.chn	15 min	14Jan09_164811.chn
6.0"	15 min	14Jan09_122751.chn	15 min	14Jan09_170433.chn

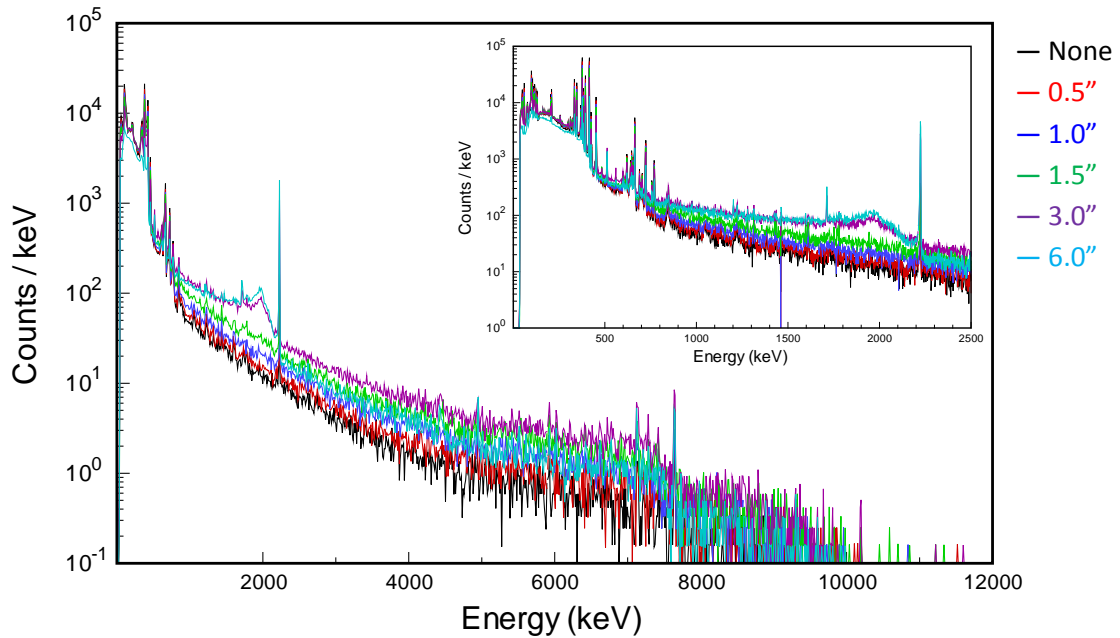


Figure 60: Gamma spectrum versus LANL polyethylene reflector thickness; the inset shows the region between 0 and 2500 keV

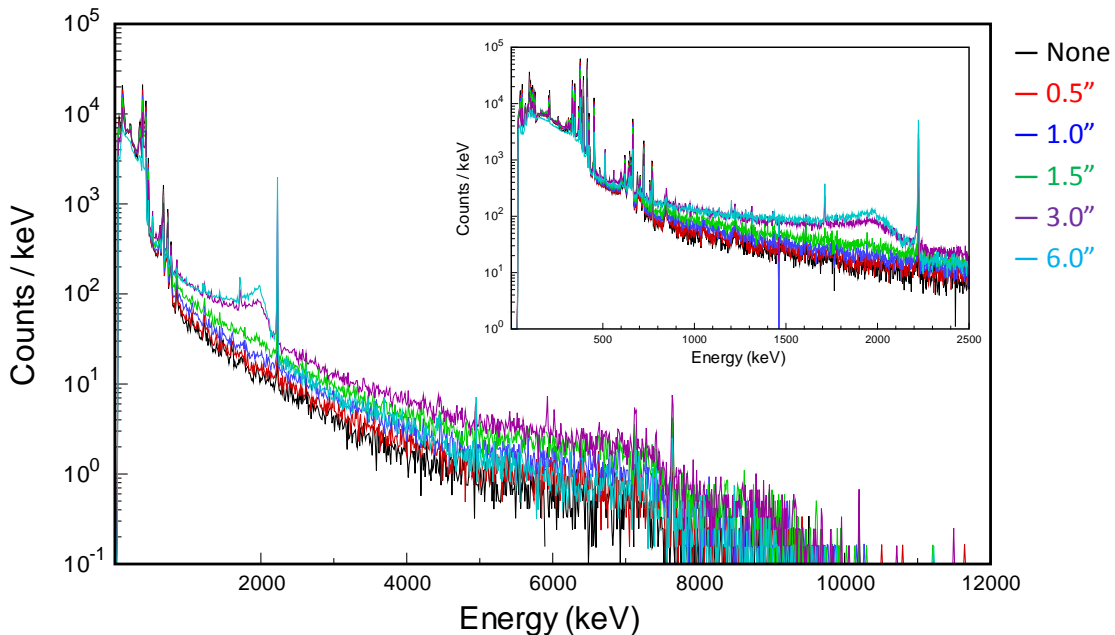


Figure 61: Gamma spectrum versus SNL polyethylene reflector thickness; the inset shows the region between 0 and 2500 keV

8.4 Californium Source in Polyethylene Reflectors

In order to characterize the polyethylene reflectors independently from the plutonium source, measurements were conducted where the californium neutron calibration source (see the section “Neutron Calibration Source and Moderators”) was placed at the center of the polyethylene reflectors. These measurements can be used to confirm the accuracy of radiation transport models of the polyethylene reflectors.

8.4.1 Gross Neutron Counting Measurements

Table 32 lists the SNAP count rate measured for the californium source in each of the polyethylene reflectors. The gross neutron count rate is plotted versus the polyethylene reflector thickness in Figure 62. Observe that the trend in neutron count rate versus polyethylene thickness for the californium source is dissimilar from the same trend for the plutonium source (see Figure 47). This is because the spontaneous fission neutron spectrum of californium-252 is not identical to the spectrum of neutrons emitted by the plutonium source, which is influenced by the interaction cross-sections of plutonium. Consequently, it is recommended that the measurements in Table 32 should not be used to estimate neutron transmission through the polyethylene. Neutron transmission is a strong function of the incident neutron spectrum, and the californium spectrum is significantly different from the plutonium source spectrum.

Table 32: Gross neutron counter count rate versus polyethylene reflector thickness

Reflector	Front Cover On		Front Cover Off	
	Count Rate (cps)	Uncertainty (cps)	Count Rate (cps)	Uncertainty (cps)
None	12.1	0.1	14.0	0.2
0.5"	11.3	0.2	15.0	0.2
1.0"	9.7	0.2	14.3	0.2
1.5"	7.9	0.1	13.1	0.1
3.0"	4.6	0.1	7.8	0.1
6.0"	1.2	0.0	1.9	0.0

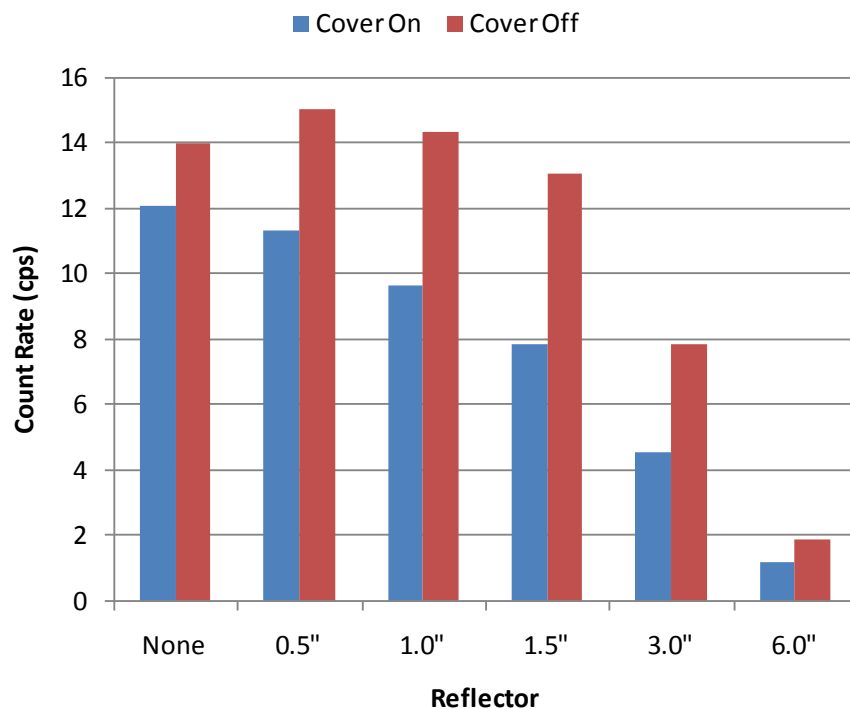


Figure 62: Gross neutron counter count rate versus polyethylene reflector thickness

8.4.2 Neutron Multiplicity Counting Measurements

Neutron multiplicity measurements collected with the NPOD when the californium source was inside the polyethylene reflectors are listed in Table 33. The NPOD count rate is plotted versus polyethylene reflector thickness in Figure 63. Figure 64 shows the multiplicity distribution measured for the 1-inch thick reflector. The distribution was very nearly Poisson for that reflector as well as for the others. As Figure 65 shows, neutron multiplicity measurements of the californium source in each reflector exhibited a variance that was only slightly higher than the mean, which is due to the spontaneous fission neutron multiplicity of californium-252.

Table 33: Neutron multiplicity measurements with the californium calibration source placed inside the polyethylene reflectors

Reflector	Segments	File
0.5"	26	09011504.dat
1.0"	26	09011503.dat
1.5"	20	09011502.dat
3.0"	28	09011500.dat
6.0"	13	09011599.dat

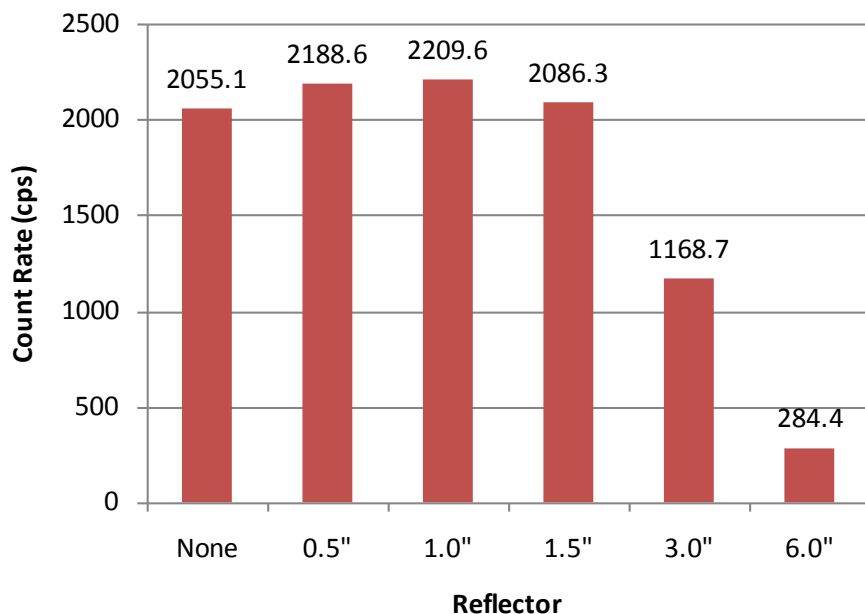


Figure 63: Neutron multiplicity counter count rate versus polyethylene reflector thickness

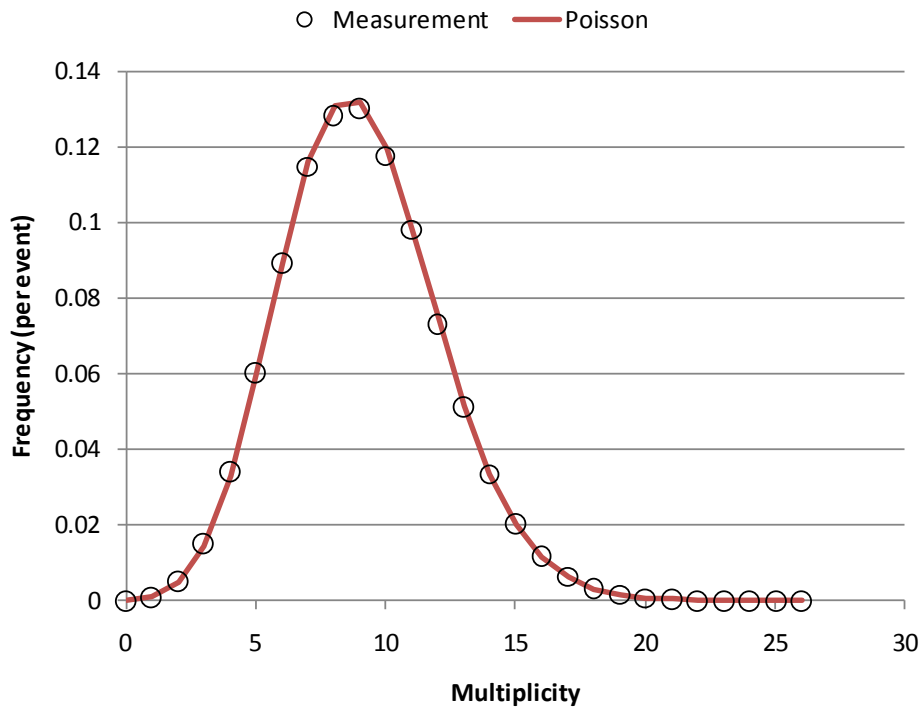


Figure 64: Neutron multiplicity distribution measured with the californium calibration source inside the 1.0-inch thick polyethylene reflector; the coincidence gate width is 4096 μ s

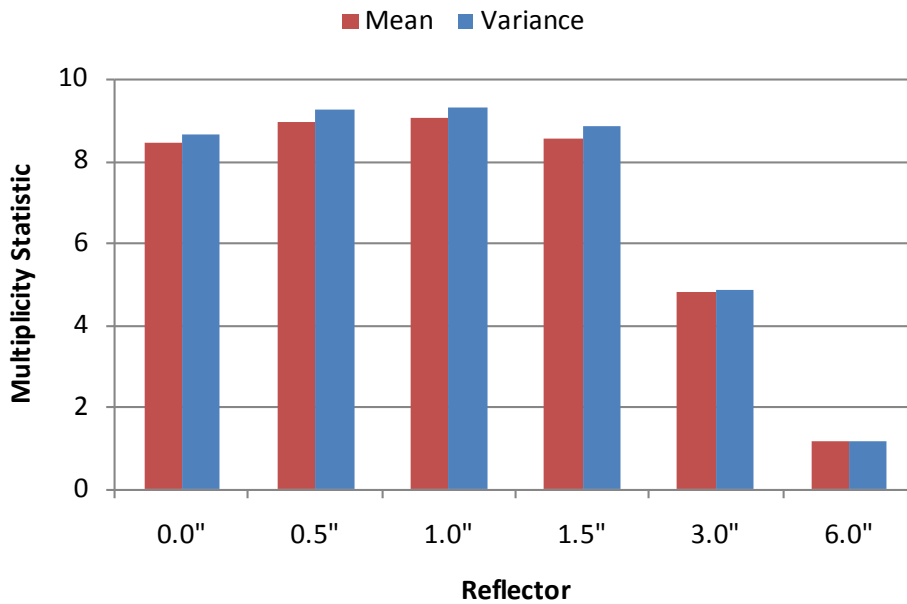


Figure 65: Neutron multiplicity distribution mean and variance versus polyethylene reflector thickness; the coincidence gate width is 4096 μ s

8.4.3 Gamma Spectrometry Measurements

Table 34 lists gamma spectrometry measurements that were collected when the californium calibration source was placed inside the polyethylene reflectors. All of these measurements were collected with the NPOD and SNAP present near the plutonium source. The spectra are plotted in Figure 66. The inset in the figure emphasizes the 2223 keV photopeak that results from neutron capture in hydrogen, primarily in the reflector.

Table 34: Gamma spectrometry measurements where the californium calibration source was placed inside the polyethylene reflectors

Reflector	Real Time	File
0.5"	15 min	15Jan09_135018.chn
1.0"	15 min	15Jan09_132240.chn
1.5"	30 min	15Jan09_124054.chn
3.0"	30 min	15Jan09_120521.chn
6.0"	60 min	15Jan09_113022.chn

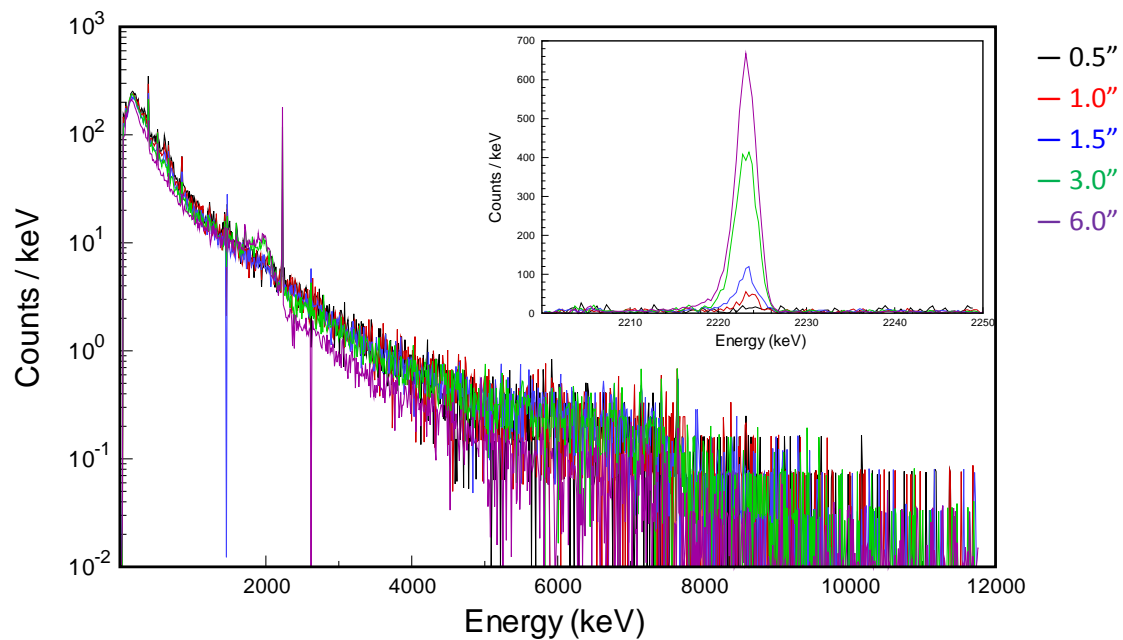


Figure 66: Gamma spectrum versus polyethylene reflector thickness; the inset shows the height of the 2223 keV photopeak from hydrogen neutron capture

9 Summary

Subcritical experiments were conducted with an α -phase, weapons-grade plutonium metal sphere in the DAF at NTS in January 2009. The experimental results will permit developers of radiation transport models and codes to validate their coupled neutron-photon transport calculations. The measurements include data acquired from three different instruments:

- A gross neutron counter (a LANL SNAP-3 detector)
- A neutron multiplicity counter (a LANL NPOD detector)
- A high-resolution gamma spectrometer (a high-efficiency HPGe detector)

The plutonium sphere was measured in six different configurations:

- Bare
- Reflected by 0.5 inch of high density polyethylene (HDPE)
- Reflected by 1.0 inch of HDPE
- Reflected by 1.5 inches of HDPE
- Reflected by 3.0 inches of HDPE
- Reflected by 6.0 inches of HDPE

All of the data acquired during this series of experiments are available upon request.

Acknowledgements

These experiments were conducted with the support and at the direction of the National Nuclear Security Administration. The experiments were also made possible by the assistance of several National Security Technologies (NSTec) and LANL personnel working at NTS. In particular, Jesson Hutchinson and Mark Smith-Nelson of LANL assisted in the operation of the instruments, which were all supplied by LANL. In addition, Avneet Sood and Erik Shores of LANL provided the models of the NPOD and SNAP detectors from which the MCNP models in this report were developed.

References

DeHoffman, Frederic. "Statistical Aspects of Pile Theory." In *The Science and Engineering of Nuclear Power, Vol. II*, 103 - 119. Addison-Wesley, 1949.

L. Lucas, L. Pibida, M. Unterweger, and L. Karam. "Gamma-Ray Emitting Test Sources for Portal Monitors used for Homeland Security." *Radiation Protection Dosimetry* Vol. 113 No. 1, 2005: 108-111.

Valentine, Timothy E. "Polyethylene-Reflected Plutonium Metal Sphere Subcritical Noise Measurements, SUB-PU-MET-MIXED-001." In *International Handbook of Evaluated Criticality Safety Benchmark Experiments, NEA/NSC/DOC(95)03/I-IX*. Organization for Economic Co-operation and Development - Nuclear Energy Agency (OECD-NEA), 2006.

Appendix A: LANL Documentation of Plutonium Source Construction



LOS ALAMOS SCIENTIFIC LABORATORY
UNIVERSITY OF CALIFORNIA
LOS ALAMOS, NEW MEXICO 87545
Telephone Ext:

OFFICE MEMORANDUM

TO : Tom McLaughlin, Q-14, MS 560

DATE: October 23, 1980

FROM : Eldon Brandon

SUBJECT : ASSEMBLY OF ^{239}Pu BALL FOR CRITICALITY EXPERIMENT

SYMBOL : CMB-11-FAB-80-65

MAIL STOP: 505

Per your instructions, one plutonium-239 sphere was fabricated and clad in stainless steel by CMB-11.

The components making up the assembly are listed in Attachment 1. The stainless steel hemisHELLS were deep drawn of 0.38-mm-thick Type 304 stainless steel to an inside radius of 38.27 mm. The flange at the equator was turned to a diameter of 84.4 mm.

The ^{239}Pu sphere was cast and turned to a mean diameter of 75.876 mm. The density was 19.655 g/cc. The chemical and isotopic analyses are included as Attachment 2.

Just prior to assembly, the Pu sphere was partially immersed in freon and wiped with cheesecloth to shrink the sphere and to remove any loose contamination. It was removed from the glovebox line and assembled in the S/S hemisHELLS. The cladding was then electron beam welded using the procedure given in Attachment 3. The assembly is shown in Attachment 4.

The assembly was monitored for alpha contamination, weighed, and prepared for shipment.

Eldon Brandon
Eldon Brandon

EB:bs

Atmtts: a/s

Distribution:

J. L. Green, CMB-11, MS 505 *143*

D. Harbur, CMB-11, MS 505

F. Miley, CMB-11, MS 505

E. Brandon, CMB-11, MS 505

File

SUMMARY OF COMPONENTS

ATTACHMENT 1

ASSEMBLY NAME Criticality Experiment DATE ASSEMBLED 10/14/80
WAS NO. None FOR WHOM Tom McLaughlin, Q-14
MASS. BY Rupprecht DATE OF MASS 10/14/80

ANALYTICAL CHEMISTRY REPORT

ATTACHMENT 2

Page 1 of 5

SAMPLE NO. = 16298

DATE REPORTED = 9-24-80

SAMPLE ID = CMB-11-H001733S1

DATE SUBMITTED = 9-11-80

SAMPLE DESCRIPTION = METAL

ANALYSES REQUESTED =
SPEC, PU, FE, GR, C, ISO, AM

SUBMITTER = CMB-11-MILEY

FORM B CODE = C680

◆ ANALYTICAL RESULTS ◆

ANALYTICAL RESULTS	QA PROCEDURE	ANALYST(S)	LA	NOTEBOOK	PAGE (C)
PU=99.52%	✓ ✓ ✓ ✓	EL, DJT	22774	99	
FE=10 PPM		DR, DJT	22774	99	
GR=335 PPM		ASB	22683	24-25	

COMMENT =

CERTIFIED BY GLENN R. WATERBURY *gw*

ANALYTICAL CHEMISTRY REPORT

***** Page 2 of 5

SAMPLE NO. = 16298

DATE REPORTED = 10-3-80

SAMPLE ID = CMB-11-H001733S1

DATE SUBMITTED = 9-11-80

SAMPLE DESCRIPTION = METAL

ANALYSES REQUESTED =
SPEC, PU, FE, GA, C, ISO, AM

SUBMITTER = CMB-11-MILEY

FORM B CODE = C680

◆ ANALYTICAL RESULTS ◆

BE <1 B <1 NA <50 MG <1
AL <5 SI <5 CA 3 CR <5
NI <5 CU <1 ZN <5 ZR <100
MD 9 AG <1 CD <10 SN <5
PB <5 BI <1

*WMM
ORL*

SPECTRO QUAL= RESULT ESTIMATED TO ORDER OF MAGNITUDE BY CONCENTRATION RANGE
SPECTRO QUANT= RESULT REPORTED BY A SINGLE NUMBER HAS A PRECISION OF 50%
RELATIVE STANDARD DEVIATION. IF THE NUMBER IS FOLLOWED BY AN \pm , THE PRECISION
IS 20%. OTHER PRECISIONS, IF OBTAINED, WILL BE SHOWN AFTER THE NUMBER.
RESULT IS BASED ON SAMPLE AS RECEIVED AND IS EXPRESSED AS UG/G OR UG/ML
UNLESS INDICATED OTHERWISE. RESULT PRECEDED BY < SYMBOL REPRESENTS OUR
PRESENT LIMIT OF DETECTION.

COMMENT =
PLATE NO. 496871,72

QA PROCEDURE =

DATA RECORDED IN LA NOTEBOOK NO. PAGE(S) =

ANALYST(S) = MYERS, CISNEROS, MONTOYA

CERTIFIED BY GLENN R. WATERBURY *GW*

ANALYTICAL CHEMISTRY REPORT

Page 3 of 5

SAMPLE NO. =

DATE REPORTED = 10-9-80

SAMPLE ID = H00-1733S1

DATE SUBMITTED = 9-11-80

SAMPLE DESCRIPTION = Metal

ANALYSES REQUESTED = Spec, Pu-Fe, Ga, C, Iso, Am

FORM B CODE = C680

SUBMITTER = Miley

◆ ANALYTICAL RESULTS ◆

Carbon - 230 ppm

Pr ES

COMMENT =

OP PROCEDURE =

DATA RECORDED IN LA NOTEBOOK NO. 21637 PAGE(S) = 15

ANALYST(S) = Archuleta, Vance

CERTIFIED BY GLENN R. WATERBURY *gw*

Page 4 of 5

CMB-1 RADIONANALYSIS REPORT

SAMPLE NUMBER				SUBMITTED BY				CODE	RECEIVED		
CMB-11-470-1733-S1				MILEY				C680	9-11-80		

MG. SAM.	X UL	Y ML	Z UL	W ML	PU1 C/M	PU2 C/M	AM1 C/M	AM2 C/M	T D	ML. VOL.
1055	25	25	25	2	21754	21861	28184	29315	7	100.

AM = 557. PARTS PER MILLION IN 9-23-80

PRINTED AND COMPUTED SEPTEMBER 23, 1980

Gm

CMB-1 ANALYTICAL CHEMISTRY REPORT

Page 5 of 5

MASS SPECTROMETRY SECTION

SAMPLE ID CMB-11-FM-H001733S1 SUBMITTER Miley
 FORM B CODE C690 DATE SUBMITTED 9/11/80 DATE REPORTED 9/29/80
 ANALYST DH, MEO SECT APPR ZER GRP APPR SW
 SAMPLE DESCRIPTION Pu metal
 REQUESTED ANALYSES Isotopic Pu
 ORIGINAL DATA RECORD AVCO 12598, 12599
 QA PROCEDURE ANC-DE-1-MS-3, R3

ANALYTICAL RESULTSURANIUM ISOTOPIC DISTRIBUTION

CUT	ATOM PERCENT				
	233	234	235	236	238

WEIGHT PERCENT				
233	234	235	236	238

PLUTONIUM ISOTOPIC DISTRIBUTION

CUT	ATOM PERCENT				
	238	239	240	241	242
A	.020	93.75	5.93	.266	.027
B	.020	93.77	5.92	.267	.028

WEIGHT PERCENT				
.238	.239	.240	.241	.242
.020	93.73	5.96	.268	.028
.020	93.74	5.94	.269	.028

URANIUM CONTENTCUT RESULTPLUTONIUM CONTENTCUT RESULT

COMMENT:

L-H ELECTRON BEAM
WELDING PROCEDURE

WELDING PROCEDURE

ATTACHMENT 3

Heat Shield-to-Work						
Vacuum		8x10 ⁻⁵				
Filament Current (A)		4.8				
High Voltage	Meter	50				
	Setting	3.45				
Beam Current	Meter	1.99				
	Setting	2.4				
Focus	Spot	SHARP				
	Meter	33.5				
	Setting	2.05				
Up Slope		0.2				
Down Slope		1.0				
Mode		TIMER				
Function		~				
% Modulation		50				
Frequency						
Timer		22				
Pulsation	Frequency	--				
	Width	--				
AC Deflection	Mode					
	Function					
	Frequency	100				
	Range	x1				
Spot Position	Amplitude	0.03				
	X	Center				
Fixture	Y	Center				
	Meter	5				
	Setting	10				
	s/rev	20				
	mm/s					

Date 10/14/80

Joint Edge Flange

By LRR/EDB

Material SS Hemishells

Item Criticality Experiment 0-14

Thickness 0.015 ea x 3.4" Ø

Part Nos. Pu: H00 173301

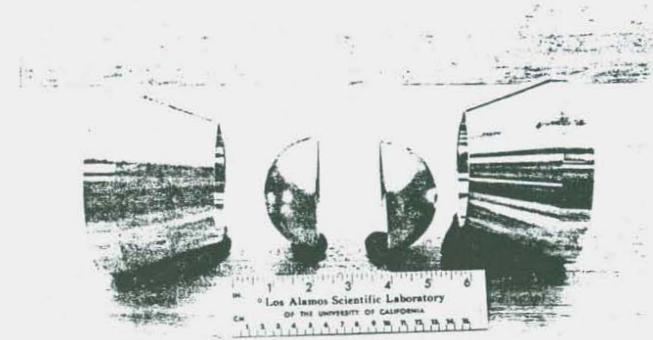
Penetration

Data Book

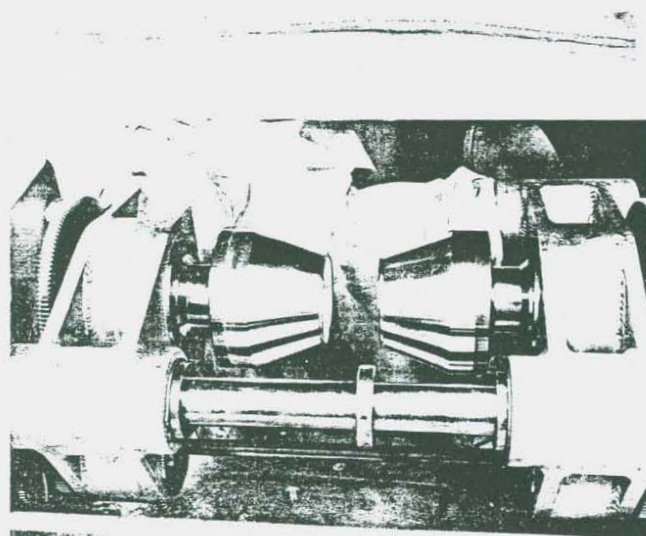
Results, Notes, Sketch:

PHOTOS OF BALL ASSEMBLY

ATTACHMENT 4



Stainless steel hemisHELLS
& aluminum welding pads



Stainless steel hemisHELLS
and welding pads in fix-
ture for electron beam
welding

Completed ball assembly



Appendix B: Polyethylene Reflector Density Measurements and Uncertainty Analysis

From: Hy D. Tran
To: John Mattingly
Subject: Densities

September 10, 2009

John,

Per your request, we measured the mass of several machined polyethylene artifacts as identified in Table 1 below. For the summary results, you can skip to the end of this memo. For all the details, please read the narrative.

Table 1. Identification numbers and descriptions

ID#	Description
RM0801041	4" OD reflector sphere, bottom
RM0801042	4" OD reflector sphere, top
RM0801043	5" OD reflector sphere, bottom
RM0801044	5" OD reflector sphere, top
RM0801045	6" OD reflector sphere, bottom
RM0801046	6" OD reflector sphere, top
RM0801047	9" OD reflector sphere, bottom
RM0801048	9" OD reflector sphere, top
RM0801049	15" OD reflector sphere, bottom
RM0801050	15" OD reflector sphere, top

The mass measurements were performed by the Length/Mass/Force metrology project in the Primary Physical Standards department at Sandia's Primary Standards Laboratory (PSL). PSL is accredited to ISO17025 by NVLAP. Although the mass measurement report that you will receive is not an accredited report, the standards, procedures, and quality system used are the same as would be used in an accredited calibration.

The mass measurement procedure used is derived from NIST Standard Operating Procedure 4 (NIST SOP-4), "substitution weighing." We use an automatic double substitution method, where we compare each item to certified master weights, in a drift-eliminating design (ABBA, where A is the master and B the unknown; we measure A, then B, then B again, then A. A straight line is fitted between the first "A" and last "A" measurement, and the "B" values are evaluated from the comparison).

The mass measurements are corrected to "true mass" per OIML R-111 or R-33 definition (OIML is the international weights and measures organization; R-111 is a recommended practice for mass). True mass is equivalent to inertial mass, or mass in a vacuum.

In order to obtain true mass values, it is necessary to know the density of each item. To obtain the density of each item, we calculated the volumes.

Appendix C: MCNP Model of the LANL SNAP-3 Detector

The document “snap.i” attached to this report is an MCNP model of the LANL SNAP-3 detector geometry and materials. To view the attachment in Adobe Acrobat or Adobe Reader, from the main menu select “View/Navigation Panels/Attachments” or click on the paperclip icon on the lower left side of the display.

Appendix D: MCNP Model of the LANL NPOD-3 Detector

The document “npod.i” attached to this report is an MCNP model of the LANL NPOD-3 detector geometry and materials. To view the attachment in Adobe Acrobat or Adobe Reader, from the main menu select “View/Navigation Panels/Attachments” or click on the paperclip icon on the lower left side of the display.

Appendix E: MCNP Model of 140% HPGe Detector

The document “hpge.i” attached to this report is an MCNP model of the 140% relative efficiency HPGe detector geometry and materials. To view the attachment in Adobe Acrobat or Adobe Reader, from the main menu select “View/Navigation Panels/Attachments” or click on the paperclip icon on the lower left side of the display.

Distribution (Electronic)

MS0782	John Mattingly	6418
MS0782	Susan H. Rhodes	6418
MS0899	Technical Library	9536



Sandia National Laboratories